A DUAL FLOW BIOREACTOR FOR CARTILAGE TISSUE ENGINEERING

Tim Spitters

2014

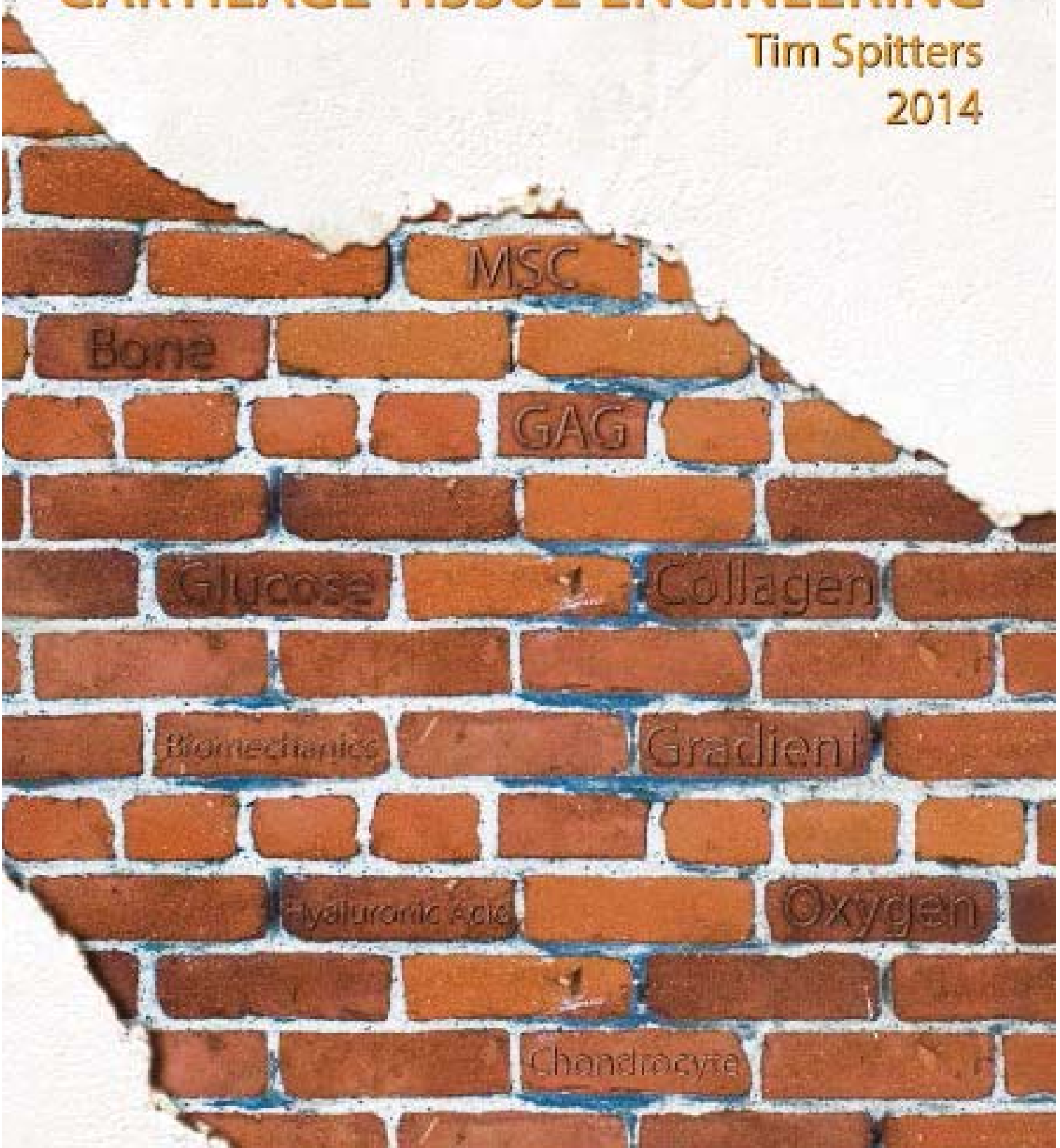

A dual flow bioreactor for cartilage tissue engineering

Tim Spitters

2014

Members of the graduation committee

Chairman:	Prof. Dr. Ir. J.W.M. Hilgenkamp	University of Twente
Promoters:	Prof. Dr. H.B.J. Karperien	University of Twente
	Prof. Dr. C.A. van Blitterswijk	University of Twente
Members:	Prof. J. de Boer	University of Twente
	Prof. Dr. Ir. N.J.J. Verdonschot	University of Twente
	Prof. Dr. H.H. Weinans	University Medical Centre Utrecht
	Dr. C. C. van Donkelaar	Eindhoven University of Technology
	Dr. Ir. D.E. Martens	Wageningen University
	Dr. R. Schulz	University of Leipzig

A dual flow bioreactor for cartilage tissue engineering
Timotheus Wilhelmus Gerardus Maria Spitters
ISBN: 978-94-6259-112-7

The research described in this book was financially supported by Project P2.02 OAcontrol of the research program of the BioMedical Materials institute, co-funded by the Dutch Ministry of Economic Affairs, Agriculture and Innovation.

The cover art was designed by Curious Media and represents a bottom up or top down approach in cartilage repair and many of the parameters that play a role in the development and homeostasis of articular cartilage.

A DUAL FLOW BIOREACTOR FOR CARTILAGE TISSUE ENGINEERING

DISSERTATION

to obtain
the degree of doctor at the University of Twente,
on the authority of rector magnificus,
Prof. Dr. H. Brinksma,
on account of the decision of the graduation committee,
to be publicly defended
on Friday April 11th, 2014 at 12.45

by
Timotheus Wilhelmus Gerardus Maria Spitters

born on December 21st, 1981
in Waalwijk, The Netherlands

This dissertation has been approved by

Prof. Dr. Marcel Karperien
Prof. Dr. Clemens A. van Blitterswijk

Table of Contents

Summary 1

Samenvatting 3

Chapter 1 General Introduction 5

Chapter 2 Bioreactors Design and Application in Musculoskeletal Tissue Engineering 11

I Gradients in Cartilage Tissue Engineering 29

Chapter 3 A dual Flow Bioreactor with Controlled Mechanical Stimulation for Cartilage Tissue Engineering 31

Chapter 4 Creating growth factor gradients to control cell behavior in three dimensional constructs 54

Chapter 5 Glucose Gradients Influence Zonal Matrix Deposition in 3D Cartilage Constructs 77

II Preclinical Evaluation of Treatment Strategies 99

Chapter 6 Delivery of Small Molecules from a Drug Delivery System into Articular Cartilage is Dependent on Synovial Clearance and Cartilage Loading 101

Chapter 7 Short communication: Are Microspheres a Treatment Option in Osteoarthritis? 121

Chapter 8 Dextran-Based Hydrogel Compositions in Cartilage Defect Repair 132

Chapter 9 General Discussion 151

Acknowledgements 157

Curriculum Vitae 159

List of Publications 160

Summary

Preventing the onset of a degenerative disease like osteoarthritis by restoring tissue function before cartilage degradation occurs will decrease health costs, reduce socio-economic burdens of patients and preserve quality of life. However, producing *ex vivo* cartilage implants of clinically relevant size remains a challenge. Culturing isolated chondrocytes in an environment that resembles their native environment can stimulate the cells to deposit and rearrange extracellular matrix that is structurally similar to native cartilage. Bioreactors and hydrogels can provide such a setting *ex vivo* (Chapter 2). Articular cartilage has a particular location in the joint. It is situated between synovial fluid and the subchondral bone plate. Together with the avascular nature of cartilage, this has an important influence on nutrient supply, growth factor distribution and action of these compounds. Its function is also determined by the mechanical stimulation cartilage is subjected to. Both these key factors are captured in one device (Chapter 3). This bioreactor is then used to test how this particular growth factor and nutrient supply influences chondrocyte behavior *in vitro* (Chapter 4 and 5). Here we find that and matrix distribution of cells cultured in the bioreactor system show trends that resemble the profiles in native cartilage.

Simulating the natural environment in a bioreactor system can also aid in the preclinical evaluation of novel biomedical therapies. Drug delivery systems are depots that can be injected in the joint to deliver drugs. As it is largely unknown how these systems behave in the knee joint, we evaluate the effect of a hydrogel system (Chapter 6) and a microsphere system (Chapter 7) on drug delivery and cartilage integrity. From our results we hypothesized that after injection of these novel treatments a personalized recovery has to be formulated to maximize drug uptake by the tissue and minimize further cartilage damage. Stabilizing a defect can also prevent cartilage degradation. Important is that cells from the surrounding tissue invade the filling material and deposit extracellular matrix components. In an *in vitro* defect model we find that providing the cells with a natural scaffold facilitates cell invasion in this sugar-based hydrogel (Chapter 8). This could aid in the understanding how we can tailor biomedical solutions to improve cartilage healing.

In summary, this thesis describes the development and validation of a novel bioreactor system that resembles the knee joint in two key aspects. Further, the potential role of this system in the preclinical evaluation of novel therapies in cartilage repair is explored.

Samenvatting

Artrose is een veel voorkomende chronische ziekte. Het voorkomen van een degeneratieve ziekte als artrose, verlaagt de ziektekosten en socio-economische belasting en verhoogt de kwaliteit van leven. Het is de uitdaging van de wetenschap de productie van natuurlijke kraakbeenimplantaten buiten het lichaam mogelijk te maken. Het kweken van geïsoleerde chondrocyten in een nagebootste natuurlijke omgeving kan de cellen aanzetten tot het aanmaken en organiseren van een extracellulaire matrix die qua structuur gelijk is aan origineel kraakbeen. Zo'n omgeving buiten het lichaam kan gecreëerd worden met behulp van bioreactoren (Hoofdstuk 2). Articulair kraakbeen heeft een specifieke locatie in het gewricht. Het wordt ingeklemd tussen synoviaal vocht en de subchondrale botplaat. Samen met de avasculaire aard van kraakbeen heeft dit een belangrijke invloed op de toevoer van voedingsstoffen, de verdeling van groeifactoren en de werking van deze moleculen. De functie wordt ook bepaald door de mechanische belasting waaraan kraakbeen onderhevig is. Deze twee uiterst belangrijke factoren hebben wij gecombineerd in één apparaat (Hoofdstuk 3). Daarnaast hebben we gekeken wat de invloed is van de specifieke toevoer van groeifactoren en nutriënten op het gedrag van chondrocyten in *vitro* (Hoofdstuk 4 en 5). In deze experimenten hebben we gevonden dat de matrix distributie overeen lijkt te komen met de matrix verdeling die in gezond kraakbeen voorkomt.

Het nabootsen van de natuurlijke omgeving in een bioreactor systeem kan ook helpen in de preklinische evaluatie van nieuwe biomedische therapieën. Drug delivery systems zijn depots die in een gewricht geïnjecteerd kunnen worden om bijvoorbeeld pijnbestrijdingsmedicijnen voor een langere tijd af te geven. Het is grotendeels onbekend hoe deze depots zich gedragen in een kniegewricht. Daarom hebben wij het effect van een hydrogel (Hoofdstuk 6) en microspheren (Hoofdstuk 7) op de medicijnafgifte en kraakbeenintegriteit getest. Deze resultaten leiden tot de hypothese dat na injectie van deze nieuwe therapieën een persoonlijk advies voor het herstel opgesteld zou moeten worden om de medicijnopname door het weefsel te maximaliseren en verdere kraakbeenschade te voorkomen. Het stabiliseren van een kraakbeen defect kan preventief werken in het voorkomen van verdere schade. Het

is dan belangrijk dat kraakbeencellen uit het omringde weefsel het opgevulde defect in kunnen groeien en daar extracellulaire matrix aanmaken. In het ontwikkelde osteochondrale model laten we zien dat cellen een op suiker gebaseerde hydrogel in kunnen groeien als ze natuurlijke aanhechtingspunten hebben (Hoofdstuk 8). Dit kan bijdragen aan de kennis hoe we biomedische oplossingen aan kunnen passen om kraakbeendefecten sneller te genezen.

Kortom, dit proefschrift beschrijft de ontwikkeling en validatie van een nieuw bioreactor systeem dat het kniegewricht in twee uiterst belangrijke aspecten nabootst. Verder is de potentiele rol van dit systeem in de preklinische evaluatie van nieuwe therapieën voor de aanmaak van kraakbeen verkend.

1

Chapter 1
General Introduction

In The Netherlands about 1.2 million individuals are affected by osteoarthritis, a degenerative joint disease, according to the Dutch Arthritis Fund. This number is expected to rise in the coming decennia due to the increase in life expectancy. During disease progression, the tissues in the joint, cartilage, bone and synovium, undergo changes due to an imbalance in anabolic and catabolic processes. The disease can be initiated by trauma, disease or age. Several surgical techniques have been developed to initiate cartilage repair and to restore tissue function. Mosaicplasty and drilling in the subchondral bone aim at restoring the cartilage defect with tissue or cells from different sites. However, these techniques are also associated with donor site morbidity and fibrocartilage formation, respectively. An even more invasive, and usually the last-option treatment strategy, is total joint replacement. Although advancements in the field of prostheses have been made, the risk of donor site morbidity and integration of the prosthesis with the surrounding tissue. Further, total joint replacement in young patients is undesirable as prostheses only last about 15 years.

Cartilage tissue engineering (CTE) can serve as an alternative to these surgical methods. Autologous chondrocyte implantation, a technique already used in the clinic, harvests the cells of the patient's own cartilage, multiplies the chondrocytes *ex vivo* and transplants them into the defect site. Although clinical results three to five years after surgery are promising, long term results have to provide evidence on the mechanical stability of the produced tissue. As an alternative to the surgical techniques described above, supports of natural and synthetic materials can be produced on which cells can deposit extracellular matrix.

Next to providing the cells with a support for growth and matrix deposition, the chemical environment of the chondrocytes is important. Cartilage is situated between synovial fluid in the joint cavity and the subchondral bone plate. Its structure can be divided in three main zones: the superficial, middle and deep zone. These have specific distributions of the main extracellular matrix components (Figure 1). These parameters cause gradients of biochemical cues through the tissue. Nutrient and growth factor concentrations determine the fate of cells and can create an environment the cells experience in the body. Glucose, oxygen and growth factor levels have a gradual distribution in cartilage. These cause a differential response of chondrocytes at different depths in the matrix. To establish the native structure of cartilage *in vitro*, gradient formation has to be taken into account as a major influence

on cell behavior [2]. So, it is important to consider the appropriate means for nutrient supply depending on the tissue to be produced. To achieve this distribution, we hypothesized that nutrient and growth factor distribution and supply similar to the native situation could induce zonal differentiation of isolated chondrocytes. Bioreactors can provide the means to create such an environment.

Bioreactors can be designed to control nutrient supply. Perfusion bioreactors have

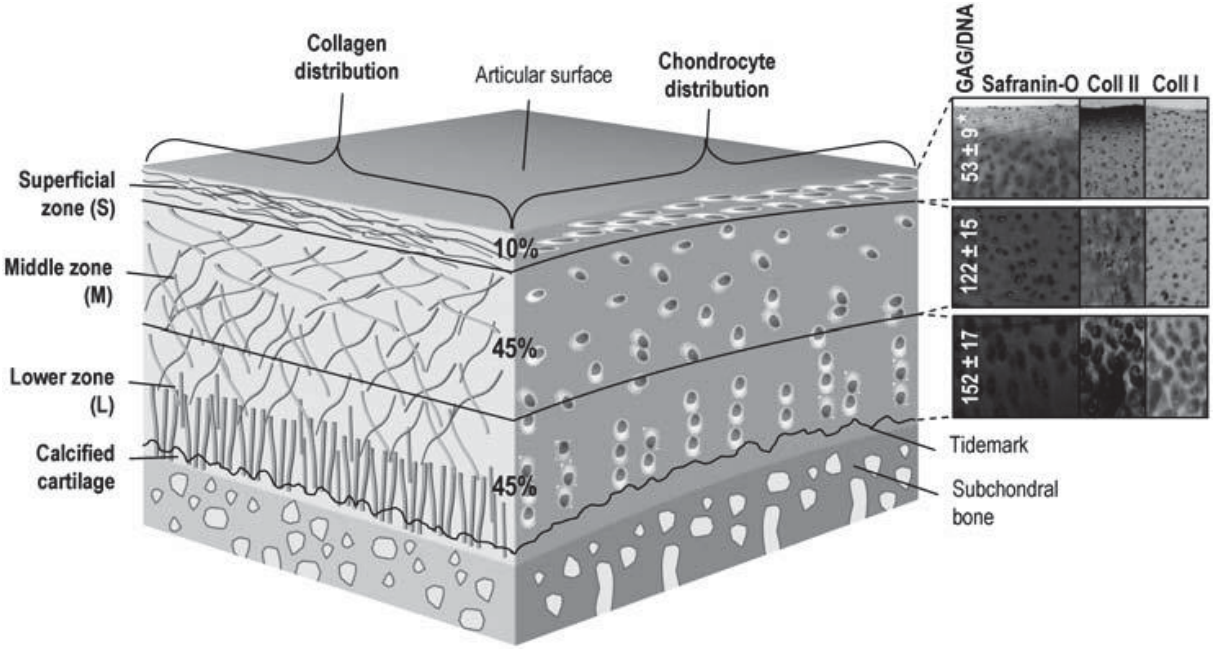

Figure 1: Zonal distribution of cells and extracellular matrix components through articular cartilage. Reproduced from [1].

been developed to keep nutrient supply constant [3, 4], supply nutrients from two sides [5, 6], apply compression [7-9], simulate articulation [10] or provide a combination of perfusion and mechanical stimulation [11, 12]. However, a combination of a dual compartment and compression did not exist yet. This is the basis of this thesis of which the outline will be discussed next.

Thesis outline

After the general introduction of chapter 1, chapter 2 describes of the state of the art bioreactor designs for musculoskeletal tissue engineering and the implication and applications of gradient in tissue culture.

Then, chapter 3 elaborates on the design and validation of a dual flow bioreactor. Here, we describe the dual compartment set-up which was validated with

computational modeling and experimentation. It was shown that the design supported gradient formation of oxygen, glucose and matrix degrading enzymes.

In chapter 4 and 5 the new bioreactor design was used to create nutrient and growth factor gradients. In chapter 4 growth factor and growth factor antagonist gradients were created through agarose constructs. Further it was attempted to create an osteochondral construct through the creation of opposing gradients of growth factors that induce chondrogenesis and osteogenesis. In chapter 5 the effect of a glucose gradient through agarose constructs seeded with chondrocytes on matrix production and distribution was explored. Here we showed zonal differences in matrix deposition after culture in a glucose gradient.

In chapter 6 the bioreactor was used as an *ex vivo* test model to evaluate the potential of a novel hydrogel drug delivery system. Here it was found that this system has a beneficial effect on the delivery of drugs into cartilage as well as retaining drugs in the joint space. Chapter 7, on the other hand, explores the feasibility of microspheres in the treatment of degenerative joint diseases. Finally, chapter 8 shows the added value of this bioreactor system in the evaluation of novel treatment options for cartilage defects.

In the final chapter the results presented in this thesis are discussed and related to current work in the field of tissue engineering. Finally, an outlook discussing future perspectives in the development of bioreactor based biomedical therapies is given.

References

1. Woodfield, T.B., et al., *Polymer scaffolds fabricated with pore-size gradients as a model for studying the zonal organization within tissue-engineered cartilage constructs.* Tissue Eng, 2005. **11**(9-10): p. 1297-311.
2. Higuera, G., et al., *Quantifying in vitro growth and metabolism kinetics of human mesenchymal stem cells using a mathematical model.* Tissue Eng Part A, 2009. **15**(9): p. 2653-63.
3. Janssen, F.W., et al., *A perfusion bioreactor system capable of producing clinically relevant volumes of tissue-engineered bone: in vivo bone formation showing proof of concept.* Biomaterials, 2006. **27**(3): p. 315-23.
4. Wendt, D., et al., *Uniform tissues engineered by seeding and culturing cells in 3D scaffolds under perfusion at defined oxygen tensions.* Biorheology, 2006. **43**(3-4): p. 481-8.
5. Chang, C.H., et al., *Cartilage tissue engineering on the surface of a novel gelatin-calcium-phosphate biphasic scaffold in a double-chamber bioreactor.* J Biomed Mater Res B Appl Biomater, 2004. **71**(2): p. 313-21.
6. Malafaya, P.B. and R.L. Reis, *Bilayered chitosan-based scaffolds for osteochondral tissue engineering: influence of hydroxyapatite on in vitro cytotoxicity and dynamic bioactivity studies in a specific double-chamber bioreactor.* Acta Biomater, 2009. **5**(2): p. 644-60.
7. Demarteau, O., et al., *Development and validation of a bioreactor for physical stimulation of engineered cartilage.* Biorheology, 2003. **40**(1-3): p. 331-6.
8. Kock, L.M., et al., *Tuning the differentiation of periosteum-derived cartilage using biochemical and mechanical stimulations.* Osteoarthritis Cartilage, 2010. **18**(11): p. 1528-35.
9. Schulz, R.M. and A. Bader, *Cartilage tissue engineering and bioreactor systems for the cultivation and stimulation of chondrocytes.* Eur Biophys J, 2007. **36**(4-5): p. 539-68.
10. Wimmer, M.A., et al., *Tribology approach to the engineering and study of articular cartilage.* Tissue Eng, 2004. **10**(9-10): p. 1436-45.
11. Schulz, R.M., et al., *Development and validation of a novel bioreactor system for load- and perfusion-controlled tissue engineering of chondrocyte-constructs.* Biotechnol Bioeng, 2008. **101**(4): p. 714-28.
12. Jovanovic, Z., et al., *Bioreactor validation and biocompatibility of Ag/poly(N-vinyl-2-pyrrolidone) hydrogel nanocomposites.* Colloids Surf B Biointerfaces, 2013. **105**: p. 230-5.

1

2

Chapter 2
Bioreactor Design and Application in Musculoskeletal Tissue Engineering

Tim WGM Spitters, Tim BF Woodfield, Marcel Karperien

Abstract

Critical size defects in skeletal muscle, bone or cartilage have a very limited healing capacity. This often leaves the patient in debilitating conditions as a result of significantly impaired limb use. At present, surgical interventions are associated with drawbacks. This, in combination with the scarcity of donor material, necessitates innovative and sophisticated tissue engineering strategies that will allow for the generation of patient-tailored large implantable constructs. To control the culture environment for reproducible production of such grafts bioreactors systems have been developed. However, most systems only culture one tissue, e.g. osteogenic differentiation without the means for vascularisation, innervation or chondrogenic differentiation, whereas in the natural situation, tissue development and homeostasis are also dependent on the crosstalk with neighbouring tissues. Therefore, bioreactor systems must be expanded to accommodate the differentiation of cells towards multiple tissue types to mimic the native environment more closely. This review focuses on the recent advancements in bioreactor design for musculoskeletal applications and addresses some of the various possibilities to mimic the complex *in vivo* environment in an *in vitro* setting.

Keywords: Bioreactor, Tissue engineering, cartilage, bone, skeletal muscle

Chapter two: Complexity in Bioreactor Design

Introduction

In the last decades, engineering musculoskeletal tissue grafts for the treatment of defects originating from trauma or removal of tumours has become of special interest as recently reviewed for cartilage defects [1], bone defects [2] and for skeletal muscle repair [3]. However, due to the complexity of these tissues, implantable constructs of clinically relevant size and structure similar to the native tissue have not been accomplished yet. To overcome these hurdles, tissue engineering aims at producing grafts that resemble the native structure of the tissue. However, it became apparent that culturing three-dimensional (3D) constructs in a conventional static manner is detrimental for nutrient supply and waste removal, resulting in necrotic cores due to nutrient deprivation. This necessitated the development of new devices for tissue engineering, called bioreactors, that can control nutrient supply and waste removal of metabolic products. Also, these bioreactors provide a closed loop system for monitoring and control of nutrient levels, pH, and tissue formation. The importance for developing bioreactors was already postulated a decade ago [4].

Early bioreactors focussed on generating an environment that facilitated homogeneous nutrient distribution and cell seeding on a biomaterial. Spinner flasks, rotating wall and perfusion bioreactor systems have been used to achieve homogeneous cell and nutrient distribution [4]. Furthermore, these devices provided hydrodynamic stimulation to the cells due to shear stress, which is one of the natural stimuli that induces extracellular matrix production [5]. In bone tissue engineering (BTE) these are parameters of great influence, but for example in cartilage tissue engineering (CTE), shear stresses induced by mechanical compression are of greater importance as they resemble the natural situation of joint loading more accurately. This illustrates the different needs in physical cues to produce functional tissues of distinct origin. This review provides an overview of the different bioreactor systems currently used in musculoskeletal tissue engineering that specifically take complex mechanical stimulation during tissue growth into account. Furthermore, the need for complexation of bioreactor systems, i.e. combining different stimulation protocols into one device, will be addressed.

Smooth muscle tissue engineering

Muscles are highly vascularized and innervated tissues. Several stem or progenitor cell types can be used to produce skeletal muscle cells, such as but not limited to satellite cells residing in the muscle and cells from the interstitial tissue, or bone marrow as reviewed by Grounds *et al* [6]. These cell sources are commonly used for tissue engineering purposes. However, to produce functional muscle, alignment of the cells and contractile motion by the cells are important. So, bioreactors should be equipped to provide physical and biochemical cues to align and mature the cells. There are two main ways to stimulate stem or progenitor cells into the myogenic lineage using physical cues, i) by stretching/relaxation of cells and ii) by electrical stimulation (schematically represented in Figure 1A and 1B). Moon *et al.* developed a bioreactor containing 10 tissue constructs anchored to a stationary bar and a moveable one. Human skeletal muscle cells seeded on porcine bladder submucosa showed alignment after 5 days and a contractile response after 3 weeks of *in vitro* culture [7]. Tissue engineered muscle constructs that were preconditioned in a bioreactor showed a 1-10% tetanic and twitch contractile specific force compared to statically cultured constructs [7]. Muscle constructs cultured in this system were implanted in an *in vivo* volumetric muscle loss model and showed functional repair of the muscle defects [8]. This showed the importance of mechanical stimulation in producing functional muscle tissues. Stretching stimulation has also been reviewed by Riehl *et al* [9].

Electrical stimulation in skeletal muscle engineering has recently been rediscovered as reviewed by Balint *et al* [10]. Donnelly *et al.* described a 6-well bioreactor in which C2C12 cells were cultured on fibrin for 9 days, of which electrical stimulation was applied for 7 days. After stimulation with a pulse width of 0.1ms, these constructs showed improved force production and excitability compared to controls [11]. In a subsequent experiment, Khodabukus and Baar showed that this system was suitable for studying tissue physiology and maturation [12].

In another approach, Hosseini *et al.* produced contractile muscle tissue in a microgrooved gelatine hydrogel after electrical stimulation (amplitude 22 mA, frequency 1 Hz, duration 2 ms) [13]. In this system, smaller grooves (50µm wide) resulted in better aligned cells than in the larger ones (100µm wide) showing that not only physical cues are important, but also environmental factors [13]. Kujala *et al.* designed a microelectrode array equipped for electrical stimulation of

cardiomyocytes. In this platform they showed that neonatal rat cardiomyocytes orientated along the electrodes. However, upon electrical stimulation (pulses at 5-5.3V/cm for up to 200ms at 1Hz) cells showed upregulation of some main cardiac markers [14]. Human aortic endothelial cells cultured on a substrate with ridge and groove topographies in a dynamic environment (shear stress: 20dyne/cm^2) showed increased elongation and orientation when a flow parallel to the topographies was applied compared to a flow that was perpendicular [15]. These studies demonstrate that surface texture of a biomaterial combined with mechanical/electrical stimulation can be exploited to organize stem or progenitor cells in tissue resembling structures.

Functionality does not only come from within the tissue, but also from the connection to other tissues. Muscle and bone are connected by tendon or ligament, providing movement of limbs. Engineering a functional connection between muscle and tendon is a challenge as the tissue border should not rupture upon a mechanical challenge. Tissue engineering strategies have focused on producing musculo-tendinous implants by creating biologically relevant scaffolds as reviewed by Turner and Badylak recently [16]. Strategies have aimed at producing muscular and tendon tissue separately and subsequently joining them together by suturing [17]. It would be highly advantageous if both tissues were produced in the same construct, so that cells themselves could arrange the connection between the two tissues. Chang *et al.* reported the development of a dual compartment bioreactor for osteochondral tissue engineering in which a cell-laden biomaterial separates two medium compartments [18]. By varying the medium composition, cells on both ends of the constructs can be differentiated towards different phenotypes. Such a concept could also be applied for engineering a functional muscle – tendon unit. It will be of paramount importance to incorporate this concept in a bioreactor that can apply stretching of the developing tissue. Furthermore, it might be worthwhile to further incorporate features allowing electrical stimulation of the tissue, since it is plausible that the combination of stretching and electrical stimulation may have a beneficial effect muscle and tendon formation over either one of the stimuli. A number of bioreactors have been developed that apply a stretching stimulus [19-21]. This assures the alignment of the fibers and strengthens the bond between muscle and tendon. Combining the mentioned bioreactor designs may result in musculo-tendinous tissue of superior mechanical strength than can be produced with current devices.

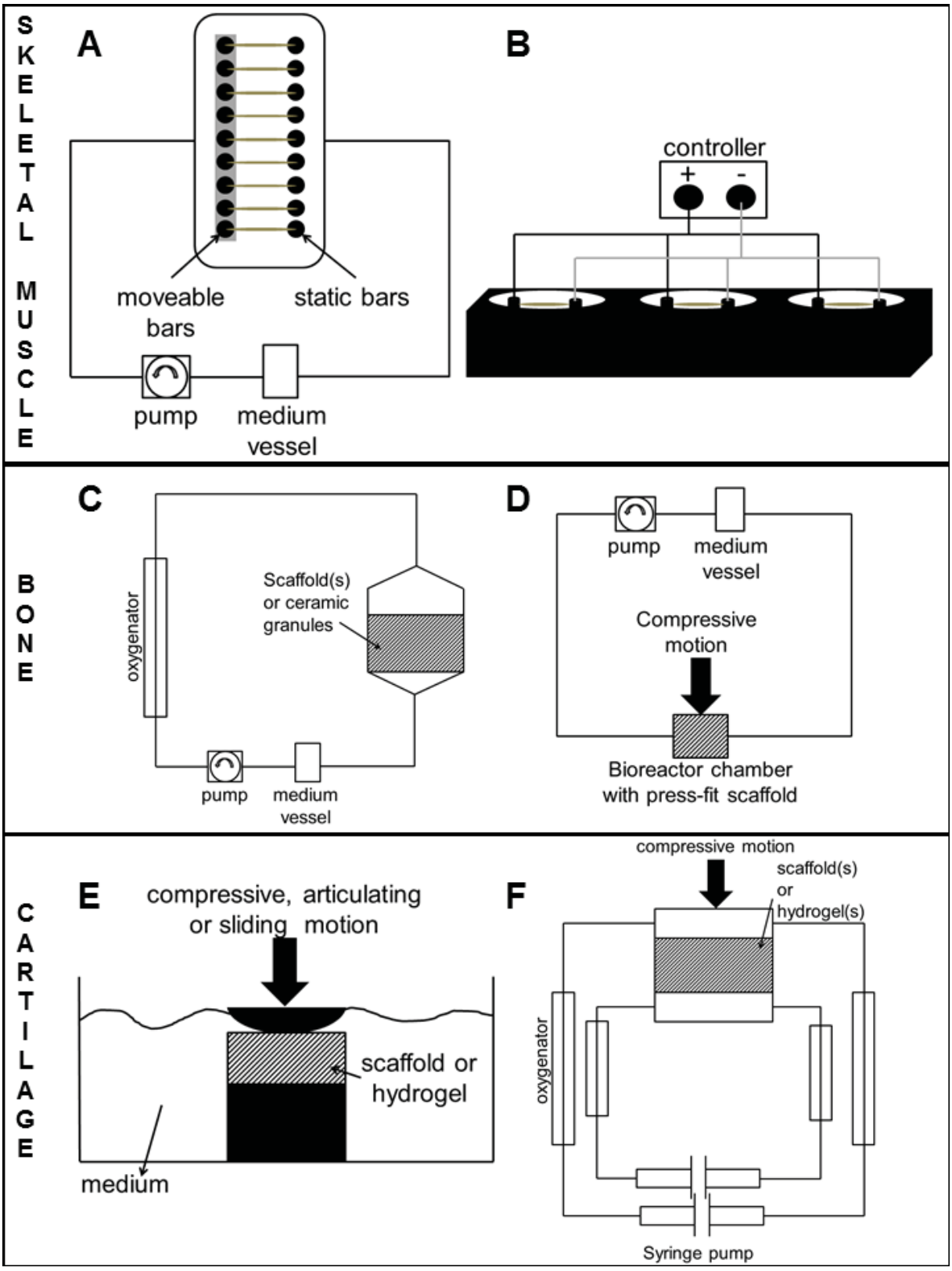

Figure 1: Schematic representations of bioreactor systems for skeletal muscle (A and B), bone (C and D) and cartilage (E and F). (A) stretching stimulation (adapted from [7]), (B) electrical stimulation(adapted from [11]), (C) (perfusion adapted from [29]), (D) combined perfusion and confined mechanical stimulation (adapted from [62]), (E) unconfined compression (adapted from [80]), (F) combined dual compartment and confined mechanical stimulation (adapted from [76]).

Muscular cells are highly metabolically active [22, 23]. Sufficient nutrient supply is thus paramount. Levenberg *et al.* investigated the effect of co-culturing myoblasts, embryonic fibroblasts and endothelial cells on a highly porous scaffolds on the development, maturation and survival of this tissue engineered muscle *in vivo* [24]. Improved function and integration of the construct was observed. Koffler *et al.* showed that a construct that was pre-vascularized *in vitro* for 3 weeks, showed improved function and integration with the host vasculature compared to a graft that was pre-vascularized for 1 day [25]. Ye *et al.* described a scaffold design consisting of 100µm hollow fibers that supplied nutrients to a parenchymal space [26]. Skeletal muscle cells were seeded between the fibers *in vitro* and transport of a cytotoxic agent from the fibers was shown by the observed cell death. After implantation, host blood vessels invaded the fibrillar network [26]. The examples described above show the beneficial effect of pre-vascularization of a tissue engineered muscle construct before implantation. However, all the grafts described were of mm-size and to be applicable in the clinic cm-size skeletal muscle constructs will be necessary. Herein still lies a major challenge. One can imagine that a combination of a hollow fiber type of scaffold or a scaffold of a precast fibrillar network in combination with mechanical (or electrical) stimulation to align smooth muscle cells - such as by exerting stretching motion [9] or sliding indentation [27] - can result in a tissue that is structurally similar to native muscle tissue, and can aid in the upscaling of vascularized tissue engineered muscle constructs.

Bone tissue engineering

The most popular bioreactor set-up in bone tissue engineering is a perfusion system [28, 29] (schematically represented in Figure 1C and 1D). More recently also oscillating fluid flow bioreactors [30] gained attention, since hydrodynamic stimulation induces anabolic and catabolic processes involved in osteogenic differentiation and bone remodeling [31-35]. Porous scaffolds, either printed [36-38] or molded polymers [39-41] or granulated ceramics [29, 42-44], can be seeded with a variety of cell sources such as bone marrow-derived stromal cells [29], adipose-derived stem cells [45] or osteoblast (precursor) cells [46, 47]. Since the bones residing in the hips and lower limbs are also subjected to compression perfusion, bioreactors are equipped with modules for mechanical compression to improve the mechanical properties of the tissue engineered grafts. Rauh *et al.* extensively reviewed spinner flasks, rotating

and perfusion bioreactors, but only briefly mentioned the combination of fluid flow and mechanical stimulation [48].

More recently, Kang *et al.* used a combined compression and ultrasound device for the stimulation of MC3-T3 E1 cells seeded on polycaprolactone/poly-L-lactic acid salt leached scaffolds [49]. Constructs that received a combined treatment showed elevated gene expression of bone related genes compared to uni-stimulated constructs. Also alkaline phosphatase (ALP) activity and calcium deposition increased after dual stimulation compared to the controls. A limitation of these studies is that they were performed under static compression [49].

In another study, perfusion combined with mechanical stimulation induced osteogenic differentiation in bone marrow derived stromal cells [50]. Biaxial compression and fluid flow combined with active nutrient exchange resulted in increased osteogenic differentiation on a decalcified bone matrix. Dynamically cultured, compressed constructs showed higher ALP activity and calcium deposition compared to the other conditions [50].

Although mechanical stretching has been investigated in three dimensional constructs to induce osteogenic differentiation [51, 52], little progress has been made in this area recently.

Like muscle tissue, bone is also a highly vascularized tissue. Strategies have been developed to pre-vascularize the construct to increase the survival of a tissue engineered bone graft *in vivo*. Wang *et al.* developed a β-tricalcium phosphate scaffold, which could be placed around the femoral artery and vein ensuring nutrient supply to the seeded osteogenic mesenchymal stem cells [53]. Other investigations explored the *in vitro* pre-vascularisation of osteogenic construct by co-culturing human umbilical vein endothelial cells (HUVEC) with osteoblasts [54]. This resulted in an upregulation in expression of endothelial and osteogenic markers, such as VEGF and collagen type I as well as microvessel formation throughout the construct compared to monocultures. In co-cultures of endothelial progenitor cells and mesenchymal stem cells on a demineralized bone scaffold, similar results were obtained [55]. While the previous studies cultured the cells in a two dimensional environment before seeding onto a scaffold, Braccini *et al.* and Scherberich *et al.* showed that constructs seeded with non-plastic expanded bone marrow-derived stromal cells (meaning directly seeded on scaffolds) or the adipose-derived stromal vascular fraction in a perfusion bioreactor system outperformed grafts seeded with

plastic expanded cells derived from the stromal vascular fraction [56, 57]. This showed that seeding of a heterogeneous population in a three-dimensional environment maintains the heterogeneity compared to the selection that results from expansion on tissue culture polystyrene plates. It is probable that seeding of whole bone marrow retains stem or progenitor cells. The use of adipose-derived progenitors in the production of vascularized osteogenic constructs was reviewed by Scherberich *et al.* [58].

Interstitial fluid flow has become of special interest recently as it resembles in many ways a more natural physical environment for cells. For this purpose an oscillating bioreactor was developed. Valonen *et al.* showed in this system the production of mechanically functional cartilage grafts and Cheng *et al.* showed the formation of cardiac tissue using slow oscillating fluid flow in combination with insulin growth factor I [59, 60]. The effect of oscillating fluid flow has yet not been combined with cyclic compression loading to explore for possible additive effects.

Cartilage tissue engineering

Perfusion bioreactors can be used to obtain scaffolds with a homogenous cell distribution for cartilage tissue engineering [61, 62]. To increase homogeneity, continuous or oscillating medium flow is used. Matrix distribution within the scaffold was shown to be homogeneous after dynamic culture and superior to scaffolds cultured statically [61]. However, chondrocytes are also subjected to interstitial fluid flow due to water displacement as a result of compression [63] and accumulated evidence shows that recreating the zonal organisation of articular cartilage in tissue engineered cartilage constructs enhances the functionality of the implantable graft [64, 65]. Thus, bioreactor systems and scaffolds have been developed to assist in the creation of this specific cell and matrix distribution. To induce a gradual cell distribution within a printed scaffold, the design of the scaffold can be adopted so that it acts as a sieve. We explored the possibility to allocate cells at high density in a perfusion bioreactor system (Figure 2A). The scaffolds consisted of “U-shaped” channels, printed in a 0-90° fashion, to capture cells. The “U-shaped” scaffold (Figure 2B) and its control (Figure 2C) were designed in such a way that they exhibited the same surface area. Cell seeding was performed in a perfusion bioreactor, which was adopted from the one described by Wendt *et al.* [61] with the channels facing the flow direction. Following cell seeding, total cell numbers were higher in the channelled

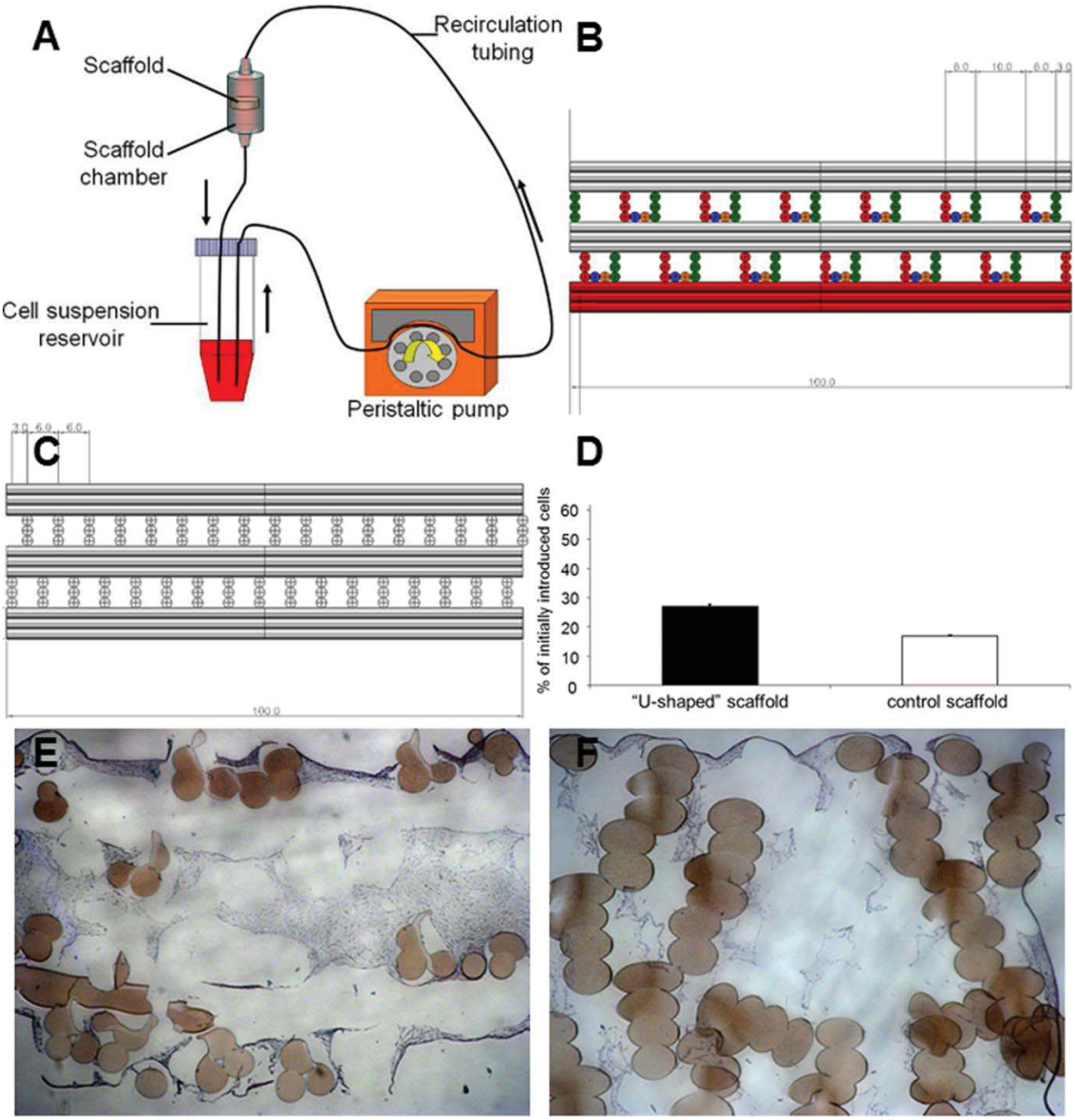

Figure 2: Conceptual design of culturing human articular chondrocytes at high density in printed polymer scaffolds. (A) A schematic overview of the bioreactor system. The black arrows indicate the flow direction and the yellow arrow indicates the pump direction.(B) 3D CAD drawing of the "U-shaped" scaffold, (C) 3D CAD drawing of the control scaffold. (D) Seeding efficiency after 18 hours dynamic seeding expressed as the percentage of loaded cells. Haematoxylin staining of human articular chondrocytes cultured for 13 days in (E) "U-shaped" scaffolds and (F) control scaffolds. Note the increased tissue formation in the "U-shaped" scaffolds.

scaffold compared to a conventional printed scaffold as confirmed by DNA quantification (Figure 2D). Furthermore, using a haematoxylin/eosin staining, we found higher amounts of tissue in the "U-shaped" scaffold (Figure 2E) compared to control scaffolds (Figure 2F) after 13 days of static culture. This showed that seeding cells at high density in controlled spaces can have beneficial effects on tissue growth

in long term culture. Ng *et al.* developed a more elaborate protocol to induce inhomogeneity in a chondrocyte hydrogel [66, 67]. Cell-laden agarose solutions of 2% and 3% were seeded on top of each other and then mechanically stimulated. In these constructs they were able to show that matrix production and mechanical strength varied zonally [66].

Another option to induce zonal differences in cell response is to expose cells at different depths in the construct to varying concentrations of nutrients, growth factors and/or growth factor antagonists. Computational modelling of oxygen concentrations within a tissue engineered cartilage construct has been shown to be dependent on the depth of the construct [68, 69]. Glutamine gradients have been reported to induce mesenchymal stem cells proliferation in printed PEGT/PBT scaffolds [70]. Furthermore, chondrocytes are also responsive to varying glucose concentrations. Heywood *et al.* showed that decreasing the glucose concentration in culture medium resulted in an increased matrix production by bovine chondrocytes [71]. Chang *et al* described a dual compartment system to culture bi-layered constructs [18]. Here, a composite scaffold, seeded with chondrocytes and osteoblasts, was used to culture an osteochondral construct by varying the medium compositions in both compartments. The integration of an osteochondral construct with the host tissue has been a point of concern [72-74]. Bi-layered scaffolds rely on the integration of the two layers. To overcome this problem, gradients can be created through a construct consisting of one material. Thorpe *et al.* correlated oxygen gradients in confined, dynamically compressed mesenchymal stem cell-seeded agarose hydrogels to zonal matrix production, although matrix proteins were quantified in only two zones [75]. In a more complex system, both compression and gradient creation were combined. In this dual compartment bioreactor the creation of glucose and catabolic enzyme gradients through bovine articular cartilage explants were shown under dynamic and static conditions [76]. Although gradients play important roles during development and tissue homeostasis [77-79], their use in tissue engineering has been limited. However, lessons from embryology have taught us that subtle differences in concentrations of growth factors, for example, can have a dramatic impact on cellular responses, and hence can exploited for the production of functional implantable tissue grafts.

The degree of functionality of a cartilage tissue graft that can be achieved depends on the mechanical and chemical cues provided during the growth and developing

phase of the construct. Wimmer *et al.* used a tribology approach to mimic the complex mechanical stimulation in the knee joint [80]. In their system a ceramic ball can compress and rotate in two directions to stimulate the articular surface of an osteochondral explant or tissue engineered construct. In a follow-up experiment they showed that zone specific proteins were either up- (cartilage oligomeric matrix protein) or downregulated (superficial zone protein) [81]. This shows that functionalizing the superficial zone requires different biochemical or mechanical stimulation. It furthermore suggests that each zone of articular cartilage may require its own mechanical stimulation regime for optimal tissue development.

Shahin and Doran reported a bioreactor that exerted complex mechanical stimulation on a cartilaginous construct [82]. Poly-glycolic acid discs loaded with P2 human fetal epiphyseal chondrocytes were compressed and sheared by rotating cylinders. Mechanically stimulated cells showed higher production of cartilage specific matrix components compared to their respective controls [82]. Mechanically stimulated constructs that were pre-cultured a perfusion bioreactor also showed higher production of cartilage specific matrix proteins compared to non-stimulated controls, although the increase was less pronounced compared to constructs that were not subjected to shear stress [82].

Combining the two latter systems, dual compartment and complex mechanical stimulation, increases the complexity of the bioreactor, but also the resemblance with the natural environment of the cartilage-bone unit (Figure 1E and 1F schematically represent the above described bioreactor systems). Current challenges in recreating functional cartilage tissue from a clinical point of view was recently reviewed by Mastbergen *et al* [83].

About 10 years ago the Group for the Respect of Excellence and Ethics in Science (GREES) recommended new technologies for the evaluation of disease-modifying osteoarthritis drugs (DMOADs) in clinical trials [84]. However, evaluation of these disease modifying drugs (DMDs) in clinical trials is expensive. *In vitro* engineered tissues can provide an environment to screen these drugs as recently reviewed by Gibbons *et al* [85]. One study showed an *in vitro* model of engineered cartilaginous tissue for the evaluation of therapeutic compounds [86]. However, the functionality of this tissue, in terms of structural and biomechanical similarity to native tissue, was not shown. As these properties influence chondrocyte behaviour, as well as drug penetration for example, it is important to produce tissues with close resemblance to

their native counterparts. Popp *et al.* described a bioreactor system in which the maturity of the cartilaginous tissue is evaluated by its density [87]. While the production of functional tissues remains a challenge, other systems are being developed to evaluate DMDs on tissue explants of patients suffering from degenerative diseases. Beekhuizen *et al.* established a cartilage-synovium co-culture model to investigate the interaction of these tissues during osteoarthritis (OA) [88]. They showed inhibition of proteoglycan production in cartilage in the presence of OA synovium. Application of triamcinolone reversed this effect in co-cultures, but not in mono-cartilage cultures. A similar observation was reported by De Vries-Van Melle *et al.* in an osteochondral explant model [89]. In this *in vitro* model it was shown that the subchondral bone is involved in the stimulation of chondrogenic differentiation of mesenchymal stem cells [89].

These last two dual tissue culture models show that compartmentalisation of bioreactors to culture multiple tissues is expected to create an environment that more closely resembles the native tissue environment and will allow for important cross talk between tissue involved in development and homeostasis.

Conclusions

Evidence has accumulated that in a degenerative disease like osteoarthritis progression of the disease is determined by the crosstalk of multiple tissues, such as bone, synovium and cartilage [90-92]. Creating an environment that resembles the *in situ* environment of these tissues as closely as possible could improve the quality and functionality of these tissue engineered grafts. The importance of a complex bioreactor design was further evidenced by Grayson *et al*. They cultured an anatomically shaped human mandibular bone implant in a bioreactor of exactly the same shape [93]. They showed that after 5 weeks of culture, bone matrix was formed throughout the complete scaffold and that the bone was structurally similar to native osseous tissue. Thus, culturing constructs with complex dimensions in a bioreactor is possible, but to reproducibly cultivate complex tissues the development should be monitored during the culture period. This was beyond the scope of this review, but its importance was reviewed by Hagenmuller *et al*. This group proposes to combine a bioreactor for mechanical stimulation with online micro-computed tomography to monitor construct development [94].

Bioreactors have great potential in the tissue engineering of complex constructs, but their design is critical and depends on the application. However, with the appropriate monitoring and control offered by advanced and compartmentalised bioreactor systems in conjunction with mechanical stimulation, reliable and reproducible tissue-engineered constructs could be produced.

2

References

1. Behery, O., et al., Treatment of Cartilage Defects of the Knee: Expanding on the Existing Algorithm. Clin J Sport Med, 2013.
2. Dawson, J.I., et al., Bridging the gap: Bone regeneration using skeletal stem cell-based strategies - Where are we now? Stem Cells, 2013.
3. Fujimaki, S., et al., Intrinsic ability of adult stem cell in skeletal muscle: an effective and replenishable resource to the establishment of pluripotent stem cells. Stem Cells Int, 2013. 2013: p. 420164.
4. Martin, I., D. Wendt, and M. Heberer, The role of bioreactors in tissue engineering. Trends Biotechnol, 2004. 22(2): p. 80-6.
5. Kim, H.J., et al., Bone regeneration on macroporous aqueous-derived silk 3-D scaffolds. Macromol Biosci, 2007. 7(5): p. 643-55.
6. Grounds, M.D., et al., The role of stem cells in skeletal and cardiac muscle repair. J Histochem Cytochem, 2002. 50(5): p. 589-610.
7. Moon du, G., et al., Cyclic mechanical preconditioning improves engineered muscle contraction. Tissue Eng Part A, 2008. 14(4): p. 473-82.
8. Concaro, S., F. Gustavson, and P. Gatenholm, Bioreactors for Tissue Engineering of Cartilage. Adv Biochem Eng Biotechnol, 2008.
9. Riehl, B.D., et al., Mechanical stretching for tissue engineering: two-dimensional and three-dimensional constructs. Tissue Eng Part B Rev, 2012. 18(4): p. 288-300.
10. Balint, R., N.J. Cassidy, and S.H. Cartmell, Electrical stimulation: a novel tool for tissue engineering. Tissue Eng Part B Rev, 2013. 19(1): p. 48-57.
11. Donnelly, K., et al., A novel bioreactor for stimulating skeletal muscle in vitro. Tissue Eng Part C Methods, 2010. 16(4): p. 711-8.
12. Khodabukus, A. and K. Baar, Defined electrical stimulation emphasizing excitability for the develop ment and testing of engineered skeletal muscle. Tissue Eng Part C Methods, 2012. 18(5): p. 349-57.
13. Hosseini, V., et al., Engineered contractile skeletal muscle tissue on a microgrooved methacrylated gelatin substrate. Tissue Eng Part A, 2012. 18(23-24): p. 2453-65.
14. Kujala, K., et al., Electrical Field Stimulation with a Novel Platform: Effect on Cardiomyocyte Gene Expression but not on Orientation. Int J Biomed Sci, 2012. 8(2): p. 109-20.
15. Morgan, J.T., et al., Integration of basal topographic cues and apical shear stress in vascular endothelial cells. Biomaterials, 2012. 33(16): p. 4126-35.
16. Turner, N.J. and S.F. Badylak, Biologic scaffolds for musculotendinous tissue repair. Eur Cell Mater, 2013. 25: p. 130-43.
17. Sawadkar, P., et al., Development of a surgically optimized graft insertion suture technique to accommodate a tissue-engineered tendon in vivo. BioResearch open access, 2013. 2(5): p. 327-35.
18. Chang, C.H., et al., Cartilage tissue engineering on the surface of a novel gelatin-calcium-phosphate biphasic scaffold in a double-chamber bioreactor. J Biomed Mater Res B Appl Biomater, 2004. 71(2): p. 313-21.
19. Lee, K.I., et al., Mechanical properties of decellularized tendon cultured by cyclic straining bioreactor. J Biomed Mater Res A, 2013. 101(11): p. 3152-8.
20. Wang, T., et al., Bioreactor design for tendon/ligament engineering. Tissue Eng Part B Rev, 2013. 19(2): p. 133-46.
21. Wang, T., et al., Programmable mechanical stimulation influences tendon homeostasis in a bioreactor system. Biotechnol Bioeng, 2013. 110(5): p. 1495-507.
22. Caffin, F., et al., Altered skeletal muscle mitochondrial biogenesis but improved endurance capacity in trained OPA1-deficient mice. J Physiol, 2013.
23. Layec, G., et al., Short-term training alters the control of mitochondrial respiration rate before maximal oxidative ATP synthesis. Acta Physiol (Oxf), 2013. 208(4): p. 376-86.
24. Levenberg, S., et al., Engineering vascularized skeletal muscle tissue. Nat Biotechnol, 2005. 23(7): p. 879-84.
25. Koffler, J., et al., Improved vascular organization enhances functional integration of engineered skeletal muscle grafts. Proc Natl Acad Sci U S A, 2011. 108(36): p. 14789-94.
26. Ye, X., et al., A biodegradable microvessel scaffold as a framework to enable vascular support of engineered tissues. Biomaterials, 2013. 34(38): p. 10007-15.
27. Kock, L.M., et al., Tuning the differentiation of periosteum-derived cartilage using biochemical and mechanical stimulations. Osteoarthritis Cartilage, 2010. 18(11): p. 1528-35.

28. Bancroft, G.N., V.I. Sikavitsas, and A.G. Mikos, Design of a flow perfusion bioreactor system for bone tissue-engineering applications. Tissue Eng, 2003. 9(3): p. 549-54.
29. Janssen, F.W., et al., A perfusion bioreactor system capable of producing clinically relevant volumes of tissue-engineered bone: in vivo bone formation showing proof of concept. Biomaterials, 2006. 27(3): p. 315-23.
30. Du, D., K.S. Furukawa, and T. Ushida, 3D culture of osteoblast-like cells by unidirectional or oscillatory flow for bone tissue engineering. Biotechnol Bioeng, 2009. 102(6): p. 1670-8.
31. Li, J., et al., Effect of oscillating fluid flow stimulation on osteocyte mRNA expression. J Biomech, 2012. 45(2): p. 247-51.
32. Li, P., et al., Fluid flow-induced calcium response in early or late differentiated osteoclasts. Ann Biomed Eng, 2012. 40(9): p. 1874-83.
33. Vaughan, T.J., M.G. Haugh, and L.M. McNamara, A fluid-structure interaction model to characterize bone cell stimulation in parallel-plate flow chamber systems. J R Soc Interface, 2013. 10(81): p. 20120900.
34. Morris, H.L., et al., Mechanisms of fluid-flow-induced matrix production in bone tissue engineering. Proc Inst Mech Eng H, 2010. 224(12): p. 1509-21.
35. Grayson, W.L., et al., Effects of initial seeding density and fluid perfusion rate on formation of tissue-engineered bone. Tissue Eng Part A, 2008. 14(11): p. 1809-20.
36. Fedorovich, N.E., et al., Scaffold porosity and oxygenation of printed hydrogel constructs affect functionality of embedded osteogenic progenitors. Tissue Eng Part A, 2011. 17(19-20): p. 2473-86.
37. Fielding, G. and S. Bose, SiO2 and ZnO dopants in three-dimensionally printed tricalcium phosphate bone tissue engineering scaffolds enhance osteogenesis and angiogenesis in vivo. Acta Biomater, 2013. 9(11): p. 9137-48.
38. Jensen, J., et al., Surface-modified functionalized polycaprolactone scaffolds for bone repair: In vitro and in vivo experiments. J Biomed Mater Res A, 2013.
39. Chung, E.J., et al., Low-pressure foaming: a novel method for the fabrication of porous scaffolds for tissue engineering. Tissue Eng Part C Methods, 2012. 18(2): p. 113-21.
40. Thadavirul, N., P. Pavasant, and P. Supaphol, Development of Polycaprolactone Porous Scaffolds by Combining Solvent Casting, Particulate Leaching, and Polymer Leaching Techniques for Bone Tissue Engineering. J Biomed Mater Res A, 2013.
41. Yan, L.P., et al., Bioactive macro/micro porous silk fibroin/nano-sized calcium phosphate scaffolds with potential for bone-tissue-engineering applications. Nanomedicine (Lond), 2013. 8(3): p. 359-78.
42. Janssen, F.W., et al., Human tissue-engineered bone produced in clinically relevant amounts using a semi-automated perfusion bioreactor system: a preliminary study. J Tissue Eng Regen Med, 2010. 4(1): p. 12-24.
43. Wang, H., et al., Comparative studies on ectopic bone formation in porous hydroxyapatite scaffolds with complementary pore structures. Acta Biomater, 2013. 9(9): p. 8413-21.
44. Ye, X., et al., Preparation and in vitro evaluation of mesoporous hydroxyapatite coated beta-TCP porous scaffolds. Mater Sci Eng C Mater Biol Appl, 2013. 33(8): p. 5001-7.
45. Brocher, J., et al., Inferior ectopic bone formation of mesenchymal stromal cells from adipose tissue compared to bone marrow: Rescue by chondrogenic pre-induction. Stem Cell Res, 2013.
46. Clarke, M.S., et al., A three-dimensional tissue culture model of bone formation utilizing rotational co-culture of human adult osteoblasts and osteoclasts. Acta Biomater, 2013. 9(8): p. 7908-16.
47. Nguyen, L.H., et al., Progenitor cells: role and usage in bone tissue engineering approaches for spinal fusion. Adv Exp Med Biol, 2012. 760: p. 188-210.
48. Rauh, J., et al., Bioreactor systems for bone tissue engineering. Tissue Eng Part B Rev, 2011. 17(4): p. 263-80.
49. Kang, K.S., et al., Effects of combined mechanical stimulation on the proliferation and differentiation of pre-osteoblasts. Exp Mol Med, 2011. 43(6): p. 367-73.
50. Li, S.T., et al., A Novel Axial-Stress Bioreactor System Combined with a Substance Exchanger for Tissue Engineering of 3D Constructs. Tissue Eng Part C Methods, 2013.
51. Diederichs, S., et al., Application of different strain regimes in two-dimensional and three-dimensional adipose tissue-derived stem cell cultures induces osteogenesis: implications for bone tissue engineering. J Biomed Mater Res A, 2010. 94(3): p. 927-36.
52. Mauney, J.R., et al., Mechanical stimulation promotes osteogenic differentiation of human bone marrow stromal cells on 3-D partially demineralized bone scaffolds in vitro. Calcif Tissue Int, 2004. 74(5): p. 458-68.

53. Wang, L., et al., Osteogenesis and angiogenesis of tissue-engineered bone constructed by prevascularized beta-tricalcium phosphate scaffold and mesenchymal stem cells. Biomaterials, 2010. 31(36): p. 9452-61.
54. Thein-Han, W. and H.H. Xu, Prevascularization of a gas-foaming macroporous calcium phosphate cement scaffold via coculture of human umbilical vein endothelial cells and osteoblasts. Tissue Eng Part A, 2013. 19(15-16): p. 1675-85.
55. Pang, H., et al., Prevascularisation with endothelial progenitor cells improved restoration of the architectural and functional properties of newly formed bone for bone reconstruction. Int Orthop, 2013. 37(4): p. 753-9.
56. Braccini, A., et al., Three-dimensional perfusion culture of human bone marrow cells and generation of osteoinductive grafts. Stem Cells, 2005. 23(8): p. 1066-72.
57. Scherberich, A., et al., Three-dimensional perfusion culture of human adipose tissue-derived endothelial and osteoblastic progenitors generates osteogenic constructs with intrinsic vascularization capacity. Stem Cells, 2007. 25(7): p. 1823-9.
58. Scherberich, A., et al., Adipose tissue-derived progenitors for engineering osteogenic and vasculogenic grafts. J Cell Physiol, 2010. 225(2): p. 348-53.
59. Cheng, M., et al., Insulin-like growth factor-I and slow, bi-directional perfusion enhance the formation of tissue-engineered cardiac grafts. Tissue Eng Part A, 2009. 15(3): p. 645-53.
60. Valonen, P.K., et al., In vitro generation of mechanically functional cartilage grafts based on adult human stem cells and 3D-woven poly(epsilon-caprolactone) scaffolds. Biomaterials, 2010. 31(8): p. 2193-200.
61. Wendt, D., et al., Uniform tissues engineered by seeding and culturing cells in 3D scaffolds under perfusion at defined oxygen tensions. Biorheology, 2006. 43(3-4): p. 481-8.
62. Schulz, R.M., et al., Development and validation of a novel bioreactor system for load- and perfusion-controlled tissue engineering of chondrocyte-constructs. Biotechnol Bioeng, 2008. 101(4): p. 714-28.
63. Greene, G.W., et al., Anisotropic dynamic changes in the pore network structure, fluid diffusion and fluid flow in articular cartilage under compression. Biomaterials, 2010. 31(12): p. 3117-28.
64. Klein, T.J., et al., Tissue engineering of articular cartilage with biomimetic zones. Tissue Eng Part B Rev, 2009. 15(2): p. 143-57.
65. Klein, T.J., et al., Strategies for zonal cartilage repair using hydrogels. Macromol Biosci, 2009. 9(11): p. 1049-58.
66. Ng, K.W., G.A. Ateshian, and C.T. Hung, Zonal chondrocytes seeded in a layered agarose hydrogel create engineered cartilage with depth-dependent cellular and mechanical inhomogeneity. Tissue Eng Part A, 2009. 15(9): p. 2315-24.
67. Ng, K.W., et al., A layered agarose approach to fabricate depth-dependent inhomogeneity in chondrocyte-seeded constructs. J Orthop Res, 2005. 23(1): p. 134-41.
68. Zhou, S., Z. Cui, and J.P. Urban, Factors influencing the oxygen concentration gradient from the synovial surface of articular cartilage to the cartilage-bone interface: a modeling study. Arthritis Rheum, 2004. 50(12): p. 3915-24.
69. Zhou, S., Z. Cui, and J.P. Urban, Nutrient gradients in engineered cartilage: metabolic kinetics measurement and mass transfer modeling. Biotechnol Bioeng, 2008. 101(2): p. 408-21.
70. Higuera, G., et al., Quantifying in vitro growth and metabolism kinetics of human mesenchymal stem cells using a mathematical model. Tissue Eng Part A, 2009. 15(9): p. 2653-63.
71. Heywood, H.K., D.L. Bader, and D.A. Lee, Glucose concentration and medium volume influence cell viability and glycosaminoglycan synthesis in chondrocyte-seeded alginate constructs. Tissue Eng, 2006. 12(12): p. 3487-96.
72. Enders, J.T., et al., A model for studying human articular cartilage integration in vitro. J Biomed Mater Res A, 2010. 94(2): p. 509-14.
73. Hunter, C.J. and M.E. Levenston, Maturation and integration of tissue-engineered cartilages within an in vitro defect repair model. Tissue Eng, 2004. 10(5-6): p. 736-46.
74. Tognana, E., et al., Adjacent tissues (cartilage, bone) affect the functional integration of engineered calf cartilage in vitro. Osteoarthritis Cartilage, 2005. 13(2): p. 129-38.
75. Thorpe, S.D., et al., Modulating gradients in regulatory signals within mesenchymal stem cell seeded hydrogels: a novel strategy to engineer zonal articular cartilage. PLoS One, 2013. 8(4): p. e60764.
76. Spitters, T.W., et al., A dual flow bioreactor with controlled mechanical stimulation for cartilage tissue engineering. Tissue Eng Part C Methods, 2013.

77. Cho, H.S., et al., Individual variation in growth factor concentrations in platelet-rich plasma and its influence on human mesenchymal stem cells. Korean J Lab Med, 2011. 31(3): p. 212-8.
78. Kim, H.K., I. Oxendine, and N. Kamiya, High-concentration of BMP2 reduces cell proliferation and increases apoptosis via DKK1 and SOST in human primary periosteal cells. Bone, 2013. 54(1): p. 141-50.
79. Zhang, J. and Y. Li, Fibroblast growth factor 21, the endocrine FGF pathway and novel treatments for metabolic syndrome. Drug Discov Today, 2013.
80. Wimmer, M.A., et al., Tribology approach to the engineering and study of articular cartilage. Tissue Eng, 2004. 10(9-10): p. 1436-45.
81. Salzmann, G.M., et al., Physicobiochemical synergism through gene therapy and functional tissue engineering for in vitro chondrogenesis. Tissue Eng Part A, 2009. 15(9): p. 2513-24.
82. Shahin, K. and P.M. Doran, Tissue engineering of cartilage using a mechanobioreactor exerting simultaneous mechanical shear and compression to simulate the rolling action of articular joints. Biotechnol Bioeng, 2012. 109(4): p. 1060-73.
83. Mastbergen, S.C., D.B. Saris, and F.P. Lafeber, Functional articular cartilage repair: here, near, or is the best approach not yet clear? Nat Rev Rheumatol, 2013. 9(5): p. 277-90.
84. Abadie, E., et al., Recommendations for the use of new methods to assess the efficacy of disease-modifying drugs in the treatment of osteoarthritis. Osteoarthritis Cartilage, 2004. 12(4): p. 263-8.
85. Gibbons, M.C., M.A. Foley, and K.O. Cardinal, Thinking inside the box: keeping tissue-engineered constructs in vitro for use as preclinical models. Tissue Eng Part B Rev, 2013. 19(1): p. 14-30.
86. Cortial, D., et al., Activation by IL-1 of bovine articular chondrocytes in culture within a 3D collagen-based scaffold. An in vitro model to address the effect of compounds with therapeutic potential in osteoarthritis. Osteoarthritis Cartilage, 2006. 14(7): p. 631-40.
87. Popp, J.R., et al., An Instrumented Bioreactor for Mechanical Stimulation and Real-Time, Nondestructive Evaluation of Engineered Cartilage Tissue. Journal of Medical Devices-Transactions of the Asme, 2012. 6(2).
88. Beekhuizen, M., et al., Osteoarthritic synovial tissue inhibition of proteoglycan production in human osteoarthritic knee cartilage: establishment and characterization of a long-term cartilage-synovium coculture. Arthritis Rheum, 2011. 63(7): p. 1918-27.
89. de Vries-van Melle, M.L., et al., An osteochondral culture model to study mechanisms involved in articular cartilage repair. Tissue Eng Part C Methods, 2012. 18(1): p. 45-53.
90. Castaneda, S., et al., Subchondral bone as a key target for osteoarthritis treatment. Biochem Pharmacol, 2011.
91. Findlay, D.M., Vascular pathology and osteoarthritis. Rheumatology (Oxford), 2007. 46(12): p. 1763-8.
92. Shim, V.B., et al., A multiscale framework based on the physiome markup languages for exploring the initiation of osteoarthritis at the bone-cartilage interface. IEEE Trans Biomed Eng, 2011. 58(12): p. 3532-6.
93. Grayson, W.L., et al., Engineering anatomically shaped human bone grafts. Proc Natl Acad Sci U S A, 2010. 107(8): p. 3299-304.
94. Hagenmuller, H., et al., Design and validation of a novel bioreactor principle to combine online micro-computed tomography monitoring and mechanical loading in bone tissue engineering. Rev Sci Instrum, 2010. 81(1): p. 014303.

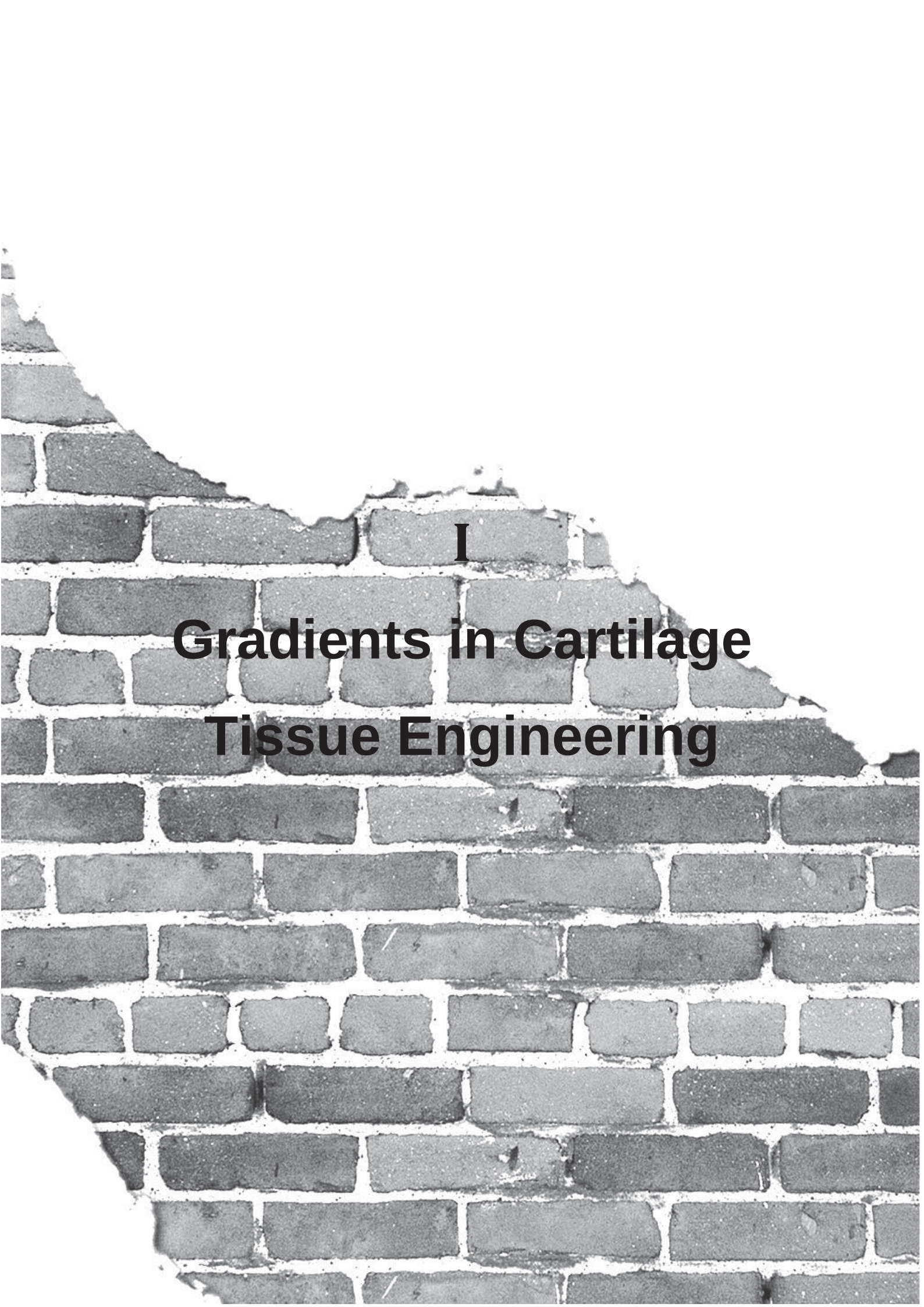

I

Gradients in Cartilage Tissue Engineering

De mens wikt, de natuur beschikt
(Man tries, nature decides)
Albert van Ooyen, 2009

Chapter 3
A dual Flow Bioreactor with Controlled Mechanical Stimulation for Cartilage Tissue Engineering

Tim W.G.M. Spitters, Jeroen C.H. Leijten, Filipe D. Deus, Ines B.F. Costa, Aart A. van Apeldoorn, Clemens A. Blitterswijk, Marcel Karperien

Abstract

In cartilage tissue engineering bioreactors can create a controlled environment to study chondrocyte behavior under mechanical stimulation or produce chondrogenic grafts of clinically relevant size. Here, we present a novel bioreactor, which combines mechanical stimulation with a two compartment system through which nutrients can be supplied solely by diffusion from opposite sides of a tissue engineered construct. This design is based on the hypothesis that creating gradients of nutrients, growth factors and growth factor antagonists can aid in the generation of zonal tissue engineered cartilage. Computational modeling predicted that the design facilitates the creation of a biologically relevant glucose gradient. This was confirmed by quantitative glucose measurements in cartilage explants. In this system it is not only possible to create gradients of nutrients, but also of anabolic or catabolic factors. Therefore, the bioreactor design allows control over nutrient supply and mechanical stimulation useful for *in vitro* generation of cartilage constructs that can be used for the resurfacing of articulated joints or as a model for studying OA disease progression.

Keywords: Dual compartment, bioreactor, gradients, mechanical stimulation, cartilage tissue engineering

Introduction

If left untreated, critical size cartilage defects will lead to degenerative diseases like osteoarthritis (OA) [1, 2]. Clinical techniques such as autologous chondrocyte implantation (ACI), matrix-induced chondrocyte implantation and microfracture have demonstrated to improve healing of critical size defects [3-5]. Although the mentioned techniques have shown positive results, the regenerated cartilaginous tissue is of less quality and neo-tissue integration with existing cartilage remains challenging [6-11]. An alternative strategy is the generation of engineered tissues of clinically relevant amounts [12] or size [13] *in vitro*, which can be used for surface defect repair. For the production of such tissue engineered constructs, bioreactor systems are essential, as they can provide control over the *in vitro* environment and allow for creating optimal conditions for neo-tissue formation [14].

Cartilage can be considered as a simple tissue, as it only contains one cell type and only two major extracellular matrix (ECM) components, proteoglycans and collagen type II. However, it is complex in the sense that it is a layered anisotropic structure which is required to absorb strong mechanical forces, distribute load and lubricate the joint [15, 16]. These functions arise in part from the zonal organization of the tissue. Collagen fibers, responsible for absorbing and distributing the load, are orientated parallel along the synovial surface and become perpendicularly orientated with depth anchoring in the subchondral bone plate. This results in a fountain-like structure with the purpose of distributing load and retrieving the tissue's original shape [17]. Glycosaminoglycans (GAGs) are distributed heterogeneously as the articular surface is almost void of these molecules and their concentration increases with depth [18]. Water is attracted by the negatively charged proteoglycans. Upon deformation, water is expelled from the tissue, which flows back when the tissue relaxes. Although several bioreactor studies have demonstrated the ability to stimulate sulphated glycosaminoglycan (sGAG) deposition, a native distribution of sGAGs in tissue engineered constructs has yet to be obtained. In addition, the fountain-like structure of collagen fibers has so far not been generated *in vitro*. As a result it remains a challenge to engineer cartilaginous tissue *in vitro* that possesses the mechanical properties of native articular cartilage.

Several bioreactors for cartilage tissue engineering have been described. In these systems, nutrients are usually supplied through perfusion, creating shear stress, or

static-like culture as in a culture dish. However, articular cartilage is not subjected to an external active flow and except for the perichondrium it does not receive nutrients from the sides. It is situated between synovial fluid and the subchondral bone plate, which physically separates the articular cartilage from the bone marrow. It has been postulated that cartilage is supplied with nutrients from the subchondral bone and from the synovial fluid [19, 20]. Applying this feature to *in vitro* culture was described by Chang *et al.*, and can be mimicked in transwell cultures. However, no mechanical stimulation can be applied in this system [21]. Chondrocytes in their natural environment are subjected to mechanical load. Therefore, bioreactors for cartilage tissue engineering that are equipped with a compression module more closely resemble cartilage's *in vivo* environment. Load can either be applied by confined [22], sliding [23] or rotating compression [24]. Demarteau *et al.* showed that under perfusion and confined compression sulphated glycosaminoglycan metabolism was increased in cell-loaded PEOT/PBT block co-polymer foam scaffolds, but this design did not originate in an heterogeneous GAG distribution as in native cartilage [22]. Kock *et al.* showed production of collagen II next to a homogenous distribution of sGAGs under sliding indentation, but this did not result in fountain like orientation of the collagen network [23]. The stimulatory effect of compression on the expression of zone specific genes was shown by Grad *et al.* indicating the importance of mechanical stimulation in the regeneration of functional chondrogenic constructs *in vitro* [25, 26].

Here, we describe a bioreactor design in which nutrient supply from both the synovial and subchondral side can be mimicked. This configuration will facilitate formation of gradients of nutrients, growth factors and growth factor antagonists through the cartilage tissue. In addition, the bioreactor is complemented with options for confined compression. We hypothesize that the ability to create gradients of relevant factors combined with confined load will aid in the generation of neo-cartilage better resembling cartilage's natural organization and mechanical properties. In this study we introduce the basic design of a dual compartment, compression equipped novel bioreactor that can be used to engineer cartilage or osteochondral constructs *in vitro*.

Materials and methods

Bioreactor design

The dynamic (Figure 1A) and static (Figure 1B) bioreactors were designed in Solidworks 2009, Edition SP4.1. The stainless steel housing of the dynamic bioreactor was produced by electrical discharge machining (EDM) effectively creating a construct chamber of 1cm^3 (Figure 1A). Removable round polymethylmethacrylaat (PMMA) windows were installed at the front and back side of the housing and allowed for placement of the construct into the chamber. Windows contained a nitrile butadiene rubber (NBR) O-ring ensuring a tight seal preventing leakage and infection.

The complete chamber has a height of 13 mm and a width and depth of 10mm. Explants were placed in a 4mm high insert. Articular cartilage constructs were placed in a square insert (Figure 1C). Osteochondral plugs were placed in a round insert (Figure 1C). The inserts were placed in the reactor chamber on top of a 4,5mm high perforated polycarbonate plate (Figure 1C, bottom) that allowed for diffusion of nutrients and metabolites. The square inserts were combined with a 4,5mm high perforated metal compression insert and the round inserts were combined with a 7mm diameter rounded Teflon head (Figure 1D). Above and below the inserts are medium reservoirs with an approximate volume of 270µL.

Culture medium within the channels of the perforated plates is refreshed by diffusion from the top and bottom medium reservoirs. The medium reservoirs are in turn refreshed by laminar flow of medium from four 10mL syringes (Hamilton, Reno, USA) which are driven by a syringe pump (kdScientific, Holliston, USA).

A stainless steel plunger is attached to the compression insert. This plunger applies top down compressional force on the tissue engineered constructs by means of a separate steppenmotor. The exerted force is continuously monitored by a Futek pressure sensor (model LSB200, type FSH00105) and is configured and controlled via labVIEW software (National Instruments, Austin, USA).

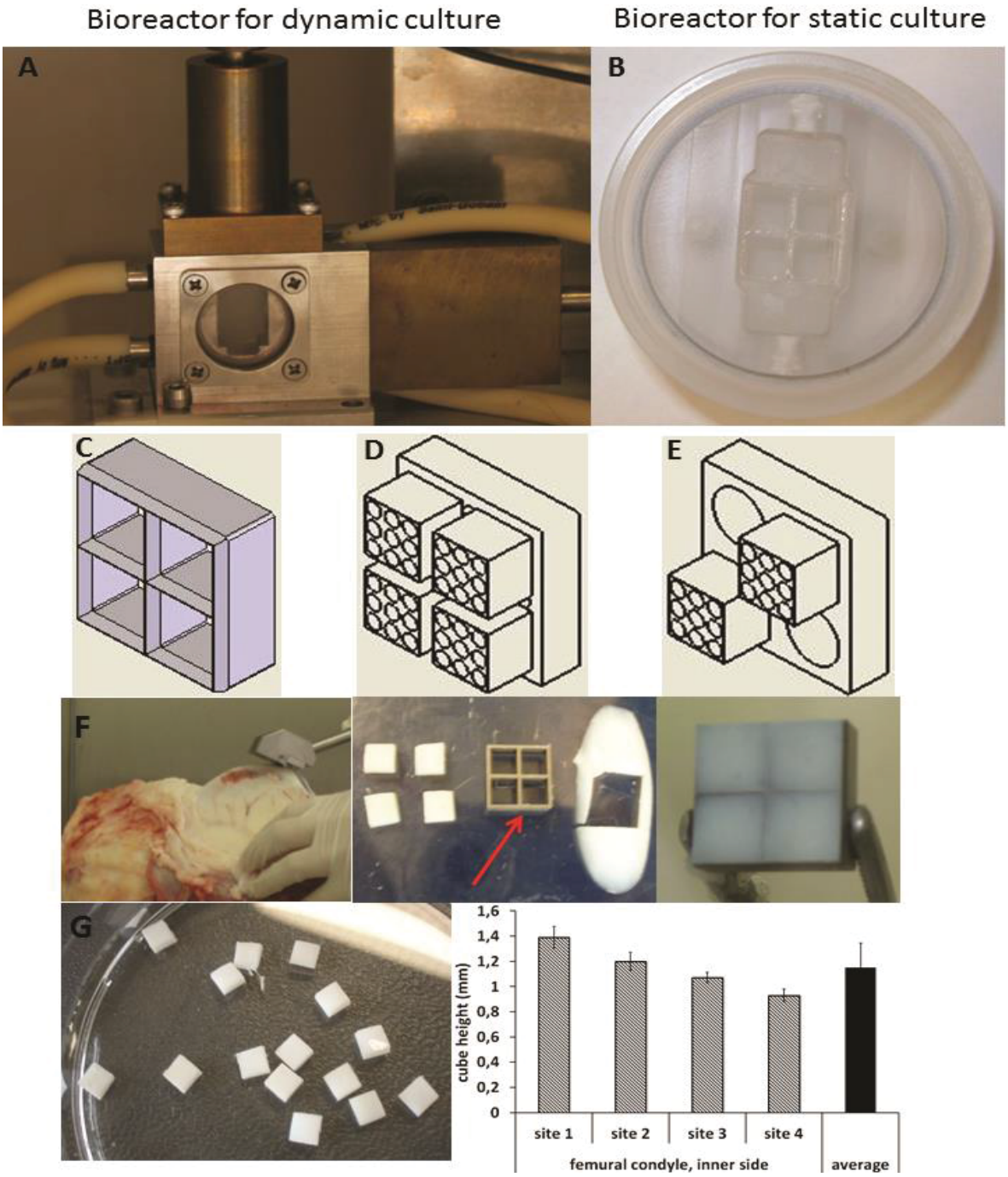

Figure 1: A novel bioreactor for articular cartilage explants. (A) A lateral view of the mechano-dual flow bioreactor. (B) A top view of dual compartment bioreactor for static culture. (C) A knife (top) for explant punch harvesting, an insert to accommodate squared cartilage explants (second from top) for bioreactor culture, an insert to house a cylindrical osteochondral explant (second from bottom) and a perforated plate to support explants (bottom). (D) A 4-module compression insert for the square explant samples (left) and a rounded compression module for the cylindrical explants (right). (E) A plunger to harvest osteochondral explants (top) and a cartilage slicer to slice off full thickness cartilage slices (bottom). (G) Reproducible standardized articular cartilage cubes are obtained using the cartilage slicer in combination with the square knife (left). The inset shows explants in the knife, The height of the cubes depended on the region of harvest. Cubes of one region were equal in height (right).

Additionally, we also designed a polycarbonate static bioreactor, which is identical to the dynamic bioreactor in the sense that samples of the same dimensions can be

inserted and the volume of both medium reservoirs are identical to the dynamic bioreactor (Figure 1B). The inlets were provided with a screw rod to enable the insertion of this bioreactor in a dynamic system. The device was placed in a custom-made four well plate during culture. The static bioreactor lacked modalities for mechanical compression.

Material source

Knees of 10-12 month old calves were collected from the local abattoir. Femoral condyles were sterily exposed by removing the muscles and patella.
For the articular cartilage explant model, cartilage slices were made with a custom made slicer (figure 1E, bottom) to obtain slices of equal height. Since this slicer could not slice through the calcified zone of the cartilage, it was ensured that slices did not contain bone contamination. Cubes of 4.5mm by 4.5mm by 1-1.4mm in height were punched from the slices with a 4-frame stainless steel knife (figure 1C, top) and a puncher. The cubes were then transferred to the polycarbonate insert (Figure 1C, second from the top) and loaded into the bioreactor chamber together with the metal compression and perforated bottom inserts. Explants were always cultured with the synovial side oriented upwards and the subchondral side downwards. The 4 explants were consistent in size. The thickness of the explants depended on the region of harvesting (figure 1F).
For the osteochondral model, 7mm diameter osteochondral plugs were punched from the condyles. These explants were about 6mm in height to assure that cartilage and bone were properly attached after explantation. Afterwards bone was removed to adjust the explant's height to 3mm and they were transferred to a polycarbonate insert (Figure 1C, third from the top) and loaded into the chamber together with the Teflon compression and perforated bottom insert.

Computational modeling

Computational fluid dynamics (CFD) of the fluid flow and diffusion in culture conditions were set-up and solved in the MEMS module (microfluidics – flow with species transport – Incompressible-Navier Stokes) in Comsol Multiphysics version 3.5a software (Comsol, Zoetermeer, The Netherlands).

The Navier-Stokes equation that was solved for incompressible fluid dynamics is as defined by Eq. 1:

$$\rho\frac{\partial u}{\partial t} = -\eta\nabla^2 u + \rho(u\cdot\nabla)u + \nabla p = F \qquad (1)$$

$$\nabla\cdot u = 0$$

where ρ is the fluid density (kg m^{-3}), u is the velocity field (m s^{-1}), t is the time (s), η is the dynamic viscosity of the fluid (kg m^{-1} s^{-1}), ∇ is the del operator, p is the pressure (Pa) and F represents other forces (gravity or centrifugal force), which in this case equals 0. It was assumed that medium could not flow through the cartilage explants. Fluid flow was set at a velocity of 2.65 x 10^{-3} m/s (=0.5 mL/min).

Species transport was coupled to Navier-Stokes. Glucose and oxygen concentrations in the bioreactor chamber were modeled in steady state using the following assumptions: i) walls in different conditions were considered rigid and impermeable, ii) no-slip boundary conditions were applied to surfaces, iii) the glucose diffusion constant ($Đ$) in water was set to 9.0 x 10^{-10} m^2/s and in cartilage was 3.0 x 10^{-10} m^2/s [27, 28]. Initial concentration of glucose in the top compartment was 25 mmol/L, representing high glucose DMEM, and was 0mmol/L in the bottom compartment, representing DMEM without glucose. The glucose consumption rate of chondrocytes in cartilage was considered to be 0.62 x 10^{-10} mol/(m^3*s) (calculated from [29]).

For the computation of oxygen gradients, we corrected for the difference in oxygen consumption in different layers [30]. Therefore, the explants were divided into ten different zones with the top two layers having a different consumption rate compared to the bottom eight layers. The rationale behind this division was described by Heywood *et al.*, where oxygen consumption rates were measured in superficial and deep zone chondrocytes. Superficial zone cells were isolated from the top 20% of the tissue depth and deep zone cells from the remaining 80% [30]. Oxygen diffusion constant ($Đ$) in water was 3.05 x 10^{-9} m^2/s and in cartilage was 2.2 x 10^{-9} m^2/s [31]. Initial oxygen concentration in the top compartment was 0.254mmol/L, representing 100% air saturation, and 0.127mmol/L in the bottom compartment, representing 50% air saturation. The oxygen consumption rate in the top two zones was 3.53 x 10^{-6} mol/(m^3*s) and in the bottom eight zones 6.758 x 10^{-6} mol/(m^3*s). Consumption rates were calculated after Heywood *et al* [30].

It has to be noted that for glucose the consumption rate was assumed homogenous throughout the cartilage. However, as oxygen consumption rates are different in various layers, the same probably also holds for glucose consumption, but this is not supported by literature data.

Explants culture

Static culture

Cartilage explants were transferred to polycarbonate 4-chamber (comparable to figure 1C) inserts and placed in the static bioreactor (figure 1B). A ring was used to separate the two medium compartments and the bioreactor was placed in a custom made 4-well plate. The top and bottom compartments were filled with differentiation medium (DMEM, 100U/mL penicillin/100μg/mL streptomycin, 20mM ascorbic acid, 40μg/mL proline, 100μg/mL sodium pyruvate, 1%Insulin, Transferrin and Selenium premix,). In specific experiments, medium in the top compartment was supplemented with 1,5mg/mL hyaluronidase or collagenase. Volumes used were identical to those used in the dynamic bioreactor. Explants were cultured for 7 days without medium change in a humidified atmosphere at 37ºC.

Dynamic culture

Cartilage explants in the 4-chamber polycarbonate inserts were placed between a compression module insert (figure 1D) and a perforated cover plate in the bioreactor chamber (figure 1A). The reactor was connected to a syringe pump with syringes of 10mL creating two separate medium compartments. Both compartments were filled with 30mL of differentiation medium saturated with 20% air. The concentration of glucose in the top compartment was 25 mmol/L and in the bottom compartment was 0 mmol/L. Medium flow was 0.5 mL/min. The culture was performed for 3 days at 37ºC in an incubation unit, which has been previously described [12].

Viability

Cell viability in the chondral and osteochondral model was assessed after 24 hours of culture with 3 cycles of 1 hour compression followed by 7 hours of rest with a live/dead assay according to manufacturer's protocol (Invitrogen, New York, USA).

Live (green) and dead (red) cells were visualized with a separate FITC and Texas Red filters on a fluorescence microscope (Nikon Eclipse E600, USA) and microphotographs were taken with Qcapture acquisition software. These pictures were overlaid in Photoshop and the areas of dead cells and the total area were analyzed with ImageJ.

Histology

For histology, explants were dissected top to bottom and fixed in 10% buffered formalin at 4^{o}C overnight and decalcified in 12.5% ethylenediaminetetraacetic acid (EDTA) dissolved in H_2O (pH=8.0) at 4^{o}C for 4 weeks. The EDTA solution was refreshed every 7 days. Decalcified explants were embedded in Cryomatrix™ (Thermo Fisher Scientific, USA). The cryomatrix blocks were sectioned in a cryotome into 10 µm thick longitudinal sections and then mounted onto Superfrost® Plus (Thermo Fisher Scientific, USA) glass slides.

Safranin-O staining

Safranin-O staining was performed as previously described [32]. In short, sections were hydrated for 10 minutes in demi water and stained with Fast Green for 3 minutes, rinsed in 1% acetic acid and subsequently stained with Safranin-O for 5 minutes and dehydrated in 96% EtOH, 100% EtOH and xylene for 2 minutes each. Section were dried and mounted with mounting medium.

Picrosirius Red

To visualize collagen fibers sections were stained with the Picrosirius Red staining kit (BioSciences, San Jose, USA) according to the manufacturer's protocol. Shortly, sections were hydrated for 10 minutes in demi water, stained with Haematoxylin for 8 minutes and rinsed in distilled water followed by staining with Picrosirius Red. The stained sections were washed in 70% EtOH for 45 seconds and dehydrated in a graded ethanol series. Collagen fibrils were visualized using a Nikon polarization filter.

Microphotographs were taken using a light microscope (Nikon Eclipse E600, USA) and Qcapture acquisition software. Image analysis was performed using Image J software

Glucose analysis

After 3 days of dynamic culture, explants were physically separated into a top, middle and bottom part, weighed and, after mincing, dissolved in 50µL of PBS. After 3 days of incubation at room temperature the glucose concentration was analyzed using a Vitros DT60II medium analyzer (Ortho-Clinical Diagnostics, USA), assuming that chondrocytes were inactive and not consuming glucose. Ten samples per zone were analyzed and glucose content was corrected for the weight of the cartilage.

Statistical analysis

Statistical analysis was performed using a one-way ANOVA using SPSS version 19 followed by Tukey post-hoc testing. Differences were considered statistically significant at $P<0.05$ and are indicated with an asterisk.

Results

Computational modeling of oxygen and glucose gradients

To predict whether our bioreactor design allowed for the formation of biological relevant gradients of bioactive molecules a computational model was made using glucose and oxygen as representative molecules. We modeled the design with the square cartilage only explants. Additionally, two different types of inlets were modeled, namely a horizontal inlet and a diagonal inlet. The model predicted that with both inlets biological relevant gradients were formed for both oxygen and glucose (Figure 2). Interestingly, the two types of inlets created gradients that differed in concentration difference and distribution. The gradients generated by the horizontal inlets were larger than those created by the diagonal inlets. Thus, by a simple adaptation in the orientation of the inlets the concentration gradients within the explant could be varied in a controlled manner.

Experimental measurement of glucose gradient in explants.

In the square cartilage explants without compression, some cell death was observed at the lateral sites of the explant likely due to sample processing [37, 38]. Hardly any cell death was observed in the top, in the center or bottom of the cartilage explant either in static or dynamic culture. Cartilage explants were successfully cultured for up to 7 days without loss of viability (data not shown). This showed that limitation of diffusion by confinement of the explant was not a limiting factor for chondrocyte survival. To validate the predicted gradient (Figure 3A), cartilage explants were subsequently dynamically cultured for 3 days using medium containing 25 mmol/L of glucose in the top compartment and medium containing 0 mmol/L of glucose in the bottom compartment. Figure 3B shows the glucose concentration in the top, middle and bottom layer of the explants after 3 days of culture. The concentration decreased with depth and the concentration in the top layer significantly differed from the one in the bottom layer. The decrease in concentration from top to bottom suggests that a gradient can be formed during 3 days of culture. However, the experimental values did not fully comply with the computational model. This is most likely due to the fact that the diffusion coefficient of glucose through the tissue, in contrast to the model, is not homogenous, but differs from zone to zone. Another possibility could be that permeability of the tissue is higher than what is assumed in our model [33, 34].

Regardless, we validated the formation of a biologically relevant gradient using the dual flow-approach.

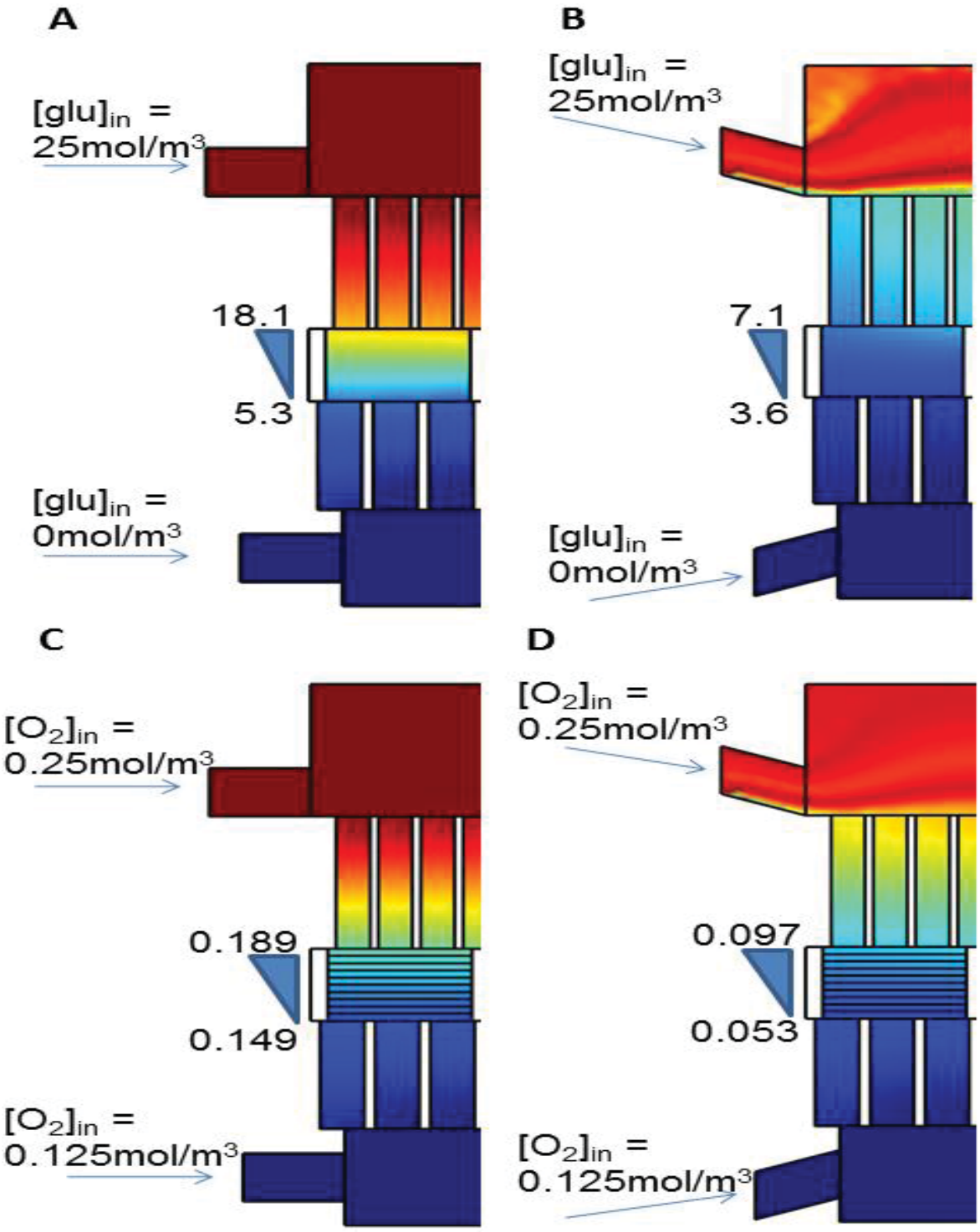

Figure 2: Computational modeling of the glucose and oxygen gradient formation within the explants in the dual flow bioreactor with two different designs. Prediction of the glucose gradient when horizontal (A) or diagonal (B) inlets are used. Prediction of the oxygen gradient when horizontal (C) or diagonal (D) inlets are used. Dark red represents a [glu] of 25mmol/L and dark blue represents a [glu] of 0mmol/L and concentration decreases from dark red via orange and yellow to dark blue. The same holds for the $[O_2]$.

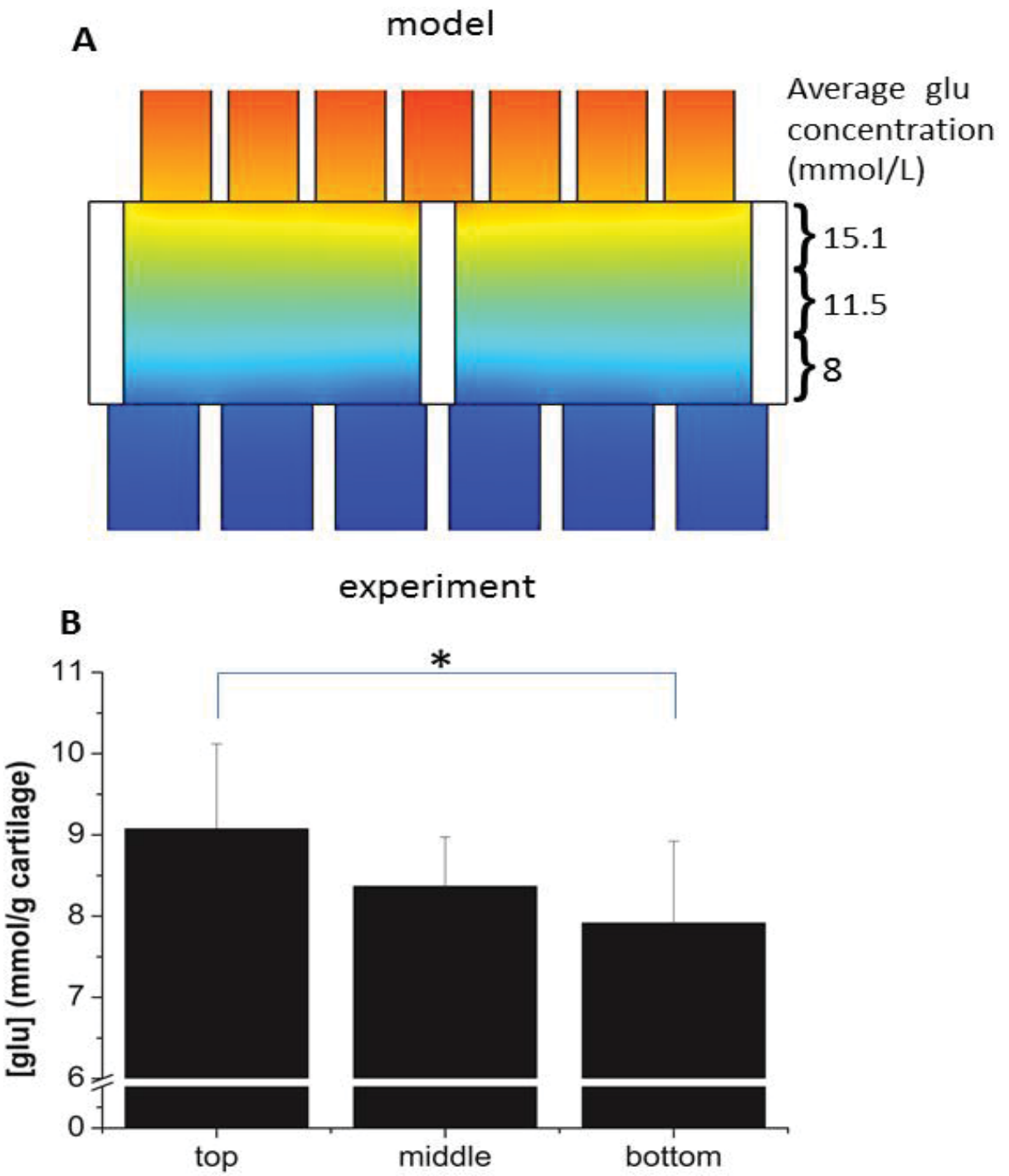

Figure 3: Predicted and experimental glucose concentrations in different zones of articular cartilage. (A) Quantification of the modeled gradients, (B) Quantification of the glucose concentration in different zones after 3 days of dynamic culture (*=P<0,05, n=10). The data is represented as the mean glucose concentration/gram cartilage +/- the standard deviation of the mean.

Gradient formation of cartilage degrading enzymes

We next assessed whether gradients in the explants could also be obtained by larger molecules like proteins. For this we used enzymes involved in cartilage degradation as model compounds. Several enzymes involved in cartilage degradation enter the

cartilage via the synovial fluid [35, 36]. In our models we mimicked this by culturing explants using two physically separated medium compartments that are located on either side. The medium on the synovial side of the explant was supplemented with either hyaluronidase or collagenase. After 7 days of culture, explants were stained for sGAGs and collagens. Safranin-O and Picrosirius Red staining revealed a loss of sulphated GAGs or collagen, respectively, at the synovial side of the cartilage as compared to a freshly isolated sample (Figure 4A and C). Moreover, there was no loss at the lateral sides or the subchondral side indicating the absence of leakage. Quantification of the histological section showed a significant decrease in matrix components (Figure 4B and D). In addition, no matrix degradation on the lateral sides

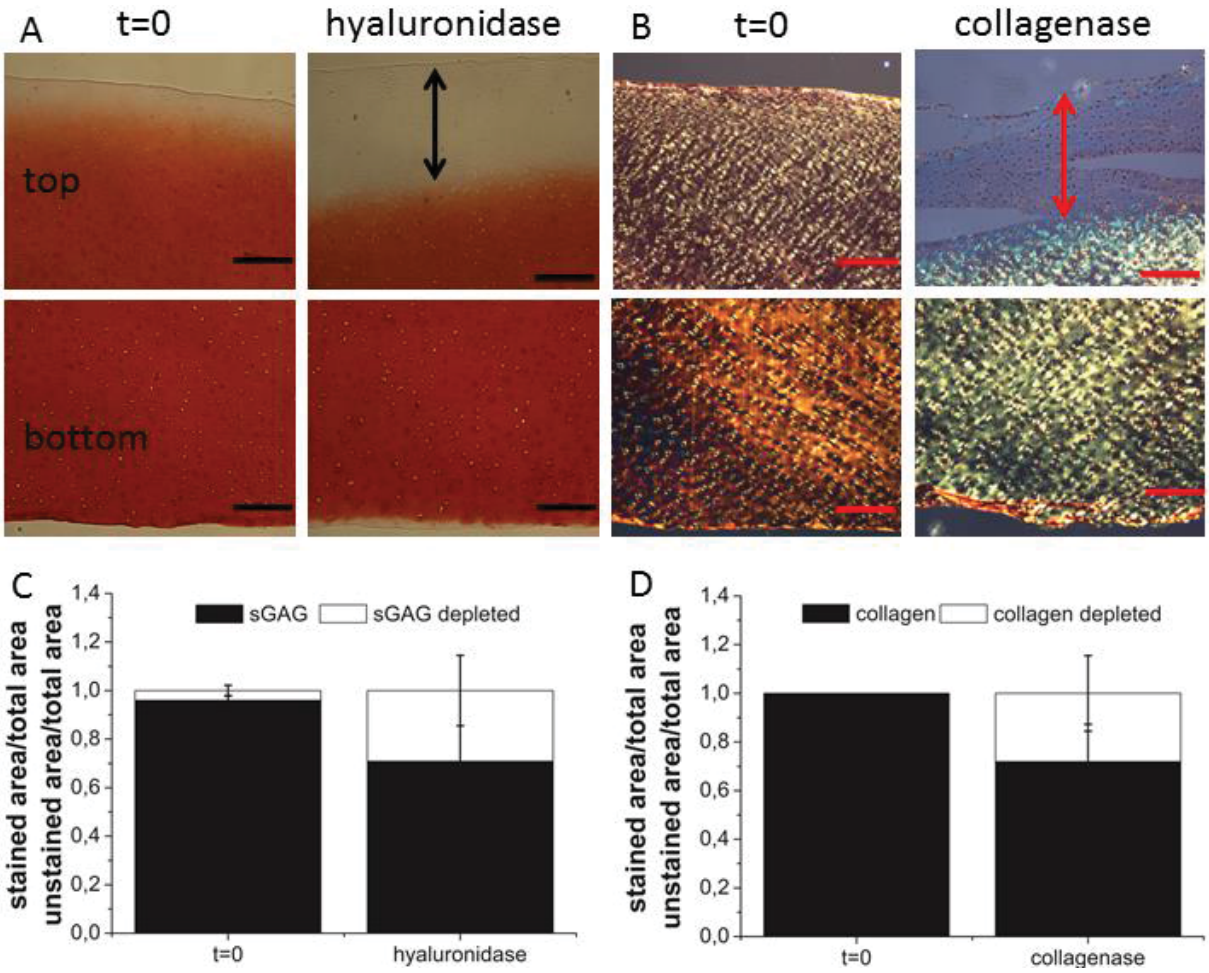

Figure 4: Matrix degradation in a static dual compartment system. (A) Safranin-O stained explants cultured without and with hyaluronidase on top. A representative example out of 9 slides is shown. (B) Picrosirius Red stained explants cultured without and with collagenase on top (polarized light pictures). A representative example out of 7 slides is shown. (C) Quantification of GAG depletion in histological samples (n=9 slides from 4 explants). (D) Quantification of collagen depletion in histological samples (n=7 slides from 4 explants). The upward standard error bars belong to the bars representing the nonstained parts (red) and the downward errors bars to the stained parts (blue). Black and red arrow indicate the depth of matrix degradation.

of the explants could be observed. This strongly suggests that the system does not suffer from leakage ensuring that the additives from the top compartment can only reach the bottom compartment via diffusion through the tissue. Taken together, our bioreactor set up this system allows for the creation of gradients of molecules of choice through cartilage explants.

Compression and cell viability.

We next examined the effect of compression on chondrocyte viability. Square cartilage explants were compressed for 24 hours (1 hour compression, 7 hours rest with 0.25MPa compressive load (~2.5% strain) at 0,33Hz) and a live dead assay was performed. In remarkable contrast to static or dynamic culture of cartilage explants which showed negligible cell death in top and bottom cell layers of the explant (data not shown), considerable cell death was observed after 24 hours at the top and bottom of the explant (Figure 5). Most cell death was noted at the top edges of the explant (Figure 5, arrow), while cell death in the top central part of the explant was reduced (Figure 5, asterisk). Chondrocytes in the middle of the explant did not show evidence of increased cell death. Cell death at the lateral sites was more pronounced than in static or dynamic culture.

We reasoned that the square compression plate which tightly fitted in the cartilage inserts used for explant culture was responsible for the increased cell death in particular at the top lateral sites of the explant. This design was not compatible with tissue expansion and deformation upon compression likely resulting in high stresses at the borders of the explant resulting in the observed cell death. To test this we redesigned the inset for explant culture in the bioreactor and the compression module. The new inset is designed for culturing cylindrical osteochondral plugs with a width of 7mm. The top of the compression module was rounded and made out of Teflon instead of metal. The rounded tip is compatible with tissue deformation at the lateral sides. Like the square cartilage explants, the cylindrical osteochondral plugs could be isolated and cultured in the bioreactor either statically or dynamically without noticeable cell death of chondrocytes anywhere in the explant for up to 2 weeks (data not shown). Interestingly and in marked contrast to the previous design. 24 hours of compression (1 hour compression, 7 hours rest with 0,25MPa compressive load (~2.5% strain) at 0,33Hz) dramatically reduced the thickness of layers with cell death at the top, bottom, and lateral sites of the cartilage explants from on average 8% to

less than 0.2% of total construct height or width (Figure 5). Also, the cell death at the top lateral sites was markedly reduced.

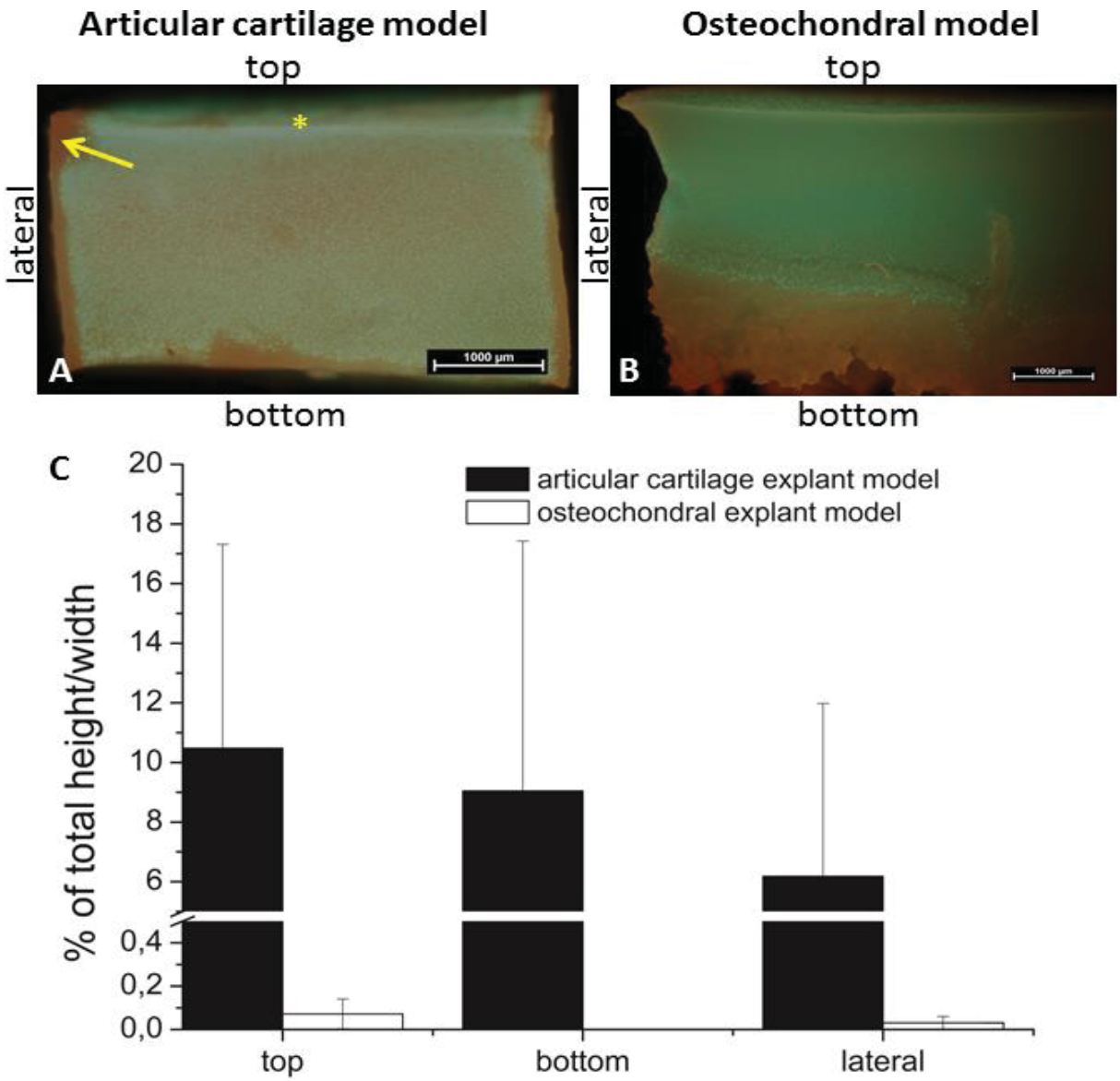

Figure 5: Design validation. Live/dead assays were performed on cartilage explants and on the cartilage in osteochondral explants after compression (24 hours (1 hour compression, 7 hours rest) with 0,25MPa compressive load (~2.5% strain) at 0,33Hz). In both constructs, cell death was only noted in layers at the periphery of the cartilage explants but not in the center. A) Live/dead staining of a compressed cartilage explant. The arrow indicates the area where most cell death is observed. The asterisk indicates the top center of the explant. B) Live/dead staining of a compressed osteochondral explant. The red staining in the lower part of the explant is due to non-specific binding of the ethidium homodimer to mineralized bone matrix. A representative example out of 3 specimens is shown. C) Quantification of A and B. The thickness of the layers was measured and expressed as % +/- standard deviation of the total height at the top or bottom or width of the cartilage explant at the lateral sites. (n=5 (articular cartilage model), n=3 (osteochondral model)).

Discussion

This study reports on the development of a novel bioreactor for cartilage tissue engineering. Our design is unique due to the incorporation of both confined cyclic mechanical loading and nutrient supply via diffusion from both the top and bottom separately. This form of nutrient supply resembles the natural situation in native cartilage. The combination of both features in one bioreactor set up generates a system that more closely resembles the native environment of articular cartilage compared to previously reported bioreactors [22-24]. We successfully succeeded in culturing cartilage explants and osteochondral plugs in our bioreactor for up to 2 weeks in static or dynamic flow without any significant cell death in the cartilage layers. In the square cartilage explants some cell death was noted in peripheral layers at the lateral sites of the construct. These likely arise as a consequence of cutting the cartilage [37, 38]. The data do indicate, however, that in our design diffusion of nutrients, oxygen and waste products from top or bottom is sufficient to keep middle zone chondrocytes alive.

Computational modeling predicted that our design is suitable for the formation of gradients of small molecules like glucose and oxygen in cartilage explants. The formation of these gradients can be manipulated with simple modifications in the design by changing the position of the inlets for dynamic flow or by varying the nutrient concentrations above or below the construct. The design allows to explore the effect of gradients of a wide variety of molecules on healthy and tissue engineered cartilage [31, 39] and to test the hypothesis that gradients of signaling molecules are important for reconstructing cartilage's zonal architecture. For nutrients, like glucose, there is little known how the gradient in articular cartilage looks like. Since middle and deep zone chondrocytes rely on diffusion from either the synovial fluid or subchondral bone compartment it is likely that such gradient exist. In line with this, Heywood et al described differences in metabolic responses in chondrocyte subpopulations, which may be involved in establishing specific zonal phenotypes [31, 40]. We performed two experiments to demonstrate the formation of a gradient in tissue explants cultured in our bioreactor by varying the concentration of compounds in the top and bottom compartment. First we used glucose as a model compound for nutrients and added a concentration of 25mM in the top compartment and 0mM in the bottom compartment. Experimentally, a glucose gradient was

detected across the cartilage explant. This experimental gradient did it did not exactly match the predicted one by computational modeling. In computational models it is assumed that the glucose consumption rate in cartilage is homogenous, however in reality it is not [30]. This is an important notion as it may also hold true for other nutrients as well as growth factors. For secreted soluble growth factors the abundance, their zonal distribution and the affinity and abundance of receptors for these factors will also play an important role. All these parameters, of which many are still unknown will affect the diffusion of growth factors and nutrients and thus the nature of a gradient. Fundamental knowledge regarding diffusion coefficients of many nutrients and growth factors in cartilage is also lacking. All these factors likely contribute to the deviation in our modeled glucose gradient versus the experimentally determined values. It should be noted that the computational modeling and the experimental gradient across a cartilage explant were studied in the absence of mechanical load. Mechanical compression likely affects the diffusion of molecules in the cartilage as it results in water displacement. However, the true nature of the effects remains largely unknown. Our bioreactor can function as an enabling technology that can facilitate in depth studies of these topics.

Besides glucose, two proteins were used to study the formation of a gradient, namely hyaluronidase and collagenase. These enzymes were added in the top compartment mimicking their presence in synovial fluid as in osteoarthritis [35, 36]. By studying the depletion of sGAGs and collagen from the tissue using histological staining the formation of gradients could be easily studied. The results show that the absence of leakage at the lateral sites of the explant and the formation of a top down gradient. They demonstrate the feasibility of our design to build gradients of proteins in explants.

Next to culturing explants in an environment that mimics the natural situation in several key features, we hypothesize that creating gradients in a controlled way can contribute to the development of tissue engineered grafts closely resembling cartilage's natural architecture *in vitro*. Current research focuses on elucidating what concentration ranges stimulate the expression of zone specific proteins like superficial zone protein, cartilage intermediate layer protein and cartilage oligomeric matrix protein [41]. Introduction of gradients may contribute to native matrix distribution in tissue engineered cartilage. In addition, the effect of compression on these developing constructs can be studied in depth using this bioreactor.

Although rotating compression can best simulate the natural load of the joint, it is less controllable than confined or sliding compression, as different forces are exerted on the tissue (indentation and rotation) and each can have different effects on the tissue. Since load is an important feature in cartilage development, we complemented the two compartment bioreactor with confined compression. When confined compression was applied to square cartilage explants using a tight fit perforated metal plate substantial cell death was noted at the periphery of the explant particularly at the top lateral sites. This is likely explained by the design of the bioreactor's insets which did not allow tissue deformation as response upon load resulting in high stresses at the periphery of the construct and consequently cell death. This issue could be easily solved by adapting the inset for explant culture as well as the module used for confined compression. The new inset is compatible with the culture of cylindrical cartilage explants. Cylindrical osteochondral plugs can be easily isolated using standardized orthopedic equipment. For confined compression a rounded module was used made out of teflon. The mechanical properties of teflon better resemble the mechanical properties of native cartilage compared to metal. In addition, the rounded surface of the tip is compatible with tissue expansion at the lateral sites upon load. Using this new design negligible cell death was observed at the periphery of the cartilage explant. Besides the possibility for tissue expansion at the lateral sites upon load, the use of Teflon instead of metal for compression and the cylindrical shape of the explant may also contribute to improved cell survival upon load. Using this new design it will be possible to culture chondral or even osteochondral explants or tissue engineered constructs for prolonged periods of time in the bioreactor and study the role of compression.

Our system is advantageous over current mechano-perfusion bioreactor systems for cartilage tissue engineering as it is not based on convection but on diffusion from physiologically relevant sides. This more closely mimics the natural environment of articular cartilage. This strategy allows us to take advantage of a two compartment system generating biologically relevant gradients in a tissue engineered construct or explant culture. These gradients can be modulated by applying different concentrations of molecules of interest in each compartment. In addition, the gradient can be controlled by changing the orientation of the medium inlets.

By using simple modifications of our system we can include other tissues such as bone and synovial tissue. This would further increase the resemblance of the micro-

environment generated in our system to the native environment of cartilage. Moreover, with the addition of bone by explant culture of osteochondral plugs and/or synovium it is able to function as a more accurate *ex-vivo* model for degenerative cartilage diseases such as osteoarthritis when compared to standard explants cultures. Particularly, it incorporates the idea that osteoarthritis is not a single tissue disease but a multifactorial joint disease [42-45].

In summary, we have developed a unique bioreactor system that captures two key features of cartilage's natural environment. It has the ability to create gradients of nutrients and growth factors and apply confined cyclic compression. We believe that this will aid in development of an *in vitro* environment for cartilage homeostasis facilitating neo-cartilage formation. Therefore, our bioreactor holds the potential to grant deeper insight in fundamental concepts of cartilage biology, model degenerative cartilage diseases like osteoarthritis and stimulate the development of novel therapeutics for such diseases.

References

1. Linden, B., *Osteochondritis dissecans of the femoral condyles: a long-term follow-up study.* J Bone Joint Surg Am, 1977. **59**(6): p. 769-76.
2. Messner, K. and J. Gillquist, *Cartilage repair. A critical review.* Acta Orthop Scand, 1996. **67**(5): p. 523-9.
3. Kon, E., et al., *Articular Cartilage Treatment in High-Level Male Soccer Players: A Prospective Comparative Study of Arthroscopic Second-Generation Autologous Chondrocyte Implantation Versus Microfracture.* Am J Sports Med, 2011.
4. Steadman, J.R., W.G. Rodkey, and K.K. Briggs, *Microfracture to treat full-thickness chondral defects: surgical technique, rehabilitation, and outcomes.* J Knee Surg, 2002. **15**(3): p. 170-6.
5. Bartlett, W., et al., *Autologous chondrocyte implantation versus matrix-induced autologous chondrocyte implantation for osteochondral defects of the knee: a prospective, randomised study.* J Bone Joint Surg Br, 2005. **87**(5): p. 640-5.
6. Knutsen, G., et al., *Autologous chondrocyte implantation compared with microfracture in the knee. A randomized trial.* J Bone Joint Surg Am, 2004. **86-A**(3): p. 455-64.
7. Knutsen, G., et al., *A randomized trial comparing autologous chondrocyte implantation with microfracture. Findings at five years.* J Bone Joint Surg Am, 2007. **89**(10): p. 2105-12.
8. Kreuz, P.C., et al., *Is microfracture of chondral defects in the knee associated with different results in patients aged 40 years or younger?* Arthroscopy, 2006. **22**(11): p. 1180-6.
9. Kreuz, P.C., et al., *Results after microfracture of full-thickness chondral defects in different compartments in the knee.* Osteoarthritis Cartilage, 2006. **14**(11): p. 1119-25.
10. Mithoefer, K., et al., *The microfracture technique for the treatment of articular cartilage lesions in the knee. A prospective cohort study.* J Bone Joint Surg Am, 2005. **87**(9): p. 1911-20.
11. Mithoefer, K., et al., *High-impact athletics after knee articular cartilage repair: a prospective evaluation of the microfracture technique.* Am J Sports Med, 2006. **34**(9): p. 1413-8.
12. Janssen, F.W., et al., *A perfusion bioreactor system capable of producing clinically relevant volumes of tissue-engineered bone: in vivo bone formation showing proof of concept.* Biomaterials, 2006. **27**(3): p. 315-23.
13. Santoro, R., et al., *Bioreactor based engineering of large-scale human cartilage grafts for joint resurfacing.* Biomaterials, 2010. **31**(34): p. 8946-52.
14. Martin, I., D. Wendt, and M. Heberer, *The role of bioreactors in tissue engineering.* Trends Biotechnol, 2004. **22**(2): p. 80-6.
15. Huang, C.Y., et al., *Experimental verification of the roles of intrinsic matrix viscoelasticity and tension-compression nonlinearity in the biphasic response of cartilage.* J Biomech Eng, 2003. **125**(1): p. 84-93.
16. Schumacher, B.L., et al., *A novel proteoglycan synthesized and secreted by chondrocytes of the superficial zone of articular cartilage.* Arch Biochem Biophys, 1994. **311**(1): p. 144-52.
17. Shirazi, R., A. Shirazi-Adl, and M. Hurtig, *Role of cartilage collagen fibrils networks in knee joint biomechanics under compression.* J Biomech, 2008. **41**(16): p. 3340-8.
18. Klein, T.J., et al., *Tissue engineering of articular cartilage with biomimetic zones.* Tissue Eng Part B Rev, 2009. **15**(2): p. 143-57.
19. Imhof, H., et al., *Subchondral bone and cartilage disease: a rediscovered functional unit.* Invest Radiol, 2000. **35**(10): p. 581-8.
20. Pan, J., et al., *In situ measurement of transport between subchondral bone and articular cartilage.* J Orthop Res, 2009. **27**(10): p. 1347-52.
21. Chang, C.H., et al., *Cartilage tissue engineering on the surface of a novel gelatin-calcium-phosphate biphasic scaffold in a double-chamber bioreactor.* J Biomed Mater Res B Appl Biomater, 2004. **71**(2): p. 313-21.
22. Demarteau, O., et al., *Development and validation of a bioreactor for physical stimulation of engineered cartilage.* Biorheology, 2003. **40**(1-3): p. 331-6.
23. Kock, L.M., et al., *Tuning the differentiation of periosteum-derived cartilage using biochemical and mechanical stimulations.* Osteoarthritis Cartilage, 2010. **18**(11): p. 1528-35.
24. Wimmer, M.A., et al., *Tribology approach to the engineering and study of articular cartilage.* Tissue Eng, 2004. **10**(9-10): p. 1436-45.
25. Grad, S., et al., *Effects of simple and complex motion patterns on gene expression of chondrocytes seeded in 3D scaffolds.* Tissue Eng, 2006. **12**(11): p. 3171-9.

26. Grad, S., et al., *Chondrocyte gene expression under applied surface motion.* Biorheology, 2006. **43**(3-4): p. 259-69.
27. Allhands, R.V., P.A. Torzilli, and F.A. Kallfelz, *Measurement of diffusion of uncharged molecules in articular cartilage.* Cornell Vet, 1984. **74**(2): p. 111-23.
28. Maroudas, A., *Distribution and diffusion of solutes in articular cartilage.* Biophys J, 1970. **10**(5): p. 365-79.
29. Zhou, S., Z. Cui, and J.P. Urban, *Nutrient gradients in engineered cartilage: metabolic kinetics measurement and mass transfer modeling.* Biotechnol Bioeng, 2008. **101**(2): p. 408-21.
30. Heywood, H.K., M.M. Knight, and D.A. Lee, *Both superficial and deep zone articular chondrocyte subpopulations exhibit the Crabtree effect but have different basal oxygen consumption rates.* J Cell Physiol, 2010. **223**(3): p. 630-9.
31. Malda, J., et al., *Oxygen gradients in tissue-engineered PEGT/PBT cartilaginous constructs: measurement and modeling.* Biotechnol Bioeng, 2004. **86**(1): p. 9-18.
32. Moreira Teixeira, L.S., et al., *High throughput generated micro-aggregates of chondrocytes stimulate cartilage formation in vitro and in vivo.* Eur Cell Mater, 2012. **23**: p. 387-99.
33. Korhonen, R.K., et al., *Fibril reinforced poroelastic model predicts specifically mechanical behavior of normal, proteoglycan depleted and collagen degraded articular cartilage.* J Biomech, 2003. **36**(9): p. 1373-9.
34. Seifzadeh, A., D.C. Oguamanam, and M. Papini, *Evaluation of the constitutive properties of native, tissue engineered, and degenerated articular cartilage.* Clin Biomech (Bristol, Avon), 2012. **27**(8): p. 852-8.
35. Fernandes, J.C., J. Martel-Pelletier, and J.P. Pelletier, *The role of cytokines in osteoarthritis pathophysiology.* Biorheology, 2002. **39**(1-2): p. 237-46.
36. Kapoor, M., et al., *Role of proinflammatory cytokines in the pathophysiology of osteoarthritis.* Nat Rev Rheumatol, 2011. **7**(1): p. 33-42.
37. Amin, A.K., et al., *Chondrocyte death in mechanically injured articular cartilage--the influence of extracellular calcium.* J Orthop Res, 2009. **27**(6): p. 778-84.
38. Secretan, C., K.M. Bagnall, and N.M. Jomha, *Effects of introducing cultured human chondrocytes into a human articular cartilage explant model.* Cell Tissue Res, 2010. **339**(2): p. 421-7.
39. Zhou, S., Z. Cui, and J.P. Urban, *Factors influencing the oxygen concentration gradient from the synovial surface of articular cartilage to the cartilage-bone interface: a modeling study.* Arthritis Rheum, 2004. **50**(12): p. 3915-24.
40. Heywood, H.K., D.L. Bader, and D.A. Lee, *Glucose concentration and medium volume influence cell viability and glycosaminoglycan synthesis in chondrocyte-seeded alginate constructs.* Tissue Eng, 2006. **12**(12): p. 3487-96.
41. Coates, E.E. and J.P. Fisher, *Phenotypic variations in chondrocyte subpopulations and their response to in vitro culture and external stimuli.* Ann Biomed Eng, 2010. **38**(11): p. 3371-88.
42. Castaneda, S., et al., *Subchondral bone as a key target for osteoarthritis treatment.* Biochem Pharmacol, 2011.
43. Findlay, D.M., *Vascular pathology and osteoarthritis.* Rheumatology (Oxford), 2007. **46**(12): p. 1763-8.
44. Shim, V., et al., *A multiscale framework based on the Physiome markup languages for exploring the initiation of osteoarthritis at the bone cartilage interface.* IEEE Trans Biomed Eng, 2011.
45. Aspden, R.M., *Osteoarthritis: a problem of growth not decay?* Rheumatology (Oxford), 2008. **47**(10): p. 1452-60.

3

Chapter 4
Creating growth factor gradients to control cell behavior in three dimensional constructs

Tim W.G.M. Spitters, Jacqueline R.M. Plass, Marcel Karperien

Abstract

Growth factor gradients play an important role in cell guidance during embryonic development, but also have a pivotal role in tissue homeostasis. Therefore, we hypothesized that growth factor and growth factor antagonist gradients can create an environment for hydrogel-embedded expanded cells to guide cell fate in a tissue-engineered construct. To test this hypothesis, gradients were established by culturing C_2C_{12}-laden agarose cubes in a dual compartment bioreactor in which the top and the bottom of the constructs are exposed to distinct media. When Wnt3A was present in the top compartment and its antagonist DKK present in the bottom compartment, a gradient of active Wnt signaling from top to bottom of the construct was established as revealed by measuring a Wnt-response luciferase reporter assay. Similar findings were made using BMP2 and its antagonist Grem-1. When MSC-laden agarose cubes were cultured between chondrogenic and osteogenic differentiation medium, zones of glycosaminoglycan and mineral deposition overlapped. Future research will focus on determining the formation of complex growth factor gradients to create the optimal environment for the production of osteochondral tissue engineered constructs in this dual compartment bioreactor. In summary, we herein show proof-of principle of a dual compartment system for the study of the effect of growth factor gradients on tissue engineered constructs consisting of multiple tissues. Furthermore, we provide evidence that opposing gradients of agonists and antagonists rather than gradients of individual factors are needed to effectively establish differential cell responses in a three-dimensional tissue engineered construct.

Keywords: growth factor, bioreactor, cartilage, tissue engineering, antagonist

Chapter four: Growth Factor Gradients

Introduction

Concentration differences of biomolecules play an important in biological processes such as proliferation, differentiation and maintaining tissue homeostasis [1-3]. During embryonic development gradients of Wnt regulate the formation of the anterior-posterior axis as reviewed by Arkel *et al* [4]. Likewise, ecto-, endo- and mesoderm are formed by complex morphogen gradients [5]. Following this, gradients of morphogens direct individual cells of the germ layers towards the appropriate tissue during organogenesis [6-8].

During early stages of development, at which extracellular matrix (ECM) is not yet being produced, these gradients are formed by free diffusion [9]. However, once the ECM becomes structurally denser it also plays an important role in the creation of gradients. Heparan sulphate is described as an actuator in the control of morphogen diffusion and signaling as reviewed by Yan *et al* [10]. One of the morphogen families, the fibroblast growth factor (FGF) family, specifically interacts with heparan sulphate [11]. FGFs are involved in regulation of cell migration and proliferation and therefore heparan sulphate mediated gradients can aid in the spatial organization of cellular proliferation and migration [12].

Three well-described morphogens that form gradients during embryogenesis are Wnt, BMP and Hedgehog [13]. Members of the Hedgehog family have been shown to be involved in the chondrogenic differentiation of chondrocyte precursor cells and promote chondrocyte hypertrophy [14-16]. TGF-β isoforms have been tied to articular cartilage formation [17-19] and BMPs are known to induce osteogenesis as well as chondrogenesis [20]. The activity of these morphogens is counteracted by antagonists, such as Gremlin (Grem), Frizzled (FRZ) and Dickkopf-1 (DKK1). Opposing expression of agonists and antagonists help in establishing gradients of morphogen activity. In articular cartilage the activity of BMP en WNT is counteracted by - among others - GREM1, FRZ and DKK1 [21, 22]. These antagonists play an important role in establishing articular cartilage homeostasis by preventing chondrocyte hypertrophy.

Attempts to produce articular cartilage *in vitro* have shown the possibilities of using expanded cells to engineer cartilaginous tissue [23, 24]. However, many attempts lead to fibrocartilage, which illustrates that the reproducibility of engineering cartilage *in vitro* remains a challenge [25]. Mesenchymal stem cells seem to behave as growth

plate chondrocytes rather than mature articular chondrocytes and isolated articular chondrocytes have a tendency to undergo hypertrophic differentiation in *in vitro* cartilage cultures. This is unlike healthy articular cartilage which is largely protected from undergoing hypertrophic differentiation [26]. So, continuing on the fundaments of developmental biology, recreating an environment that supports the spatial distribution of morphogens could lead to self-organizing signals in a tissue-engineered construct. Initially, free diffusion would create gradients of growth factors present in the medium, where - in time - ECM components would aid in the preservation and reorganization of these gradients.

Since creating these gradients in a reproducible manner is a challenge, a previously reported bioreactor system will be used to aid in this matter [27]. In the present work, gradients of Wnt, BMP and TGF have been tested in their ability to induce spatial changes in protein expression and matrix production.

Materials and Methods

Growth factors (antagonists)

Wnt3A, DKK1, BMP2, GREM1 and TGFβ3 were purchased from R&D Systems. Final concentrations in the medium were 1000ng/mL for Wnt3A and DKK1, 200ng/mL BMP and Grem and 100ng/mL for TGFβ3.

Cell sources

C_2C_{12} cells were cultured up to 90% confluency in Dulbecco's Modified Eagle's Medium (DMEM, Gibco) supplemented with 10% fetal bovine serum (FBS, Lonza) and 100U/mL penicillin/100µg/mL streptomycin (pen/strep, Gibco) before transfection or stimulation.

C_2C_{12} cells stably transfected with a BRE-LUC (C_2C_{12} BRE-LUC) plasmid [28] were cultured upto 90% confluency in DMEM supplemented with 10% FBS, pen/strep and 700mg/mL geniticin (G418, Gibco) for selection before stimulation.

Bovine chondrocytes (bCHs) were obtained by harvesting articular cartilage from both condyles, mincing the tissue and incubating it in collagenase type II (150U/mL, Worthington) at 37°C for 18 hours. After digestion, the collagenase mixture was filtered through a 20µm cell strainer and the filtrate was centrifuged at 300g for 10 minutes at 4°C. Then, the pellet was washed in PBS and centrifuged again. This process was repeated once more before cells were resuspended in DMEM containing pen/strep, 20mM ascorbic acid (asap, Sigma), 40µg/mL proline (Sigma), 100µg/mL sodium pyruvate (Sigma) and 1% Insulin Transferrin and Selenium premix (ITS, Gibco) and used immediately after isolation.

Goat bone marrow-derived stromal cells (gMSCs) were isolated by adherence and frozen after two passages on tissue culture plastic. After thawing, cells were cultured up to 90% confluency in αMEM (Gibco) supplemented with 15% FBS, pen/strep, 0.2mM asap, 2mM L-glutamine (L-glut, Gibco), 1ng/mL basic fibroblast growth factor (bFGF, Instruchemie) before stimulation.

Before stimulation, cell constructs were prepared by combining 40µL cell suspension with 40µL 1% agarose solution, resulting in cells embedded in 0.5% agarose, and pipetted in customized polycarbonate four-chamber inserts. After solidifying, the inserts were placed in a previously described dual compartment bioreactor (Spitters,

2013). The top compartment was filled with 2mL medium and the bottom compartment with 10mL medium. C_2C_{12} cells were cultured in DMEM supplemented with 10% FBS and pen/strep. C_2C_{12} BRE-LUC cells were cultured in DMEM supplemented with 10% FBS, pen/strep and G418. bCH differentiation medium consisted of DMEM supplemented with pen/strep, asap, proline, sodium pyruvate, ITS and 10^{-7}M dexamethasone (dex). gMSCs were cultured in medium supplemented with 15% FBS, pen/strep, asap, L-glut and beta-glycerol phosphate (BGP).

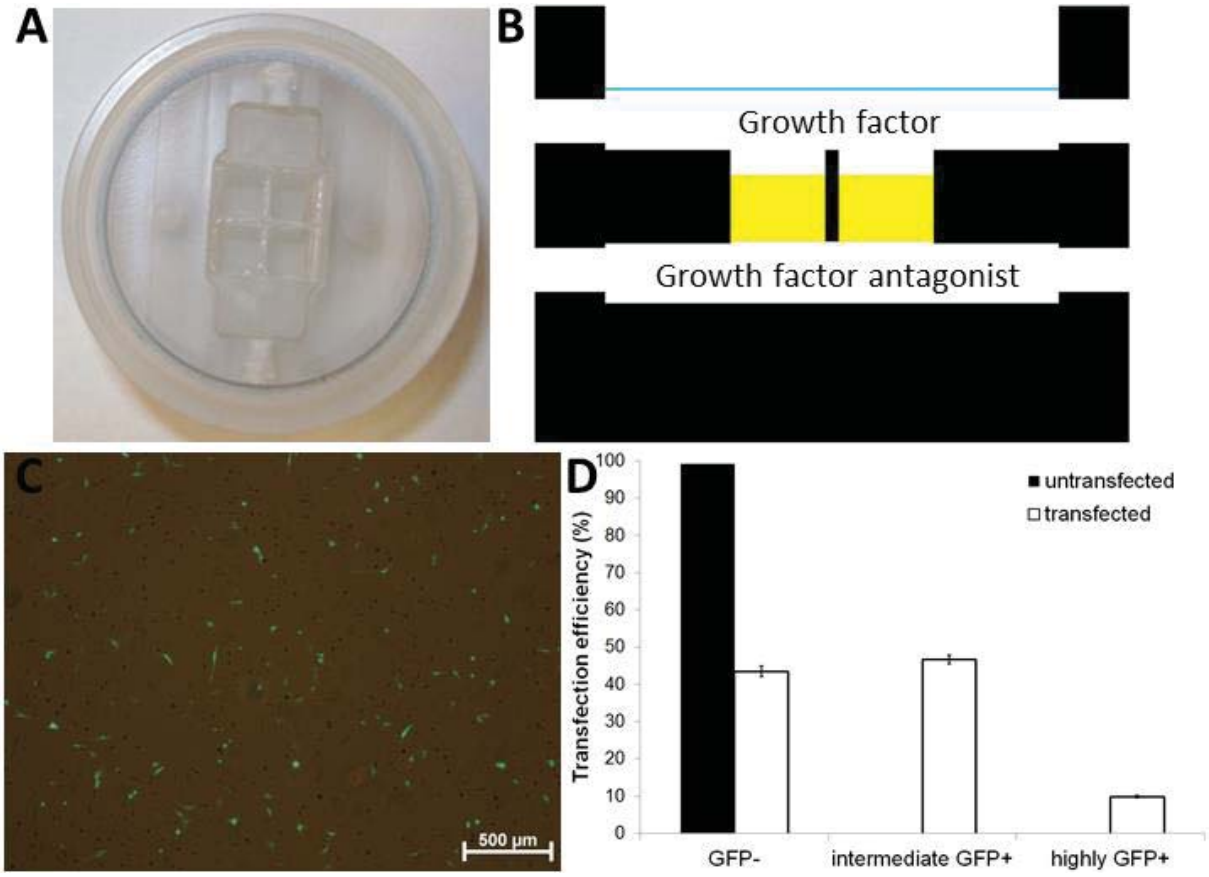

Figure 1: (A) A static dual compartment bioreactor, (B) schematic representation of a dual bioreactor depicting in which compartment the growth factors and their antagonists where present (also see Table 1). Transfection efficiency was determined by transfecting C_2C_{12} cells with a plasmid containing a GFP reporter and culturing the cells for the same time period as the experimental conditions. (C) Brightfield/FITC overlay showing GFP distribution in transfected C_2C_{12} cells. (D) Quantification of C_2C_{12} transfected cells by fluorescent automated cell sorting (FACS).

Cell concentration, culture period and growth factor concentrations are indicated in Table 1. Figure 1A and 1B show a photographic representation of the bioreactor and a schematic overview where constructs and growth factors where situated. After culture, constructs for biochemical analysis were divided in a top, middle and bottom zone.

Transfection

After trypsinization, C_2C_{12} cells were replated at a density of 4400 cells/cm^2 in a T175 flask in 35mL of medium and left to adhere overnight. To measure Wnt signaling, 1µg TOPFLASH plasmid was transfected using lipofectamine L-2000 (Invitrogen) according to the manufacturer's protocol. The plasmid/lipofectamine solution was added to the cells and transfection was continued overnight. After transfection, the cells were trypsinized and embedded in agarose and left to adapt to the new environment overnight before stimulation. To check the transfection efficiency, C_2C_{12} cells were transfected with a plasmid encoding green fluorescent protein (GFP) according to the protocol described above. Figure 1C shows an overlay of bright field and GFP indicating the GFP positive cells.

Fluorescence Activated Cell Sorting (FACS)

Flow cytometry analysis of transfected cells was performed using a FACSCalibur with CellQuest Software (BD Immunocytometry Systems, Heidelberg, Germany). The percentage of cells showing positive expression of GFP fluorescence in FL-1 (n = 5) was determined using untransfected cells as a control.

FACS analysis showed that about 60% of the cells was GFP positive of which 10% was strongly positive and 50% moderately. This quantity was consistent among flasks (Figure 1D).

Biochemical analysis

Luciferase (LUC) activity

After the culture period, transfected cells were frozen in Glo lysis buffer (Promega, USA) overnight. Next 50µL lysis buffer was transferred to a white 96-well plate and 50µL luciferase substrate was added and luminescence was read immediately at a Victor. LUC activity was corrected for DNA quantity.

Alkaline phosphatase (ALP) activity

Before analysis, constructs were incubated in an ALP lysis buffer (content) and went through a freeze/thaw cycle. ALP content was measured using a CDP star kit. For this purpose, 10µL sample was added to a well of a white 96-well plate and 40µL substrate was added. After 15 minutes incubation, luminescence was read using a spectrophotometer LS50B (Perkin Elmer) using Wallac software. ALP activity was corrected for DNA content.

Glycosaminoglycan (GAG) content

Before analysis, constructs were incubated in a proteinase K (PK) digestion buffer (1ug/mL PK, 1µg/mL pepstatin A, 18.5µg/mL iodoacetamide, Sigma) and went through a freeze/thaw cycle. GAG content was measured with a 1,9-Dimethyl-Methylene Blue (DMMB) assay. Therefore, 25µL sample was added to a transparent 96-well plate and 5µL 2.3M NaCl solution was added. Then 150µL DMMB solution was added and absorbance was read at a plate reader. GAG content was quantified with a chondroitin standard curve and corrected for DNA content.

DNA quantification

DNA content was quantified with a CyQuant kit (Invitrogen, USA) according to manufacturer's protocol and fluorescence was measured at 480nm using a spectrophotometer LS50B (Perkin Elmer). DNA concentrations were calculated from a λ DNA standard curve.

Histology

For histology, constructs were removed from the insert and fixated in 10% buffered formalin at 4^{o}C overnight. Subsequently, constructs were embedded in Cryomatrix^{TM} (Thermo Fisher Scientific, USA). The cryomatrix blocks were sectioned in a cryotome (Shendon) into 10 µm thick longitudinal sections and then mounted onto Superfrost® Plus (Thermo Fisher Scientific, USA) glass slides. Before staining, slides were warmed up and washed in demi water for 10 minutes.

Alcian Blue staining

Sections were stained with an Alcian Blue solution (pH 1) for 30 minutes. Excess staining solution was washed away in running tap water and sections were dehydrated in 96% EtOH, 100% EtOH and xylene for 2 minutes each. Section were air dried and mounted with mounting medium.

Combined Alkaline Phosphatase and Safranin-O staining

Powder of one Fast Blue RR Salt capsule was dissolved in 48mL dH_2O. Then, 2mL naphtol AS-MX Phosphate Alkaline Solution was added and the solution was homogenized (Sigma, USA). Subsequently, sections were submerged in this solution and incubated for 30 minutes. Afterwards the excess staining solution was washed away in demi water and sections were stained with a 6% Safranin-O for 1 minute and dehydrated in 96% EtOH, 100% EtOH and xylene for 2 minutes each. Section were air dried and mounted with mounting medium.

Results

Gradients of Dickkopf-1 and Gremlin-1 counteract gradients of Wnt3A and BMP2, respectively

C_2C_{12} cells were transfected with a plasmid containing a TCF/LEF-responsive promoter immediately upstream of a luciferase reporter. A gradient of Wnt3A was created from top to bottom through a cell-laden agarose construct opposing a gradient of Dickkopf-1 (DKK1). When the Wnt3A gradient was counteracted with DKK1, luciferase activity gradually and significantly decreased from top to bottom. Without an opposing DKK1 gradient, luciferase activity in top and bottom compartments was not different while activity in the middle zone was decreased. A similar pattern was observed in constructs without stimulation (Figure 2A). Interestingly, when DKK1 was not added to the bottom compartment the luciferase activity in the bottom zone tended to increase compared to the middle zone. The culture plate is produced from polycarbonate which is impermeable for oxygen, which only is supplied from the top. Therefore, the oxygen concentration is expected to decrease with increasing depth. Thus, a hypoxia-induced response of the Wnt pathway could be responsible for the increased luciferase activity in the bottom zone [29, 30].

C_2C_{12} cells transfected with a plasmid containing BMP-responsive element upstream of a luciferase reporter gene and were cultured in opposing Gremlin-1 (GREM1) and BMP2 gradients. Luciferase activity was significantly higher when the construct was stimulated with BMP in the bottom compartment compared to the unstimulated condition. Like with Wnt3A stimulation, stimulation with BMP only resulted in atypical U-shaped activity profile with lowest activity in the middle zone of the construct. This is likely due to decreased metabolic activity of cells in this zone as a consequence of nutrient or oxygen deprivation. Interestingly, in the presence of GREM1, the U-shaped activation pattern changed in a gradient of BMP activity with highest reporter activity in zones of the construct nearest the source of BMP and lowest activity in the zone closest to the source of GREM1.

Bioactivity of growth factors and growth factor antagonists was checked in conventional two-dimensional culture conditions. This showed bioactivity of all proteins (data not shown).

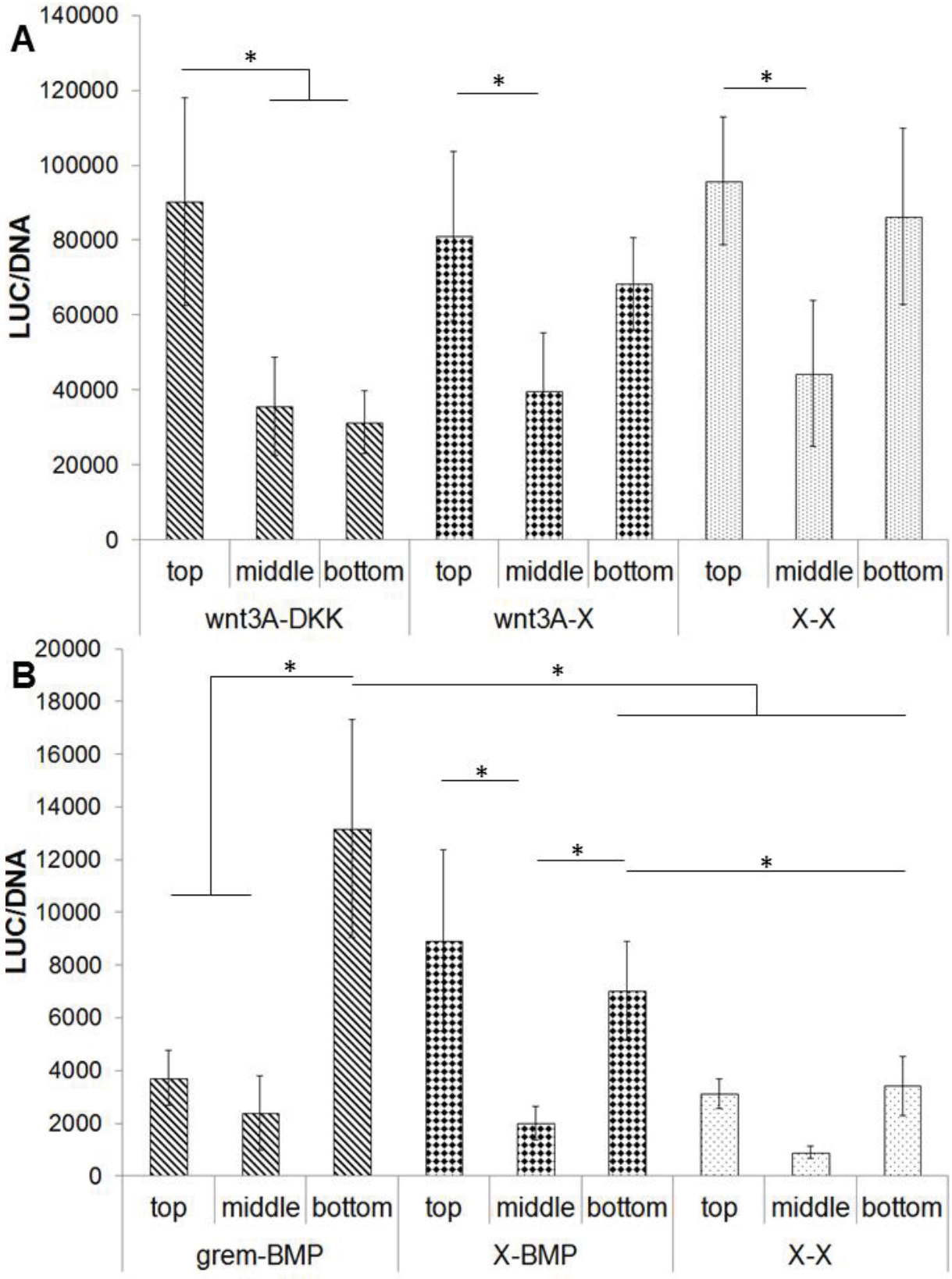

Figure 2: Gradients of growth factor antagonists showed downregulation of luciferase activity in a reporter assay. (A) Luciferase activity was decreased when a gradient of Dickkopf-1 (DKK) was used to downregulate a TCF-LEF reporter, n=8 cubes. Data are expressed as mean relative luciferase activity corrected for DNA +/- standard deviation. (B) Luciferase activity was decreased when a gradient of Gremlin (Grem) was used to counteract BMP2 activity on a BRE reporter, n=8 cubes. Data are expressed as mean relative luciferase activity corrected for DNA +/-standard deviation. * = $P < 0.05$

A BMP2 gradient stimulated zonal differentiation of C_2C_{12} cells

Agarose gels were seeded with five million cells and 200 ng/mL BMP2 was added to medium in the top compartment. In the absence of BMP2, the median alkaline phosphatase (ALP) activity corrected for DNA (ALP/DNA) in the bottom zone of the unstimulated condition tended to increase compared to the top and middle zone. In the BMP2-stimulated condition ALP/DNA values in the top zone tended to increase compared to middle zone. Also, in this condition the ALP/DNA values in the bottom zone tended to increase compared to the middle zone (Figure 3). Median ALP/DNA values in the top zone of the BMP2-stimulated constructs tended to be higher than ALP/DNA values in the top zone of the unstimulated constructs (Figure 3).

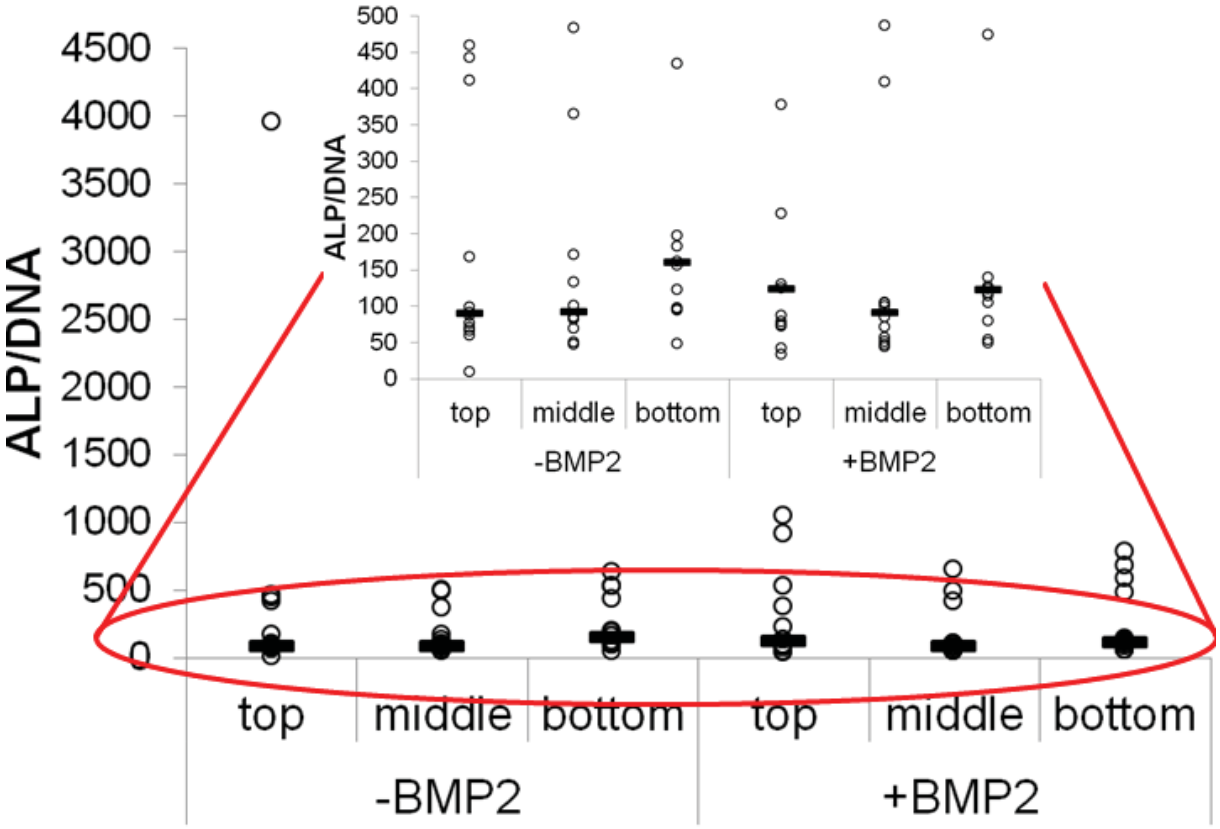

Figure 3: BMP2 gradient induced zonal ALP production in C_2C_{12} cells. (A) boxplot of ALP/DNA values after 3 days of culture with or without BMP2 added to the top compartment, n=12 cubes.

A gradient of transforming growth factor β3 induced zonal chondrogenic differentiation in goat bone marrow derived stem cells

So far, our results illustrate the regulation of cell behavior via the created gradients in a well-characterized cell line. We were then interested in elucidating whether these gradients could also induce zonal differentiation of primary bone marrow derived stem cells (BMSCs).

For this purpose, BMSCs of a goat (gBMSCs) were seeded at a density of $10x10^6$ cells/mL in agarose gels and stimulated either with transforming growth factor β3 (TGFβ3) in the top compartment to induce chondrogenic differentiation, dexamethasone (dex) in the bottom compartment to induce osteogenic differentiation or a combination of TGFβ3 in the top and dex in the bottom compartment to induce both chondrogenic and osteogenic differentiation at opposite sides of the construct. After seven days of culture, Alcian Blue staining was observed following TGFβ3 and the combined stimulation (Figure 4A-C). Alcian Blue staining in the combined condition was more prominent compared to the chondrogenic condition. In the TGFβ3 only condition, Alcian Blue staining was also observed in the bottom region of the construct, whereas this was absent in the combined stimulation. The magnifications show that Alcian Blue staining in the TGFβ3 and the combined condition was observed between the cells, whereas in the dex-only stimulated constructs Alcian Blue staining was mostly found in the pericellular region. This suggested that the dex gradient had an inhibitory effect on glycosaminoglycan expression. A combined Safranin-O/Alkaline phosphatase (Saf-O/ALP) staining was performed to show zonal distribution of a chondrogenic and osteogenic marker. No Saf O staining was detected clearly indicating the absence of a mineralized matrix. In contrast, ALP positive cells were present in each construct. The pattern in ALP-staining was comparable to the Alcian Blue staining following stimulation with TGFβ3 and the combined stimulation with TGFβ3 and dex. A lower but more homogeneous ALP staining throughout the construct was observed after stimulation with dex only compared to the other two conditions (Figure 5A-C).

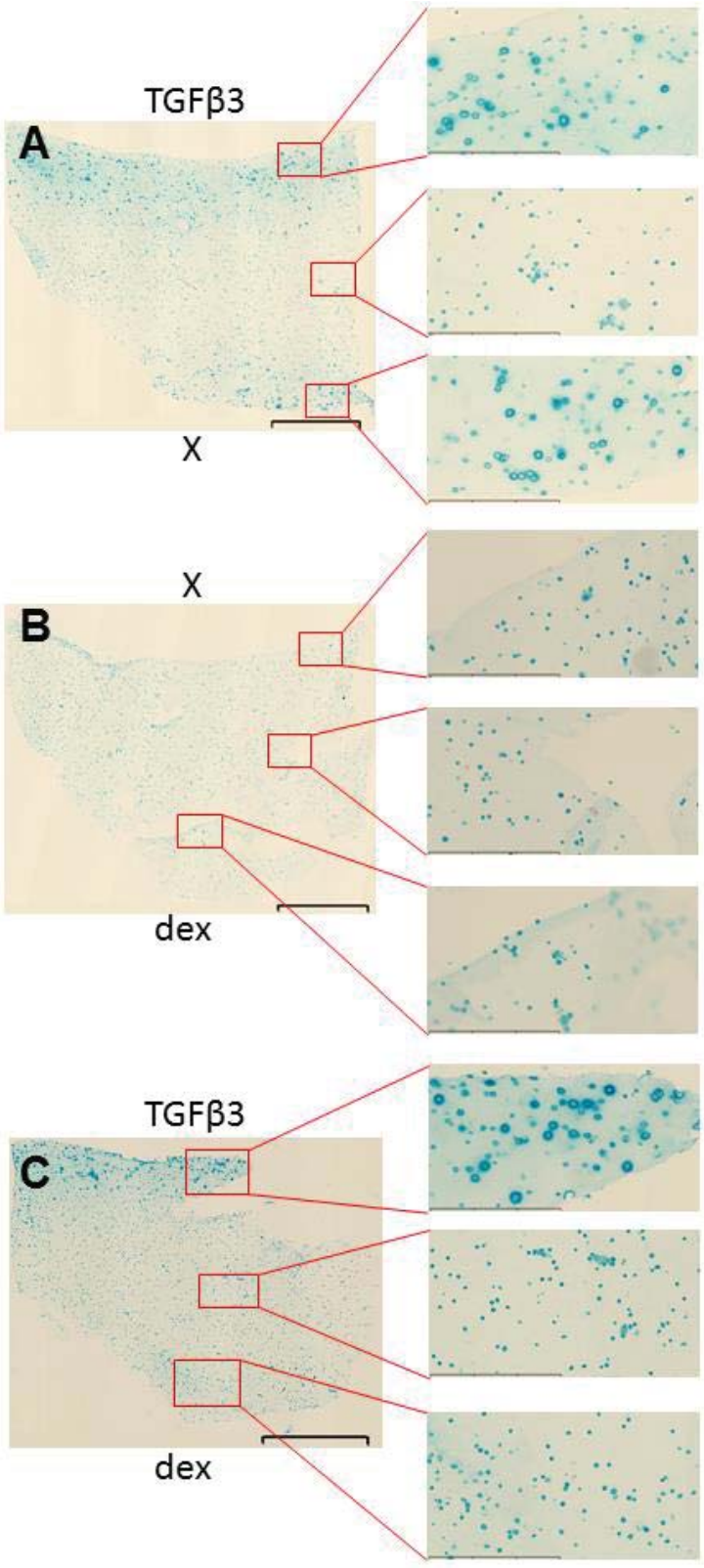

Figure 4: Alcian Blue staining of combined TGFβ3 and dexamethasone stimulation showed only positive staining in the top zone compared to only TGFβ3 stimulation. (A) TGFβ3 stimlation, n=1 cube, (B) dex stimulation, n=1 cube, (C) combined TGFβ3 and dex stimulation, n=2 cubes. Scale bar of the overview figures and magnifications represents 1mm and 300µm respectively.

Quantification of cellular capacity for chondrogenesis (GAG/DNA) and osteogenesis

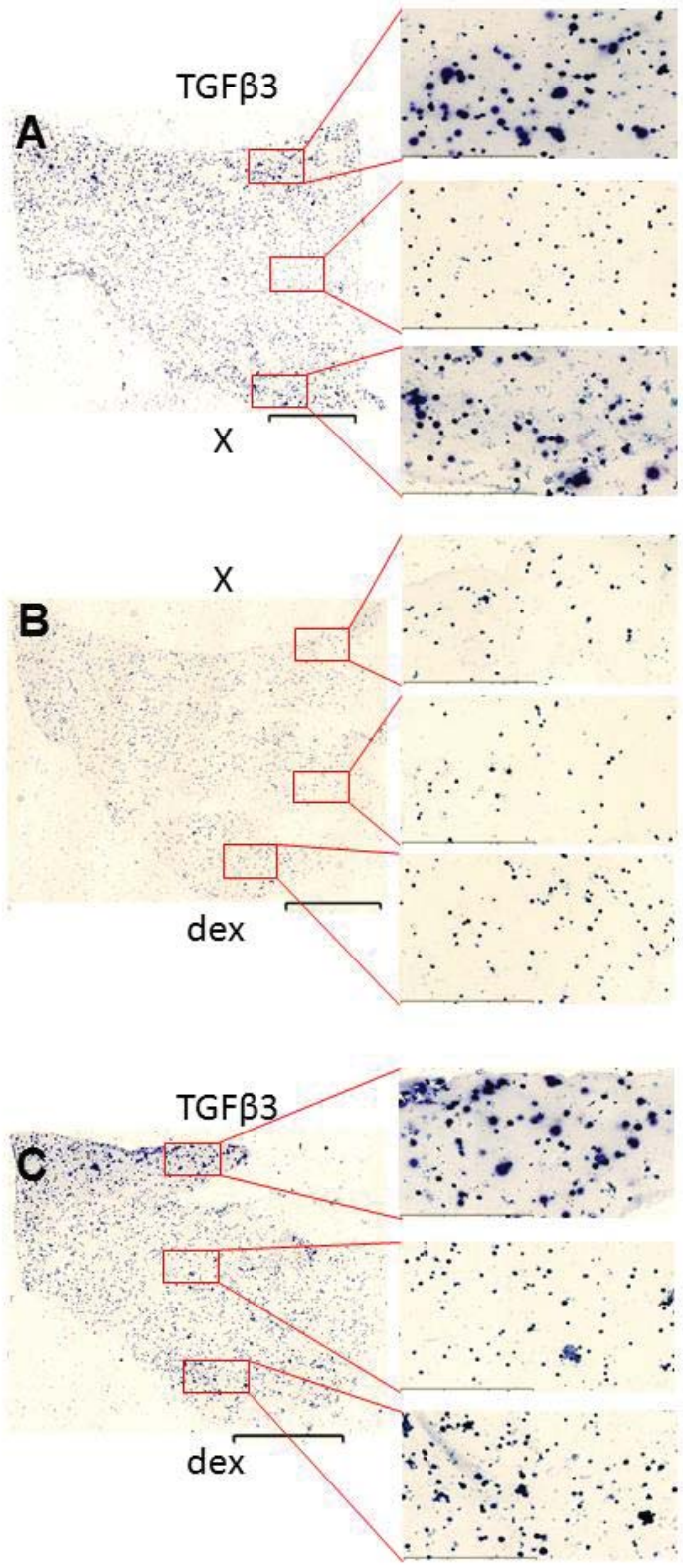

Figure 5: Combined Safranin-O and alkaline phosphatase staining of combined TGFβ3 and dexamethasone stimulation showed a similar pattern compared to only TGFβ3 stimulation. (A) TGFβ3 stimlation, n=1 cube, (B) dex stimulation, n=1 cube, (C) combined TGFβ3 and dex stimulation, n=2 cubes. Scale bar of the overview figures and magnifications represents 1mm and 300µm respectively.

(ALP/DNA) in the different zones of the constructs confirmed the results obtained by the histological stainings. Following both TGFβ3 and combined TGFβ3 and dex stimulation GAG/DNA values in the top zone were higher than the values in the middle zone. The values remained low in the condition in which dex was present in the bottom compartment, while the GAG/DNA ratio slightly increased in the condition with TGFβ3 only. (Figure 6A). This suggested that high dex concentrations have an inhibitory effect on GAG production. A comparable pattern was observed in ALP/DNA values when the dex only conditions was compared with the combined stimulation with TGFβ3 and dex. In the first condition, similar but low ALP/DNA values were observed in all zones, whereas ALP/DNA levels in the top zone of the combined stimulation was significantly higher compared to the other two zones (Figure 6B). These results show the complex influences of gradients of differentiation inducing factors on gBMSC differentiation. In our experiments the concentrations of TGFβ3 in combination with dex was found to be optimal in the top zone of the construct favoring better differentiation of the cells into the chondrogenic lineage.

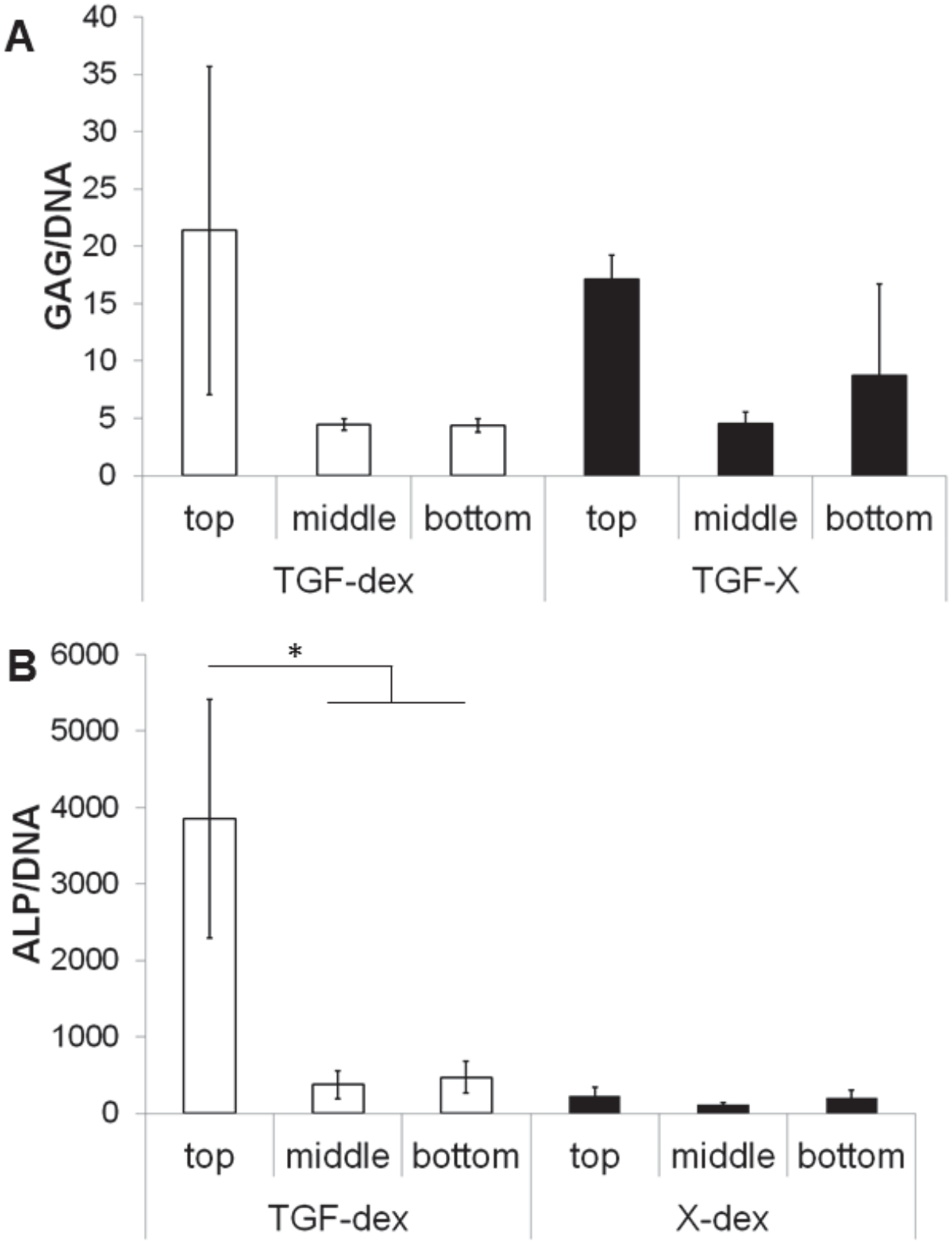

Figure 6: Biochemical analysis after TGFβ3, dexamethasone or combined TGFβ3 and dexamethasone stimulation revealed increased GAG deposition and ALP activity in the top zone of a MSC-laden agarose cube after dual stimulation. (A) GAG/DNA ratios per zone, (B) ALP/DNA ratios per zone, n=3 cubes. * = $P < 0.05$

Discussion

Morphogen gradients are indisputably important during development, where they guide cell migration, proliferation and differentiation [1-3]. But also in tissue homeostasis gradients play an important role. Dickkopf-1, Frizzled-related protein and Gremlin-1 have been shown to preserve the native articular phenotype [21]. A recent study showed that mesenchymal stem cells express a growth plate genotype rather than a mature articular genotype [26]. Based on these and other observations, it was hypothesized that such gradients could help in stimulating zone specific differentiation within a cell-laden hydrogel construct.

During embryonic development growth factor antagonists and agonists are equally important to establish gradients of growth factor for guiding cell fate [29-31]. In fact, expression of agonists and antagonists are clearly linked to each another and are often reciprocal. Gradients of well-studied morphogens in developmental biology, such as Wnt and BMP, were created in a dual compartment bioreactor. Antagonists of these growth factors, DKK and GREM1 [21, 22], were used to inhibit the induced upregulation of a luciferase reporter. Interestingly, in the conditions without these antagonists luciferase activity showed a typical U-shaped pattern with highest and comparable expression in the top and bottom zones of the construct. Hence, in these conditions it was not possible to demonstrate a gradient of agonist activity. In contrast, when an opposing gradient of the antagonist was present, there was a very clear distinction in activity with high reporter activity in the zone closest to the source of the agonist and lowest activity in the zone closest to the source of the antagonist. In all conditions the activity in the middle zone was low, most likely due to the lower metabolic activity of these cells as a consequence of nutrient or oxygen deprivation. This could indicate that without a growth factor antagonist it is more difficult to create a reproducible growth factor gradient through a tissue engineered construct over time. Culturing C_2C_{12} cells in a BMP2 gradient without an opposing Gremlin-1 gradient did not result in the expected gradual alkaline phosphatase response. Culturing these cells in a BMP gradient with an opposing gradient of its antagonist Gremlin-1 could assist in creating a more robust cellular response upon BMP stimulation. Although no significant differences were detected, these data gave an indication about the biological response that could be expected.

Several studies report the induction of the Wnt pathway by low oxygen tension and hypoxia-mediated BMP signaling in chondrocytes [32-34]. However, as in our experiments there is no evidence provided for this, it is hypothesized that the lower activity in the middle of the constructs was caused by oxygen deprivation.

Mesenchymal stem cells (MSCs) have been under intense investigation for tissue engineering purposes thoroughly [35]. Despite the strategies used, scaffolds, ceramics or hydrogels, the focus has been mainly on engineering one type of tissue [24, 36, 37]. Gradients, however, can facilitate in creating an environment that can differentiate MSCs into two different lineages within one construct. Several groups have explored the possibilities of guiding cell differentiation through gradients [38, 39]. Chang *et al.* also used a dual compartment bioreactor in which a hybrid gelatin-bone construct was cultured. They reported histologically cartilaginous matrix following 4 weeks of culture in the gelatin zone [38]. A biphasic scaffold was used while only the hydrogel part was injected with cells. In our study, we focus on the differentiation of cells into different lineages within a monophasic construct. Thorpe *et al.* showed differences in matrix production between top and bottom zones of constructs in the presence of gradients [39]. However, their system is not suitable for creating opposing gradients as described in the current study. In accordance with their study we did not find a clear distinction in zones with typical chondrogenic versus osteogenic differentiation. This might be, at least in part, due to the relatively short culture time. Alternatively, key components of either differentiation path might be lacking. Differentiation towards either lineage requires dexamethasone, although in different concentrations. Maintaining these concentrations at the proper depths in the construct is a challenge, but will be pivotal in the differentiation of MSCs. Agents antagonizing or neutralizing dexamethasone can assist in maintaining a dex-gradient. The above described interactions of growth factors and growth factor gradients show that this novel direction in cartilage tissue engineering involves complex stimulation of cells [40]. Maintaining a defined distribution of growth factors concentration will be significant in the guidance of cellular processes in tissue engineered constructs. Opposing gradients of agonists and antagonists is a new way to establish defined gradients of growth factor activity which may simulate developmental processes *in vitro* more closely than in current tissue engineered protocols.

Future experiments will focus on culturing tissue engineered constructs in defined complex growth factor and growth factor antagonist gradients, like Gremlin-1 opposing BMP2 and Dickkopf-1 opposing Wnt3A.

In summary, in this study we hypothesized on the importance of creating an *in vitro* environment that contains complex biochemical gradients. These could aid in generating more complex tissue engineered constructs. Furthermore, culturing constructs in these gradients could add to the knowledge of complex cellular responses in an environment that resembles the cell's native 3D-environment

References

1. Kim, H.K., I. Oxendine, and N. Kamiya, *High-concentration of BMP2 reduces cell proliferation and increases apoptosis via DKK1 and SOST in human primary periosteal cells.* Bone, 2013. 54(1): p. 141-50.
2. Cho, H.S., et al., *Individual variation in growth factor concentrations in platelet-rich plasma and its influence on human mesenchymal stem cells.* Korean J Lab Med, 2011. 31(3): p. 212-8.
3. Zhang, J. and Y. Li, *Fibroblast growth factor 21, the endocrine FGF pathway and novel treatments for metabolic syndrome.* Drug Discov Today, 2013.
4. Arkell, R.M., N. Fossat, and P.P. Tam, *Wnt signalling in mouse gastrulation and anterior development: new players in the pathway and signal output.* Curr Opin Genet Dev, 2013. 23(4): p. 454-60.
5. Idkowiak, J., G. Weisheit, and C. Viebahn, *Polarity in the rabbit embryo.* Semin Cell Dev Biol, 2004. 15(5): p. 607-17.
6. Jing, J., et al., *BMP Receptor 1A Determines the Cell Fate of the Postnatal Growth Plate.* Int J Biol Sci, 2013. 9(9): p. 895-906.
7. Liu, F. and S. Wang, *Molecular cues for development and regeneration of salivary glands.* Histol Histopathol, 2013.
8. Rockich, B.E., et al., *Sox9 plays multiple roles in the lung epithelium during branching morphogenesis.* Proc Natl Acad Sci U S A, 2013.
9. Christian, J.L., *Morphogen gradients in development: from form to function.* Wiley Interdiscip Rev Dev Biol, 2012. 1(1): p. 3-15.
10. Yan, D. and X. Lin, *Shaping morphogen gradients by proteoglycans.* Cold Spring Harb Perspect Biol, 2009. 1(3): p. a002493.
11. Matsuo, I. and C. Kimura-Yoshida, *Extracellular modulation of Fibroblast Growth Factor signaling through heparan sulfate proteoglycans in mammalian development.* Curr Opin Genet Dev, 2013. 23(4): p. 399-407.
12. Rogers, K.W. and A.F. Schier, *Morphogen gradients: from generation to interpretation.* Annu Rev Cell Dev Biol, 2011. 27: p. 377-407.
13. Perrimon, N., C. Pitsouli, and B.Z. Shilo, *Signaling mechanisms controlling cell fate and embryonic patterning.* Cold Spring Harb Perspect Biol, 2012. 4(8): p. a005975.
14. Enomoto-Iwamoto, M., et al., *Hedgehog proteins stimulate chondrogenic cell differentiation and cartilage formation.* J Bone Miner Res, 2000. 15(9): p. 1659-68.
15. Vortkamp, A., et al., *Regulation of rate of cartilage differentiation by Indian hedgehog and PTH-related protein.* Science, 1996. 273(5275): p. 613-22.
16. Wei, F., et al., *Activation of Indian hedgehog promotes chondrocyte hypertrophy and upregulation of MMP-13 in human osteoarthritic cartilage.* Osteoarthritis Cartilage, 2012. 20(7): p. 755-63.
17. Pei, M., et al., *Histone deacetylase 4 promotes TGF-beta1-induced synovium-derived stem cell chondrogenesis but inhibits chondrogenically differentiated stem cell hypertrophy.* Differentiation, 2009. 78(5): p. 260-8.
18. Kim, H.J. and G.I. Im, *Combination of transforming growth factor-beta2 and bone morphogenetic protein 7 enhances chondrogenesis from adipose tissue-derived mesenchymal stem cells.* Tissue Eng Part A, 2009. 15(7): p. 1543-51.
19. Choi, S., et al., *Chondrogenesis of periodontal ligament stem cells by transforming growth factor-beta3 and bone morphogenetic protein-6 in a normal healthy impacted third molar.* International journal of oral science, 2013. 5(1): p. 7-13.
20. Cao, L., et al., *Vascularization and bone regeneration in a critical sized defect using 2-N,6-O-sulfated chitosan nanoparticles incorporating BMP-2.* Biomaterials, 2014. 35(2): p. 684-98.
21. Leijten, J.C., et al., *Gremlin 1, frizzled-related protein, and Dkk-1 are key regulators of human articular cartilage homeostasis.* Arthritis Rheum, 2012. 64(10): p. 3302-12.
22. Suzuki, D., et al., *BMP2 differentially regulates the expression of Gremlin1 and Gremlin2, the negative regulators of BMP function, during osteoblast differentiation.* Calcif Tissue Int, 2012. 91(1): p. 88-96.
23. Behery, O., et al., *Treatment of Cartilage Defects of the Knee: Expanding on the Existing Algorithm.* Clin J Sport Med, 2013.
24. Lee, J.K., et al., *Clinical translation of stem cells: insight for cartilage therapies.* Crit Rev Biotechnol, 2013.
25. Jeng, L., H.P. Hsu, and M. Spector, *Tissue-engineered cartilaginous constructs for the treatment of caprine cartilage defects, including distribution of laminin and type IV collagen.* Tissue Eng Part A, 2013. 19(19-20): p. 2267-74.

26. van Gool, S.A., et al., *Fetal mesenchymal stromal cells differentiating towards chondrocytes acquire a gene expression profile resembling human growth plate cartilage.* PLoS One, 2012. 7(11): p. e44561.
27. Spitters, T.W., et al., *A dual flow bioreactor with controlled mechanical stimulation for cartilage tissue engineering.* Tissue Eng Part C Methods, 2013.
28. Zilberberg, L., et al., *A rapid and sensitive bioassay to measure bone morphogenetic protein activity.* BMC Cell Biol, 2007. 8: p. 41.
29. Criscimanna, A., et al., *PanIN-specific regulation of Wnt signaling by HIF2alpha during early pancreatic tumorigenesis.* Cancer Res, 2013. 73(15): p. 4781-90.
30. Theilhaber, J., et al., *Gene Expression Profiling of a Hypoxic Seizure Model of Epilepsy Suggests a Role for mTOR and Wnt Signaling in Epileptogenesis.* PLoS One, 2013. 8(9): p. e74428.
31. Kamiya, N., et al., *Acute BMP2 upregulation following induction of ischemic osteonecrosis in immature femoral head.* Bone, 2013. 53(1): p. 239-47.
32. Sykova, E. and S. Forostyak, *Stem cells in regenerative medicine.* Laser Ther, 2013. 22(2): p. 87-92.
33. Ghasemi-Mobarakeh, L., et al., *Advances in electrospun nanofibers for bone and cartilage regeneration.* J Nanosci Nanotechnol, 2013. 13(7): p. 4656-71.
34. Milner, D.J. and J.A. Cameron, *Muscle repair and regeneration: stem cells, scaffolds, and the contributions of skeletal muscle to amphibian limb regeneration.* Curr Top Microbiol Immunol, 2013. 367: p. 133-59.
35. Chang, C.H., et al., *Cartilage tissue engineering on the surface of a novel gelatin-calcium-phosphate biphasic scaffold in a double-chamber bioreactor.* J Biomed Mater Res B Appl Biomater, 2004. 71(2): p. 313-21.
36. Thorpe, S.D., et al., *Modulating gradients in regulatory signals within mesenchymal stem cell seeded hydrogels: a novel strategy to engineer zonal articular cartilage.* PLoS One, 2013. 8(4): p. e60764.
37. Khan, I.M., et al., *In vitro growth factor-induced bio engineering of mature articular cartilage.* Biomaterials, 2013. 34(5): p. 1478-87.

Chapter 5
Glucose Gradients Influence Zonal Matrix Deposition in 3D Cartilage Constructs

Tim W.G.M. Spitters, Carlos M.D. Mota, Barbara Slowinska, Samuel C. Uzoechi, Dirk E. Martens, Lorenzo Moroni, Marcel Karperien

Abstract

Reproducing the native collagen structure and glycosaminoglycan distribution in tissue engineered cartilage constructs is still a challenge. Articular cartilage has a specific nutrient supply and mechanical environment due to its location and function in the body. Efforts to simulate this native environment have been reported through the use of bioreactor systems. However, few of these devices take into account the existence of gradients over cartilage as a consequence of the nutrient supply by diffusion. We hypothesized that culturing chondrocytes in an environment in which gradients of nutrients can be mimicked would induce zonal differentiation. Indeed, we show that glucose gradients facilitating a concentration distribution as low as physiological glucose levels enhanced the zonal chondrogenic capacity similar to the one found in native cartilage. Furthermore, we found that glucose consumption rates of cultured chondrocytes was higher under physiological glucose concentrations and that GAG production rates were highest in 5mmol/L glucose. From these findings we concluded that this condition is better suited for matrix deposition compared to 20mmol/L glucose standard used in a chondrocyte culture medium. Reconsidering the culture conditions in for cartilage tissue engineering strategies can lead to cartilaginous constructs that have better mechanical and structural properties, thus holding the potential of further enhancing integration with the host tissue.

Keywords: glucose, bioreactor, cartilage, tissue engineering, zonal distribution

Chapter five: Glucose gradients

Introduction

Cartilage is an anisotropic tissue involved in load distribution and facilitation of frictionless movement of joints [1, 2]. Matrix components are distributed through the tissue in such a way that these functions can be optimally executed. Collagen type II fibers run parallel to the articular cartilage surface, where its concentration is high to absorb load, and bend towards the middle zone and eventually anchor in the subchondral bone in a perpendicular fashion to optimally distribute the load to the underlying bone. Thus, there exists a collagen gradient through cartilage from a high towards a low concentration starting from the synovial to the subchondral side. Also of the other main component of cartilage matrix, the proteoglycans, which function in attracting water and retaining and transporting growth factors, a concentration gradient is present in cartilage [3, 4]. The amount of GAGs per cell (GAG/DNA) increases from synovial to the subchondral side [4]. Thus, it is the distribution of these components that is important for its function.

Glucose is a precursor of proteoglycans. After conversion to glucose-6-phosphate, it is converted to glucose-1-phosphate instead of entering the glycolysis. From there it is further converted to uridine diphosphate (UDP)-glucose and UDP-glucuronate. This molecule can then be converted in glucuronides, proteoglycans and glycosaminoglycans [5]. Thus, it can be hypothesized that glucose availability can direct proteoglycan synthesis as it is the starting molecule for carbohydrates present in proteoglycans. Besides this, glucose is also the most important energy source for chondrocytes as reviewed by Mobasheri [6]. It has been shown that across cartilage from the synovial side to the subchondral bone a glucose gradient exist [7]. Given the dual role of glucose in cartilage we hypothesize that glucose gradients are in part responsible for establishing the observed gradients in glycosaminoglycans in cartilage.

During development, gradients of morphogens guide cellular processes and time-specific organization of cells. Although there has been interest for nutrient gradients, especially oxygen, studies addressing this topic are limited [7-11]. Computational models have shown how oxygen and glucose gradients are created in a tissue engineered construct [8, 12]. In an environment with a high oxygen (O_2) concentration, O_2 consumption was inhibited when embedded chondrocytes were cultured in a high glucose concentration [7]. In another study, 5% O_2 saturation of the

medium was suggested to have a protective effect on the energy metabolism and nitric oxide production [13]. The same oxygen percentage in the medium (5%) was shown to enhance the chondrogenic capacity in pellet culture of human articular chondrocytes even after pre-culture in a high oxygen environment. At the same time expression and synthesis of catabolic markers were suppressed after culture in 5% O_2 saturation [14]. In contrast, chondrogenic markers were decreased when chondrocytes were cultured in the presence of a glucose competitor, 2-deoxy-D-glucose. When the same competitor together with insulin was added to healthy (HL) and osteoarthritic (OA) chondrocytes, glucose uptake was improved due to increased glucose transferase expression [16]. However, when HL and OA chondrocytes were exposed to 30mM glucose, both anabolic and catabolic genes were upregulated, even in the presence of a known pro-chondrogenic growth factor like TGF-β [17].Yu *et al.* reported recently that, when the glucose uptake was inhibited, chondrocytes lose their native phenotype and started to express catabolic factors [15].

The above described responses to different nutrient concentrations show that their effect on chondrocyte behavior is complex and still poorly understood. By creating glucose gradients we tested the hypothesis if variations in glucose levels within a cell-laden tissue engineered construct can contribute to the zonal differentiation of chondrocytes. To test this hypothesis, we cultured cell-laden hydrogels in a bioreactor system, which was designed to create defined and controlled glucose gradients [18].

Materials and Methods

Cell sources

Bovine chondrocytes (bCHs) were isolated from femoral articular cartilage by means of collagenase type II digestion (150U/mL; Worthington, USA) overnight. Subsequently, the collagenase suspension was filtered through a 200 micrometer cell strainer and centrifuged at 300g for 10 minutes at 4°C. The pellet was then washed in phosphate buffered saline (PBS) and centrifuged. This procedure was repeated once before cells were resuspended in Dulbecco's Modified Eagle's Medium (DMEM) without glucose (Gibco, USA) and counted using a Burker counting chamber. Cells were used immediately after isolation. In 96 well plates (2D experiments), 10,000 cells/cm^2 were seeded, whereas in microwell arrays and agarose hydrogels (3D experiments) 10*10^6 cells/mL were seeded.

Medium composition

Chondrocytes were cultured in DMEM supplemented with 100U/mL penicillin/100µg/mL streptomycin, 20mM ascorbic acid, 40µg/mL proline, 100µg/mL sodium pyruvate and 1% Insulin Transferrin and Selenium premix supplemented different glucose concentrations. Different glucose concentrations were prepared by mixing DMEM containing 4.5g/L glucose with DMEM without glucose. Five concentrations were prepared which are described as [0], [1.25], [2.5], [5] and [20], referring to 0, 1.25, 2.5, 5 and 20mM of glucose, respectively. The actual starting concentrations are shown in Table 1.

Table 1: Measured starting concentrations in the bulk medium in 2D experiments

Condition	[glucose] (mM)
[0]	0
[1.25]	1.48
[2.5]	2.85
[5]	5.38
[20]	23.03

Cell seeding

For 2D experiments, a cell suspension was made in five different glucose concentrations (see table 1) and 200µL was seeded in each well of a 96-well plate at a density of 10,000 cells/cm^2.

High density cultures were performed in a previously described PolyActive 300/55/45 microwell arrays (Figure 1A and 1B; Screvo B.V., The Netherlands). Each microwell was seeded with 1μL cell suspension at a density of $10*10^6$ cells/mL [19]. This custom made array existed of 9x2 wells. The wells had a volume of 1μL. Before seeding the arrays were sterilized in ethanol and subsequently washed in PBS to remove residual ethanol. After seeding, the arrays were placed in separate wells of a 6-well plate and submerged in 6mL of DMEM containing 0, 1.25, 2.5, 5 or 20mmol/L glucose.

Hydrogel cell constructs were prepared by combining the cell suspensions with the same volume of 1% agarose solution, resulting in cells embedded in 0.5% agarose, and pipetted in custom-made polycarbonate four-chamber inserts (Figure 1C). After solidifying, the inserts were placed in a previously described dual compartment bioreactor [18]. Each hydrogel consisted of 80μL and contained $10*10^6$ cells/mL. The top compartment was filled with 2mL medium and the bottom compartment with 10mL medium. Monolayer and microwell array cultures were performed under normoxic (20%O_2) and hypoxic (2.5%O_2) conditions. A culture period of 7 days was maintained for all experiments. Table 2 shows the glucose concentrations in the top and bottom compartment that were used to create glucose gradients.

Table 2: Measured glucose concentrations in the top and bottom compartment.

Condition	[glucose] (mM) top compartment	[glucose] (mM) bottom compartment
20-0	23.03	0
20-5	23.03	5.38
20-20	23.03	23.03

Computational modeling

Computational fluid dynamics (CFD) was used to predict the glucose concentrations in culture conditions was set-up and solved in the transport of diluted species module in Comsol Multiphysics version 4.1 software (Comsol, The Netherlands).

Figure 1D represents a cross section of the static bioreactor chamber, depicting the top and bottom compartment, and the constructs in yellow.

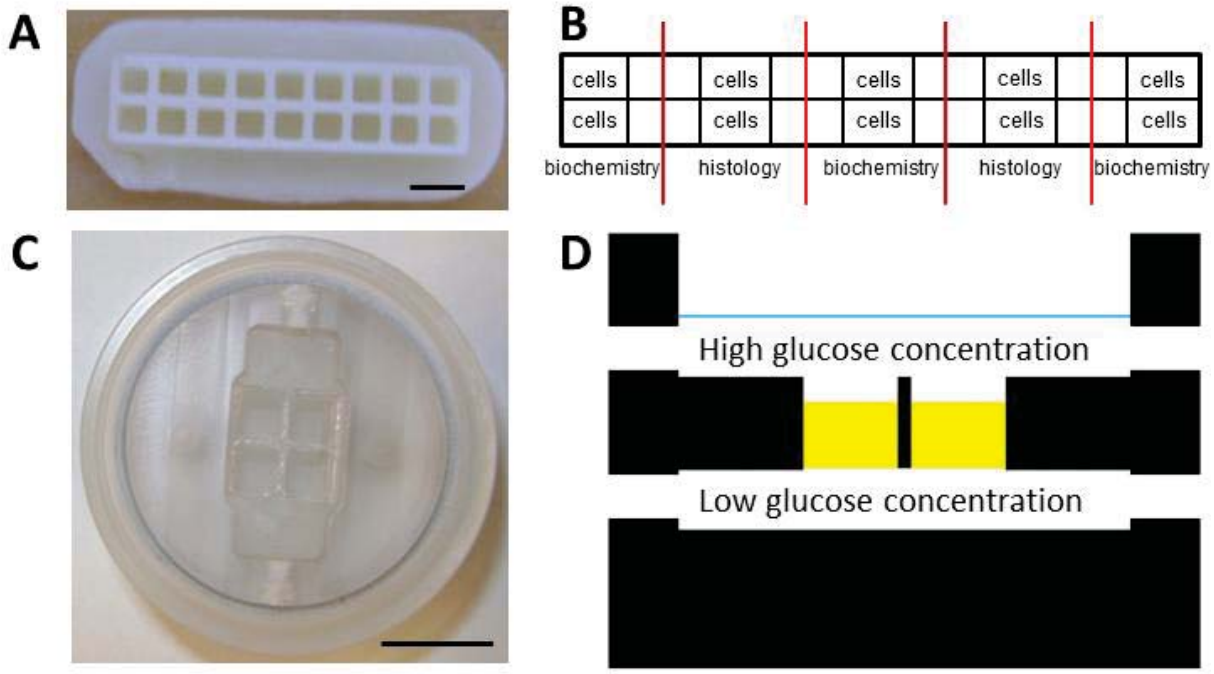

Figure 1: Culture devices and strategy. (A) Custom made microwell arrays (scalebar represents 2mm) and (B) schematic representation of cell seeding and division for analysis. (C) Static bioreactor for creating gradients (scalebar represents 10mm). (D) Schematic cross section of the bioreactor depicting the different compartments with high and low glucose concentration. The blue line depicts the height of the medium in the top compartment. The two white openings on both sides depict the in-/outlets.

The Navier-Stokes equation that was solved for incompressible fluid dynamics is as defined by Eq. 1:

$$\frac{\delta c}{\delta t} = \nabla * (D\nabla c) + R \qquad (1)$$

where ∇ is the del operator, D is the diffusion coefficient (m^2/s), c is the concentration (mol/m^3) and R is the reaction constant ($mol/(m^3*s)$).

Glucose concentrations through the constructs were modelled time-dependently using the following assumptions: i) walls in different conditions were considered rigid and impermeable, ii) no-slip boundary conditions were applied to surfaces, iii) the glucose diffusion constant (*Đ*) in water was set to 9.2 x 10^{-10} m^2/s and in 0.5% agarose was assumed equal [20]. The initial concentration of glucose in the top compartment was 20 mmol/L, representing high glucose DMEM, and was either 0, 5 or 20mmol/L in the bottom compartment, representing DMEM without glucose, with a physiological glucose concentration and high glucose DMEM respectively. Table 2 shows the actual concentrations in the compartments that were used to create glucose gradients. The glucose consumption rate of chondrocytes in the constructs

was assumed to be 1.28 x 10^{-7} mol/(L*s) (calculated from the 20mmol/L condition in Figure 2A).

It has to be noted that for glucose the consumption rate was assumed homogenous throughout the constructs and was in the same range as found in literature [21].

Biochemical analysis

Metabolite analysis

After 2D culture, the medium was removed and glucose and lactate concentrations were analyzed using a Vitros DT60II medium analyzer (Ortho-Clinical Diagnostics). Medium of three wells per condition was analyzed and the consumption and production rates were calculated and correlated with the cell content in each respective well.

Glycosaminoglycan (GAG) content

Before analysis, constructs were incubated in a proteinase K (PK) digestion buffer (1ug/mL PK, 1µg/mL pepstatin A, 18.5µg/mL iodoacetamide, Sigma) and went through a freeze/thaw cycle. GAG content was measured with a 1,9-Dimethyl-Methylene Blue (DMMB) assay. Therefore, 25µL sample was added to a transparent 96-well plate and 5µL of a 2.3M NaCl solution was added. Then, 150µL of a DMMB solution was added and absorbance was read at 520nm using a Multiskan GO plate reader (Thermo Scientific, USA). GAG content was quantified with a chondroitin sulphate standard curve and corrected for DNA content.

DNA quantification

DNA content was quantified with a CyQuant kit (Invitrogen, USA) according to manufacturer's protocol and fluorescence was measured at 480nm using a spectrophotometer LS50B (Perkin Elmer). DNA concentrations were calculated from a λ DNA standard curve.

Histology

For histology, scaffolds and constructs were dissected from top to bottom, and fixed in 10% buffered formalin. Subsequently, agarose constructs were embedded in

cryomatrix, sectioned in a cryotome into 10µm thick longitudinal sections and then mounted onto Superfrost® Plus (Thermo Fisher Scientific, U.S.A.) glass slides.

Toluidine Blue staining

Gycosaminoglycan deposition in the microwell arrays was visualized by Toluidine blue staining. Therefore, the wells were submerged shortly in Toluidine Blue (TB) solution and subsequently washed with PBS until residual TB solution was removed. Staining was visualized with a Nikon stereomicroscope (Nikon, Japan). Then, matrix volume was estimated from these staining pictures by measuring the surface of the TB staining and correcting this for the surface of the well.

Safranin-O staining

Sections were hydrated for 10 minutes in demi water and stained with Fast Green for 3 minutes, rinsed in 1% acetic acid and subsequently stained with Safranin-O for 5 minutes and dehydrated in a sequence of 96% EtOH, 100% EtOH and xylene for 2 minutes each. Sections were dried and mounted with Tissue-Tek mounting medium (Sakura Finetek Europe BV, The Netherlands).

Picrosirius Red

To visualize collagen fibers, sections were stained with the Picrosirius Red staining kit (BioSciences) according to the manufacturer's protocol. Shortly, sections were hydrated for 10 minutes in demi water, stained with Haematoxylin for 8 minutes and rinsed in distilled water followed by staining with Picrosirius Red. The stained sections were washed in 70% EtOH for 45 seconds and dehydrated in a graded ethanol series.

Slides were scanned with a Nanozoomer 2,0 RS (Hamamatsu, Japan) and pictures were captured with its proprietary NDP.Scan software (Hamamatsu, Japan).

Results

Chondrogenic response on tissue culture plastic in different glucose concentrations.

Bovine chondrocytes were cultured on tissue culture plastic using different glucose concentrations in 20%O_2 (normoxia) and 2.5%O_2 (hypoxia). Glucose levels in the medium were measured at the end of the culture period and the consumption rate was calculated as the amount of glucose consumed per cell per hour (r(glu)). Under normoxic conditions in 1.25mM, 2.5mM and 5mM glucose, glucose consumption rates during 2D culture were comparable, but decreased in 20mM (Figure 2A). However, lactate production rates in these conditions were similar for all settings (Figure 2A). This indicated that glucose uptake was affected by the high glucose concentration. Under hypoxic conditions, glucose consumption rates were similar and they tended to be higher compared to their normoxic equivalents. The same was observed for the lactate production rates (Figure 2A). This could indicate that hypoxia, regardless of the glucose concentration, maintains the native chondrocyte phenotype [22]. When the yield of lactate on glucose (Y(lac/glu)) is considered (Figure 2B), it could be observed that in all concentration the Y(lac/glu) is around 2. This is to be expected when an anaerobic metabolism is maintained.

Under normoxic conditions, total GAG production did not seem to be affected by different glucose concentrations (Figure 2C). However, under hypoxic condition the 2.5mmol/L, 5mmol/L and 20mmol/L showed higher GAG content compared to their normoxic equivalents, whereas the hypoxic 0mmol/L and 1.25mmol/L condition showed similar levels of GAG deposition (Figure 2C). Proliferation was minimal in all conditions when compared to the initial number of cells seeded (+/-39,000 cells). This could indicate that cells use the energy they produce for matrix production and maintenance instead of proliferation. However, it could be observed that cell numbers tended to be higher under lower glucose concentrations - except for the condition without glucose - regardless of the oxygen concentration (figure 2D).

The GAG production rate (rGAG) showed a similar trend as the GAG content. Under normoxic conditions there was no influence of the glucose concentration on the r(GAG), whereas under hypoxic conditions this rate showed an increase up to the setting with 2.5mM glucose and stabilized at higher glucose concentrations (Figure 2E). When the r(GAG) is considered as a function of the glucose consumption rate (r(glu)), it can be observed that highest rGAG was obtained at a glucose

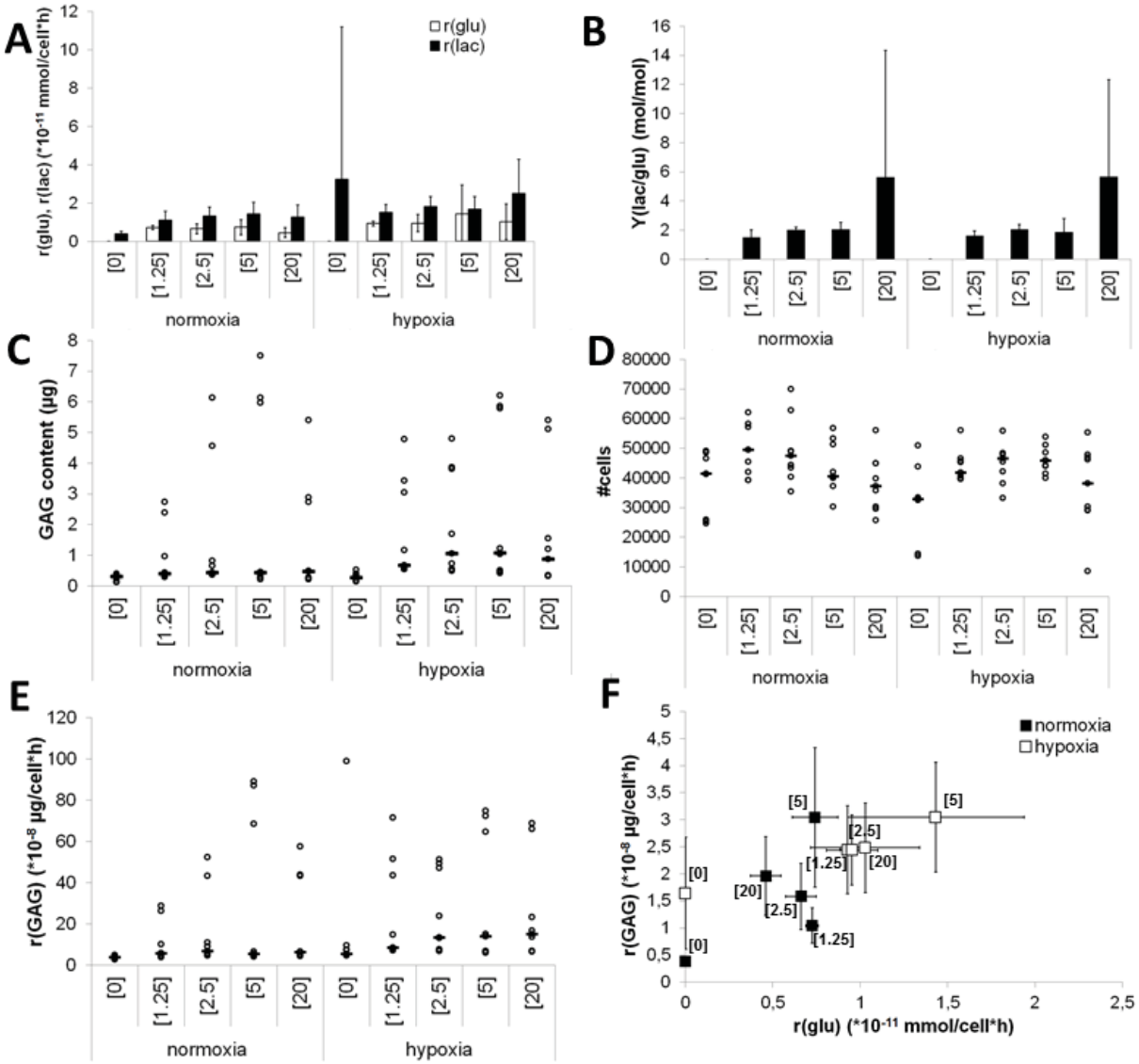

Figure 2: Metabolic response of p0 bovine chondrocytes (bCHS) to different glucose and oxygen concentrations. (A) average glucose consumption and lactate production rates of bCHs and (B) average yield of lactate on glucose. Boxplots with individual data points represent (C) Total glycosaminoglycan (GAG) production, (D) number of cells, (E) GAG production rates (grey dots represent the individual data points and the black bars the median) and (F) relation between average glucose consumption rate and average GAG production rate (error bars represented as the standard deviation) after 7 days, n=3 donors.

concentration of 5mM, although the r(glu) in this condition was lower compared to the condition with 20mM under hypoxic conditions (white squares in Figure 2F). Under normoxic conditions, rGAG seemed more optimal following culture in 5mM glucose compared to culturing in 20mM glucose (black squares in Figure 2F).

From these data it can be concluded that glucose consumption, lactate and GAG production by chondrocytes in 2D culture are slightly affected by the bulk glucose concentration, especially under low concentrations. The GAG production rate seemed optimal at 5mM glucose.

Tissue formation in microwell arrays showed an optimum under hypoxic conditions

To investigate the influence of glucose concentration on matrix production of chondrocytes seeded at high density, cells were cultured in a microwell array system and the same glucose concentrations as described above were used for cultivation. After 7 days of culture in normoxic conditions, glucose concentrations of 0mM and 1.25mM resulted in minimal Toluidine Blue (TB) staining which increased with increasing glucose concentrations. Under low oxygen tensions a similar trend was observed and the staining seemed more intense compared to high oxygen conditions (Figure 3A). Our staining observations were validated by comparing the matrix area/well area ratio in each condition. This showed similar trends as described for 2D culture. In the 0mM and 1.25mM conditions this ratio was lower compared to the other three glucose conditions in both oxygen tensions. It was also observed that in a setting with 20mM glucose the ratio decreased compared to 2.5mM and 5mM glucose regardless of the oxygen concentration - with the highest ratio observed in 2.5mM (Figure 3B). Quantification of the GAG content in the wells showed no obvious differences between glucose concentrations under high oxygen levels. Under hypoxic conditions GAG content seemed highest under 2.5mM glucose confirming the staining (Figure 3C).

These data correlated with the results shown in figure 2 indicating that matrix formation in a 3D environment could be enhanced by using physiological glucose concentrations.

Glucose gradients induced zonal differences in matrix distribution

Computational modeling of the glucose gradient with and without cellular consumptions in the hydrogel constructs cultured between two medium compartments with distinct glucose concentrations showed that after 1 hour of glucose diffusion without the presence of cells, a glucose gradient could be observed from top to bottom in the 20-0 and 20-5 condition. As assumed, the gradient in the 20-0 condition was steeper (a higher concentration difference between top and bottom) compared to the 20-5 condition (Figure 4A and B, left). A different concentration profile was predicted for the 20-20 condition, where the lowest concentration was observed in the middle of construct (Figure 4C, left). When a consumption rate of 1.28e-7 $mol*m^{-3}*s^{-1}$ (calculated from the normoxic-20mM

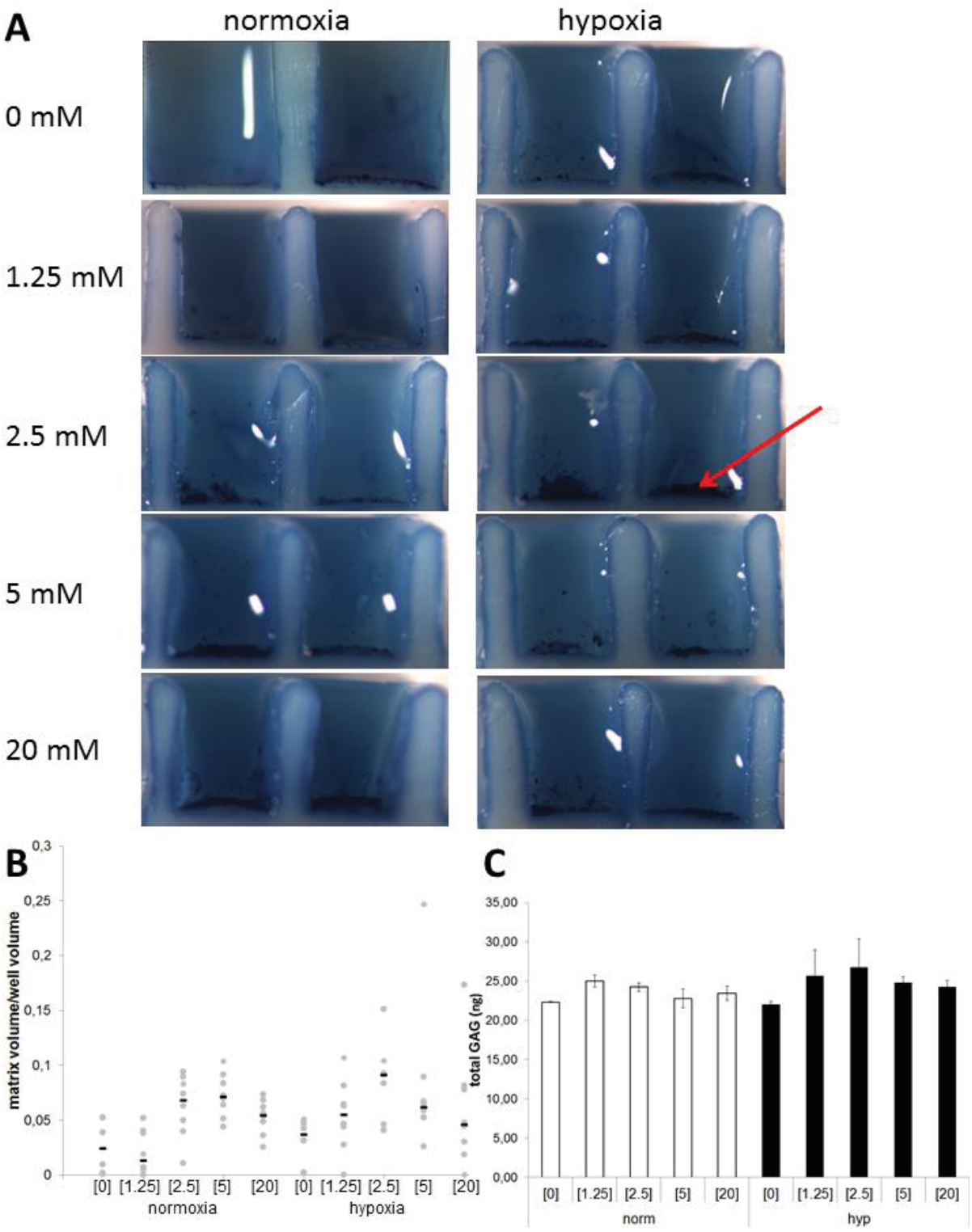

Figure 3: Chondrogenic response in printed microwells under different glucose concentrations. (A) Microtissues stained with Toluine Blue after 7 days. (arrow indicates location of cells and matrix) (B) Boxplot with individual data points quantifying the Toluidine Blue staining after 7 days, n=8 wells of 2 donors. (C) Total GAG in printed microwells.

glucose condition in Figure 2) was assumed, the glucose gradient in the 20-0 condition became steeper, whereas the gradient in the 20-5 condition did not seem to change notably compared to the gradient without consumption. In the 20-20 condition

it was observed that the width of the low concentration zone in the middle of the construct increased when compared to the gradient without consumption. At 24 hours, when in all modeled conditions the gradient became stable (data not shown), a homogeneous glucose distribution was observed in the 20-20 condition, even when glucose was consumed (Figure 4C, right). This means that the consumption rate was too small compared to the diffusion coefficient to induce changes in the glucose gradient. The gradients in the 20-0 and 20-5 conditions became less steep after 24 hours compared to the gradients after 1 hour. Although a change in the concentration distribution was observed in the 20-0 condition after 1 hour of consumption compare to no consumption, this was not observed after 24h when a cellular consumption rate was introduced in the model (Figure 4A, right). In the 20-5 condition no change in the gradient was observed after consumption (Figure 4B, right). In the 20-0 condition, the concentration distribution at equilibrium ranged from 19.7mM to 0.2mM. In the 20-5 condition this range was from 19.7mM to 5.1mM.

The effect of these gradients on cartilaginous matrix production over time is shown in Figure 5. After 7 days of culture, 10μm sections were stained with Alcian Blue (AB, Figure 5A) and Safranin-O (Saf-O, figure 5B) to visualize glycosaminoglycan distribution. This revealed zonal differences in matrix deposition in the 20-0 and 20-5 condition, whereas distribution in the 20-20 condition seemed homogeneous. In the 20-0 gradient the intensity of both AB and Saf-O staining decreased from the top to the middle of the construct where the latter was almost absent. In the bottom zone staining intensity increased compared to the middle zone. In the 20-5 condition, the AB staining appeared to be homogeneous (figure 5A), but the non-stained Saf-O zone decreased compared to the 20-0 condition and the staining appeared more homogeneously distributed (Figure 5B).

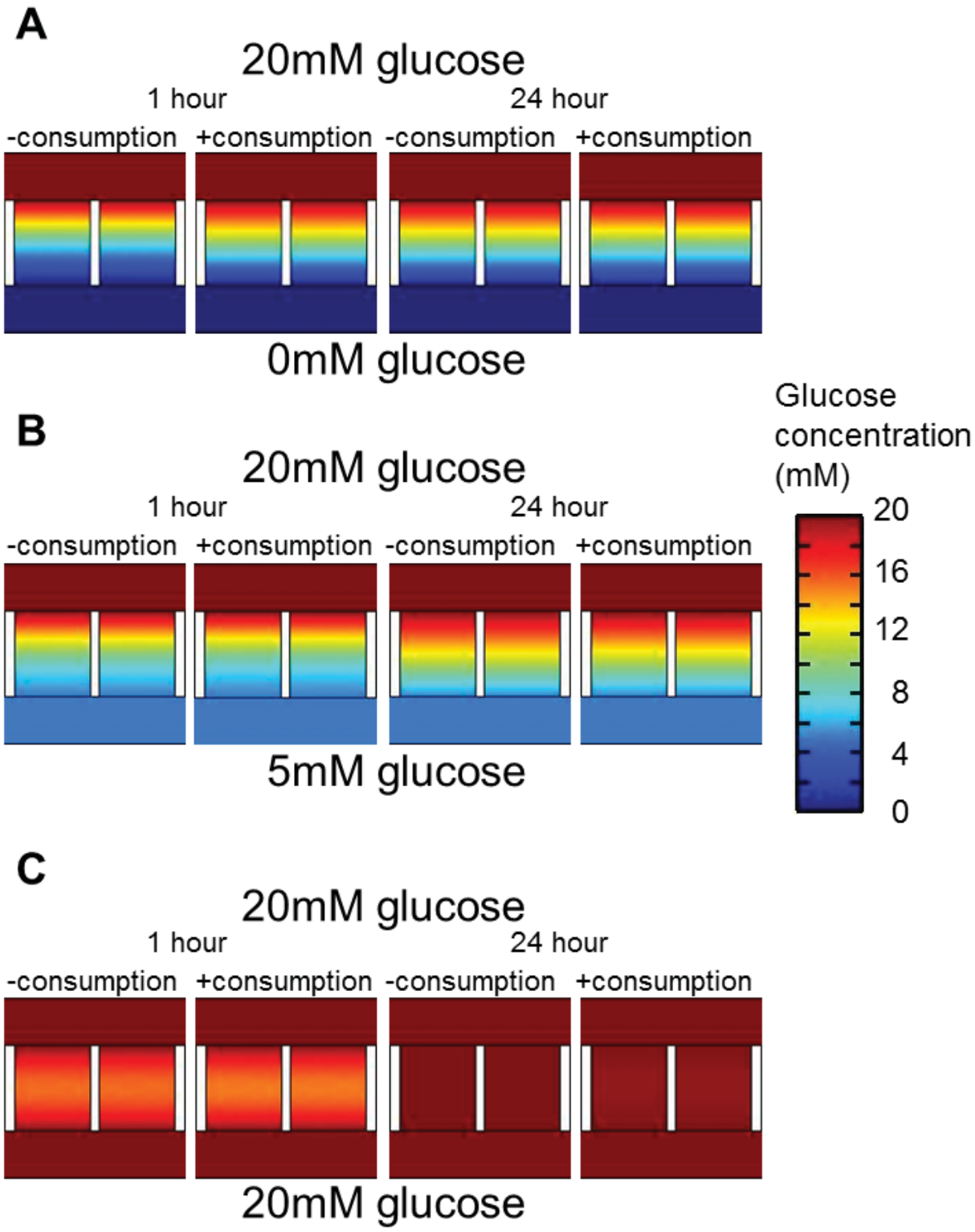

Figure 4: Modeled glucose gradients with and without consumption through constructs between different glucose concentrations. (A) Predicted glucose gradients without and with cellular glucose consumption after 1 hour (left) and 24 hours (right) after culture between 20mM and 0mM glucose. (B) Predicted glucose gradients without and with cellular glucose consumption after 1 hour (left) and 24 hours (right) after culture between 20mM and 5mM glucose. (C) Predicted glucose gradients without and with cellular glucose consumption after 1 hour (left) and 24 hours (right) after culture between 20mM and 20mM glucose.

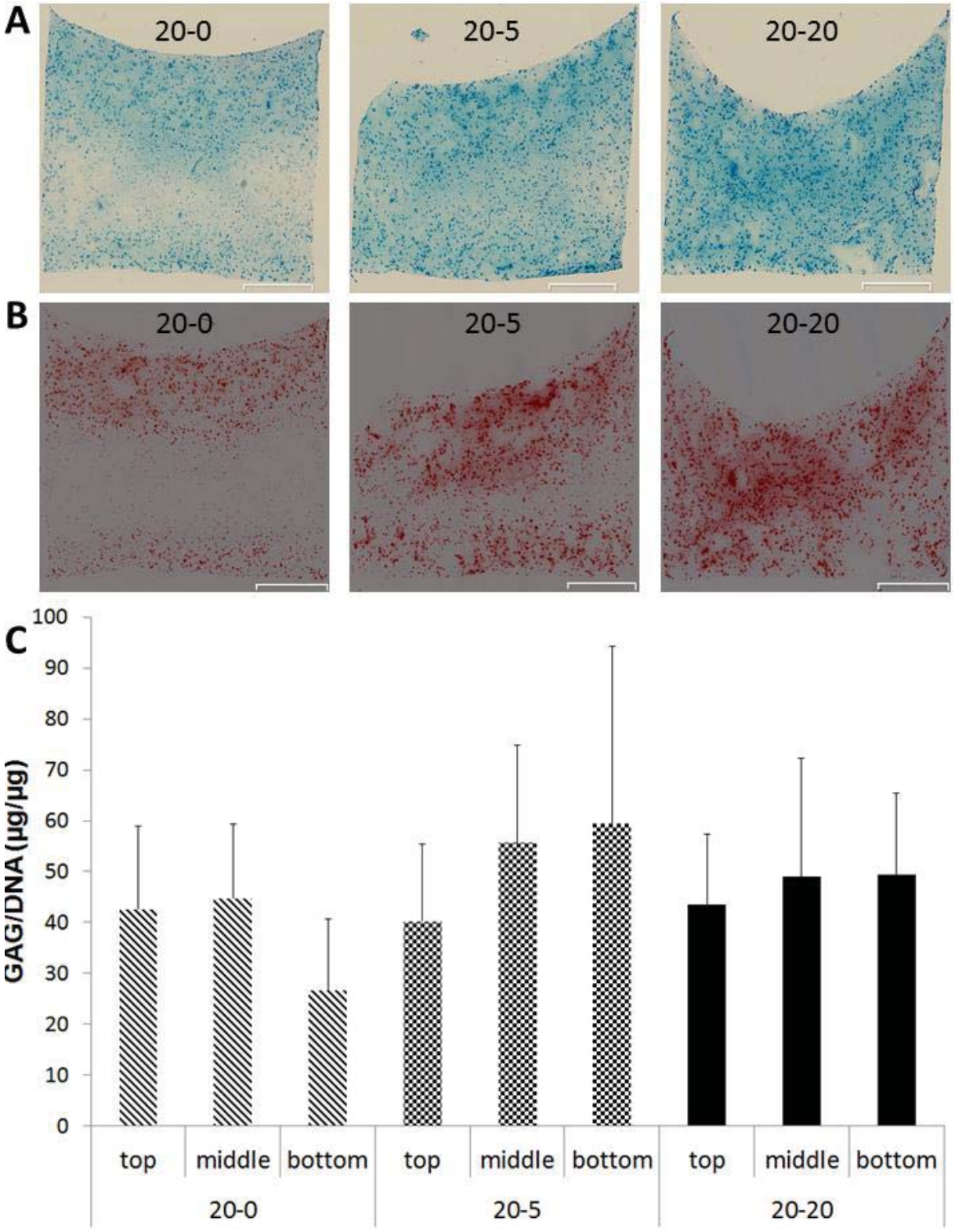

Figure 5: Chondrogenic response of p0 bovine chondrocytes embedded in agarose cultured in different glucose gradients. Constructs were cultured between medium containing 20mM glucose and 0, 5 or 20mM glucose in the top and bottom compartment respectively. (A) Alcian Blue staining after 7 days, n=2, scale bar represents 1mm. (B) Safranin-O staining after 7 days, n=2, scale bar represents 1mm. (C) zonal GAG/DNA ratios, data represents the mean of 5 cubes.

Evaluating the chondrogenicity (GAG/DNA) of the different zones showed that in the 20-5 condition an increasing trend in GAG/DNA was observed, whereas GAG/DNA was equal in all zones in the 20-20 conditions. The 20-0 condition showed as expected a decrease in GAG/DNA from middle to bottom zones (Figure 5D). Comparing the predicted gradients to the biological response of chondrocytes showed that in a gradient that includes sub-physiological concentrations (<5mM), matrix production seemed to be inhibited, but also hyper-physiological concentrations (20mM) seemed to decrease matrix deposition compared to super-physiological glucose levels (5mM < [glucose] < 10mM). Thus, between the gradients tested in this study the 20-5 condition appeared to be the best candidate to conduct further experiments with to determine the exact influence of long term cultures in nutrient gradients.

Discussion

Morphogen gradients are known to play important roles in cell migration, proliferation and terminal differentiation [23-25]. However, the influence of nutrient gradients on differentiation and tissue formation is still largely unknown. Glucose is one of the most important energy sources for chondrocytes as reviewed by Mobasheri [6]. Heywood *et al.* has studied the influence of the glucose concentration on chondrocyte behavior in a 3D environment [8]. Mathematically, glucose and oxygen gradients have been modeled assuming an equal consumption rate throughout a construct [7, 12]. Therefore, in our computational models the consumption rate of the 20mmol/L condition was also considered homogeneous as it could not be estimated from which depth chondrocytes would exert a different consumption rate. However, our experimental results suggest that bovine chondrocytes, even in a population in which chondrocytes from all zones were mixed, consume glucose at a higher rate at lower availability of this nutrient. This is similar to their oxygen consumption profile [26, 27, 28]. Further, we found that matrix production rates improved, independently from the oxygen concentration, under moderate glucose concentrations when compared to high and low concentrations. Thus, it can be concluded that culturing cells in a low glucose concentration creates an environment that is energetically more favorable for maintenance of the chondrocyte phenotype. The exact influence on the energy metabolism in a physiological glucose environment *in vitro* is not completely clear [28, 29]. Although chondrocytes predominantly exhibit an anaerobic metabolism, adenosine triphosphate (ATP) is produced by chondrocytes' mitochondria [30]. In this context, mitochondrial dysfunction has been associated with degenerative cartilage diseases like Kashin-Beck disease and osteoarthritis as reviewed by Blanco *et al.* [31, 32].

In the presence of a glucose gradient that induced a distribution to concentrations as low as physiological concentrations (20-5 condition), matrix production was enhanced in the regions in which the glucose concentration approached physiological levels. It was assumed that in those regions also the oxygen concentration ($[O_2]$) was lowest as the polycarbonate plates are impermeable for oxygen. In constructs that had a high glucose concentration in the regions with a low $[O_2]$ (20-20 condition), the chondrogenic capacity (GAG/DNA) decreased compared to 20-5 condition. In addition, in a gradient in which the bottom zone was deprived of glucose (20-0

condition) GAG/DNA values further decreased in those regions. This confirms and extends the above discussed hypothesis that low glucose concentrations create an environment to which chondrocytes can adapt more easily *in vitro*.

In this chapter, we show that a zonal distribution of GAG/DNA can be achieved by culturing bovine chondrocytes in a glucose gradient and the GAG/DNA distribution of native cartilage can be recreated [28]. However, a cartilaginous construct is not only defined by the GAG/DNA gradient. The zonal distribution and architecture of collagen fibers is also important to reconstitute proper tissue function. Collagen production has been reported to be upregulated under mechanical stimulation in bioreactor cultures [33, 34]. A zone-specific protein that is also upregulated by mechanical stimulation is lubricin, which is excreted to the synovial fluid to make it more viscous [35]. To determine the progression of the zonal development of a construct, gene expression and production of other zone specific proteins such as superficial zone protein (SZP), cartilage intermediate layer protein (CILP) and cartilage oligomeric matrix protein (COMP) should be considered as a next step in this analysis [2, 36, 37]. Furthermore, even endochondral ossification could be a target to improve construct integration upon implantation.

To summarize, we show in this proof-of-principle study how nutrient gradients can be used for zonal differentiation of chondrocytes. For further development of a cartilaginous construct these gradients can be combined with growth factor gradients to induce the upregulation of zone-specific proteins and further cellular maturation can be established by mechanical compression. This will enhance collagen production and zonal structure, which will be the focus of future work.

References

1. Huang, C.Y., et al., Experimental verification of the roles of intrinsic matrix viscoelasticity and tension-compression nonlinearity in the biphasic response of cartilage. J Biomech Eng, 2003. 125(1): p. 84-93.
2. Schumacher, B.L., et al., A novel proteoglycan synthesized and secreted by chondrocytes of the superficial zone of articular cartilage. Arch Biochem Biophys, 1994. 311(1): p. 144-52.
3. Ito, T., et al., Hyaluronan regulates transforming growth factor-beta1 receptor compartmentalization. J Biol Chem, 2004. 279(24): p. 25326-32.
4. Woodfield, T.B., et al., Polymer scaffolds fabricated with pore-size gradients as a model for studying the zonal organization within tissue-engineered cartilage constructs. Tissue Eng, 2005. 11(9-10): p. 1297-311.
5. Prydz, K. and K.T. Dalen, Synthesis and sorting of proteoglycans. J Cell Sci, 2000. 113 Pt 2: p. 193-205.
6. Mobasheri, A., Glucose: an energy currency and structural precursor in articular cartilage and bone with emerging roles as an extracellular signaling molecule and metabolic regulator. Front Endocrinol (Lausanne), 2012. 3: p. 153.
7. Zhou, S., Z. Cui, and J.P. Urban, Nutrient gradients in engineered cartilage: metabolic kinetics measurement and mass transfer modeling. Biotechnol Bioeng, 2008. 101(2): p. 408-21.
8. Heywood, H.K., D.L. Bader, and D.A. Lee, Glucose concentration and medium volume influence cell viability and glycosaminoglycan synthesis in chondrocyte-seeded alginate constructs. Tissue Eng, 2006. 12(12): p. 3487-96.
9. Malda, J., et al., Oxygen gradients in tissue-engineered PEGT/PBT cartilaginous constructs: measurement and modeling. Biotechnol Bioeng, 2004. 86(1): p. 9-18.
10. Marcus, R.E., The effect of low oxygen concentration on growth, glycolysis, and sulfate incorporation by articular chondrocytes in monolayer culture. Arthritis Rheum, 1973. 16(5): p. 646-56.
11. Marcus, R.E. and V.M. Srivastava, Effect of low oxygen tensions on glucose-metabolizing enzymes in cultured articular chondrocytes. Proc Soc Exp Biol Med, 1973. 143(2): p. 488-91.
12. Sengers, B.G., et al., Computational study of culture conditions and nutrient supply in cartilage tissue engineering. Biotechnol Prog, 2005. 21(4): p. 1252-61.
13. Fermor, B., A. Gurumurthy, and B.O. Diekman, Hypoxia, RONS and energy metabolism in articular cartilage. Osteoarthritis Cartilage, 2010.
14. Strobel, S., et al., Anabolic and catabolic responses of human articular chondrocytes to varying oxygen percentages. Arthritis Res Ther, 2010. 12(2): p. R34.
15. Rosa, S.C., et al., Expression and function of the insulin receptor in normal and osteoarthritic human chondrocytes: modulation of anabolic gene expression, glucose transport and GLUT-1 content by insulin. Osteoarthritis Cartilage, 2011. 19(6): p. 719-27.
16. Rosa, S.C., et al., Role of glucose as a modulator of anabolic and catabolic gene expression in normal and osteoarthritic human chondrocytes. J Cell Biochem, 2011. 112(10): p. 2813-24.
17. Yu, S.M., H.A. Kim, and S.J. Kim, 2-Deoxy-D-glucose regulates dedifferentiation through beta-catenin pathway in rabbit articular chondrocytes. Exp Mol Med, 2010. 42(7): p. 503-13.
18. Spitters, T.W., et al., A dual flow bioreactor with controlled mechanical stimulation for cartilage tissue engineering. Tissue Eng Part C Methods, 2013.
19. Higuera, G.A., et al., In vivo screening of extracellular matrix components produced under multiple experimental conditions implanted in one animal. Integr Biol (Camb), 2013. 5(6): p. 889-98.
20. Allhands, R.V., P.A. Torzilli, and F.A. Kallfelz, Measurement of diffusion of uncharged molecules in articular cartilage. Cornell Vet, 1984. 74(2): p. 111-23.
21. Obradovic, B., et al., Gas exchange is essential for bioreactor cultivation of tissue engineered cartilage. Biotechnol Bioeng, 1999. 63(2): p. 197-205.
22. Markway, B.D., H. Cho, and B. Johnstone, Hypoxia promotes redifferentiation and suppresses markers of hypertrophy and degeneration in both healthy and osteoarthritic chondrocytes. Arthritis Res Ther, 2013. 15(4): p. R92.
23. Cho, H.S., et al., Individual variation in growth factor concentrations in platelet-rich plasma and its influence on human mesenchymal stem cells. Korean J Lab Med, 2011. 31(3): p. 212-8.
24. Kim, H.K., I. Oxendine, and N. Kamiya, High-concentration of BMP2 reduces cell proliferation and increases apoptosis via DKK1 and SOST in human primary periosteal cells. Bone, 2013. 54(1): p. 141-50.
25. Zhang, J. and Y. Li, Fibroblast growth factor 21, the endocrine FGF pathway and novel treatments for metabolic syndrome. Drug Discov Today, 2013.

26. Heywood, H.K., M.M. Knight, and D.A. Lee, Both superficial and deep zone articular chondrocyte subpopulations exhibit the Crabtree effect but have different basal oxygen consumption rates. J Cell Physiol, 2010. 223(3): p. 630-9.
27. Rajpurohit, R., et al., Adaptation of chondrocytes to low oxygen tension: relationship between hypoxia and cellular metabolism. J Cell Physiol, 1996. 168(2): p. 424-32.
28. Heywood, H.K., et al., Cellular utilization determines viability and matrix distribution profiles in chondrocyte-seeded alginate constructs. Tissue Eng, 2004. 10(9-10): p. 1467-79.
29. Heywood, H.K., D.L. Bader, and D.A. Lee, Rate of oxygen consumption by isolated articular chondrocytes is sensitive to medium glucose concentration. J Cell Physiol, 2006. 206(2): p. 402-10.
30. Martin, L.J., Biology of mitochondria in neurodegenerative diseases. Prog Mol Biol Transl Sci, 2012. 107: p. 355-415.
31. Blanco, F.J., I. Rego, and C. Ruiz-Romero, The role of mitochondria in osteoarthritis. Nat Rev Rheumatol, 2011. 7(3): p. 161-9.
32. Li, S., et al., Proteoglycan metabolism, cell death and Kashin-Beck disease. Glycoconj J, 2012. 29(5-6): p. 241-8.
33. Buschmann, M.D., et al., Mechanical compression modulates matrix biosynthesis in chondrocyte/agarose culture. J Cell Sci, 1995. 108 (Pt 4): p. 1497-508.
34. Kock, L.M., et al., Tuning the differentiation of periosteum-derived cartilage using biochemical and mechanical stimulations. Osteoarthritis Cartilage, 2010. 18(11): p. 1528-35.
35. Grad, S., et al., Chondrocyte gene expression under applied surface motion. Biorheology, 2006. 43(3-4): p. 259-69.
36. Bernardo, B.C., et al., Cartilage intermediate layer protein 2 (CILP-2) is expressed in articular and meniscal cartilage and down-regulated in experimental osteoarthritis. J Biol Chem, 2011. 286(43): p. 37758-67.
37. Zaucke, F., et al., Cartilage oligomeric matrix protein (COMP) and collagen IX are sensitive markers for the differentiation state of articular primary chondrocytes. Biochem J, 2001. 358(Pt 1): p. 17-24.

5

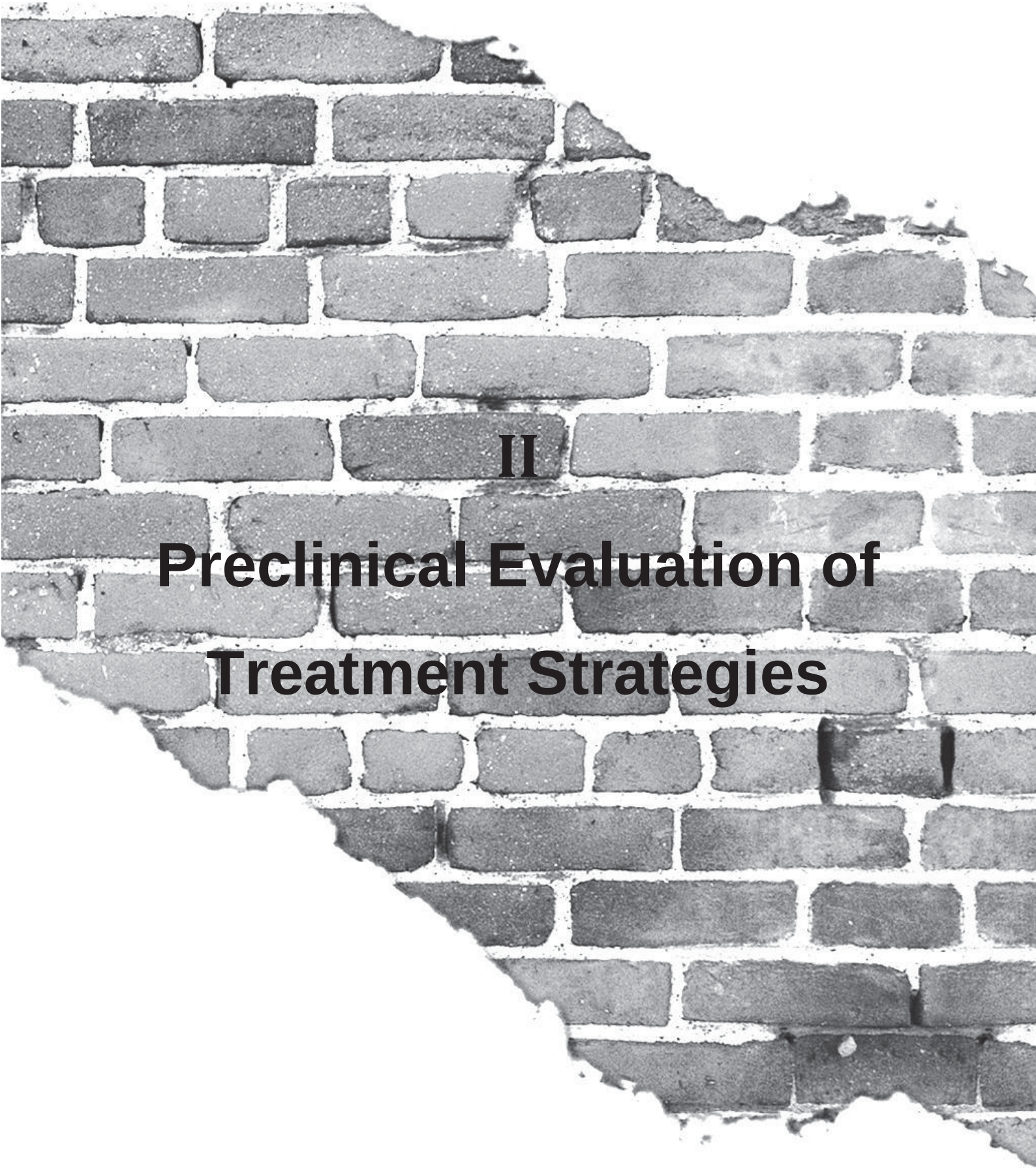

II

Preclinical Evaluation of Treatment Strategies

ka warea te ware. ka akea te rangarita.
(Onwetenheid is de onderdrukker. Waakzaamheid de bevrijder.)
(Ignorance the oppressor. Vigilance the liberator.)
Tiki Taane, Maori Singer

Chapter 6
Delivery of Small Molecules from a Drug Delivery System into Articular Cartilage is Dependent on Synovial Clearance and Cartilage Loading

Tim W.G.M Spitters, Dimitrios Stamatialis, Audrey Petit, Mike G.W. de Leeuw, Marcel Karperien

Abstract

Purpose: Determine the influence of synovial clearance, the amount of compressive load, the frequency, and tissue relaxation on small molecule delivery into articular cartilage.

Methods: Bromophenol blue (BPB) loaded hydrogels were placed on top of bovine articular cartilage explants and were compressed in a dual flow bioreactor. Subsequently, dye penetration in the tissue was visualized by microscopic evaluation and coefficients were estimated based on Fick's law.

Results: Mimicking synovial clearance revealed that dye penetration of BPB when released from a drug delivery system placed on top of a cartilage explant was enhanced compared to direct injection of bromophenol blue into a simulated synovial fluid. The data suggest that the dye penetrated the tissue faster under static conditions compared to continuous compression.

Conclusions: In this study we show the penetration behavior of a model small molecule into articular cartilage under compressive conditions. We also show the beneficial effect of injecting a drug depot compared to conventional intra-articular injection. This study offers new insights in small molecule delivery in articular cartilage aiding in the development of new therapies for treatment of degenerative diseases like osteoarthritis.

Keywords: physically crosslinked hydrogel, drug delivery, bioreactor, osteoarthritis, intra-articular

Introduction

Osteoarthritis (OA) is a degenerative disease that affects articular cartilage and surrounding tissues in the joint [1-4]. Evidence is accumulating that aberrant joint loading is one of the causative factors initiating the onset of OA [5-9]. Unloading of the joint by distraction has been hypothesized as a possibility to trigger a regenerative response by the body [10-13]. In this procedure, the femur and tibia are pulled from each other thereby decreasing the compressive load on the affected tissue [7]. In animal models it showed promising results and is now being evaluated in a clinical setting, where also positive results are obtained [14-19]. This technique is, however, highly invasive. Therefore, less invasive treatment options need to be explored. Common practice entails still oral and intra-articular drug administration, which aim at alleviating pain and other clinical symptoms to improve quality of life [20-24]. Although short-term pain relieve is achieved after intra-articular drug administration, patients require recurring injections to stay pain-free, as drugs are quickly cleared from the synovial fluid [25]. Therefore, the injected dose is usually high and the effect of these recurrent high doses are not well known. Currently, attempts are made to boost matrix production by injecting matrix components or growth factors [26, 27].

To avoid high doses on can inject a depot, so called drug delivery systems (DDSs), to locally deliver drugs (bulk or micro-encapsulated) over a prolonged period of time. This can be a suitable treatment as most OA affected joints are amenable for intra-articular injection [28-33]. The depot ensures longer retention of the drug in the joint which is slowly released. Consequently lower dosages can be used [21, 34, 35]. A tailored release, depending on material properties, is established by diffusion of the molecules from the DDS and the degradation of the material. Characterization of these systems is often done *in vitro* by assessing their degradation behavior and their release profile [36-39]. Moreover, these tests are done under static conditions which do not simulate the loaded environment the depot will be subjected to *in vivo*.

Due to a shortage of data on the behavior of drugs in the knee cavity after injection, there is also little known to which extent a drug penetrates into the cartilage tissue. The depth of penetration and its action under mechanical loading are largely unknown. Therefore, emphasis is put on creating an *in vitro* environment that can simulate key characteristics of the native joint environment, such as nutrient supply

and mechanical stimulation. These systems then can aid in the evaluation of drug delivery systems in a simulated joint environment prior to *in vivo* testing. Previously, our group has reported on a dual flow bioreactor in which articular cartilage could be supplied with nutrients from both the synovial and the subchondral sides. In addition, it is equipped to apply cyclic mechanical stimulation thus creating an environment that simulates the knee joint in two important aspects [40]. In the present work, this system is used to investigate the penetration behavior of a small molecule model compound, bromophenol blue, from a hydrogel into cartilage under compressive and hydrodynamic stimuli. The drug delivery system is added to the synovial side of the explant simulating the clinical intra-articular application and subsequently mechanical stimulation is applied. Since the hydrogel is loaded with bromophenol blue, the effect of different conditions of drug uptake by articular cartilage could be evaluated. These data can be used to determine the applicability of drug delivery systems in the knee joint further aiding in their development for clinical use.

Materials and methods

Hydrogel production

Poly(carprolactone-L-lactic acid) - poly(ethyleneglycol) - poly(carprolactone-L-lactic acid) (PCLA-PEG-PCLA) triblock copolymers were prepared by ring-opening copolymerization of caprolactone and L-lactide initiated by the PEG hydroxyl endgroups. Stannous octoate was used as a catalyst. In the second step these triblocks were hydrophobically endcapped through acetylation with an excess of acetyl chloride in the presence of triethylamine as described previously [41-43].

For the specific polymer used in these experiments the following procedure was used.

Under a nitrogen atmosphere, PEG_{1500} (20 g), ε-caprolactone (35.2 g) and L-lactide (8.8 g) were dissolved in 150 ml toluene, and dried through azeotropic distillation using a Dean Stark trap. Circa 120 ml toluene was removed by distillation.

The stirred mixture was cooled to ca. 100°C, followed by the addition of stannous octoate (0.4 ml). The mixture was stirred overnight at 120°C, after which it was allowed to cool to ambient temperature.

Dichloromethane (100 ml) was added, followed by the addition of triethylamine (9 ml). After stirring for 15 minutes at ambient temperature, excess of acetyl chloride (4 ml) was added drop by drop. The obtained mixture was stirred for 4 hours at ambient temperature.

The volatiles were evaporated under reduced pressure, followed by the addition of ethyl acetate (300 ml). After stirring for 5 minutes the mixture was filtered over a P3-glasfilter to remove triethylamine hydrochloride. Hexane was added until a precipitate was formed. The obtained mixture was stored in the freezer for 3 hours and the solvents were then decanted from the polymer. The polymer was dried under vacuum. The yield was ca. 80%.

For visualization purposes the gel was loaded with 0.025wt% bromophenol blue (BPB, a hydrophobic molecule of 670Da which is used as a model for small molecules; in comparison triamcinolone acetonide, a drug used in the palliative treatment of OA, has a molecular size of 395Da).

In vitro evaluation

Material source

Knees of 10-12 month old calves were collected from the local abattoir. Femoral condyles were exposed by removing the muscles and patella. Then, cartilage slices were made with a custom made slicer and cubical explants were punched from these slices and put into four chamber polycarbonate insert as described previously [40].

Explants culture

Three drops of hydrogel (26.5μL) loaded with bromophenol blue (BPB) (Figure 1A) were placed on the surface of the cartilage explants. Explants were placed in a custom designed bioreactor published previously (Figure 1B) [40], and compressed for 1 hour with varying load (F) (0.05MPa, 0.25MPa and 0.5MPa, at constant frequency (f) of 0.33Hz, compression time per cycle 50%). In the same manner distinct frequencies were tested (0.1, 0.33, and 1 Hz, at constant load F=0.25MPa, compression time per cycle 50%). To investigate the effect of free swelling conditions and continuous compression on BPB penetration, explants were either subjected to 1, 6, 9 or 24 hour of static culture or continuous compression (F=0.25MPa and f=0.33Hz, 3x compression cycles).

The influence of clearance was investigated by either direct injection of dissolved BPB (0,025wt%) in medium at the top compartment or placing a hydrogel loaded with an equimolar concentration of BPB on top of the explants. Then, the bioreactor was connected to a syringe pump as described previously [40] and medium flow was applied at 0.5mL/min. Medium in the syringes was changed every 20 minutes for 1 hour.

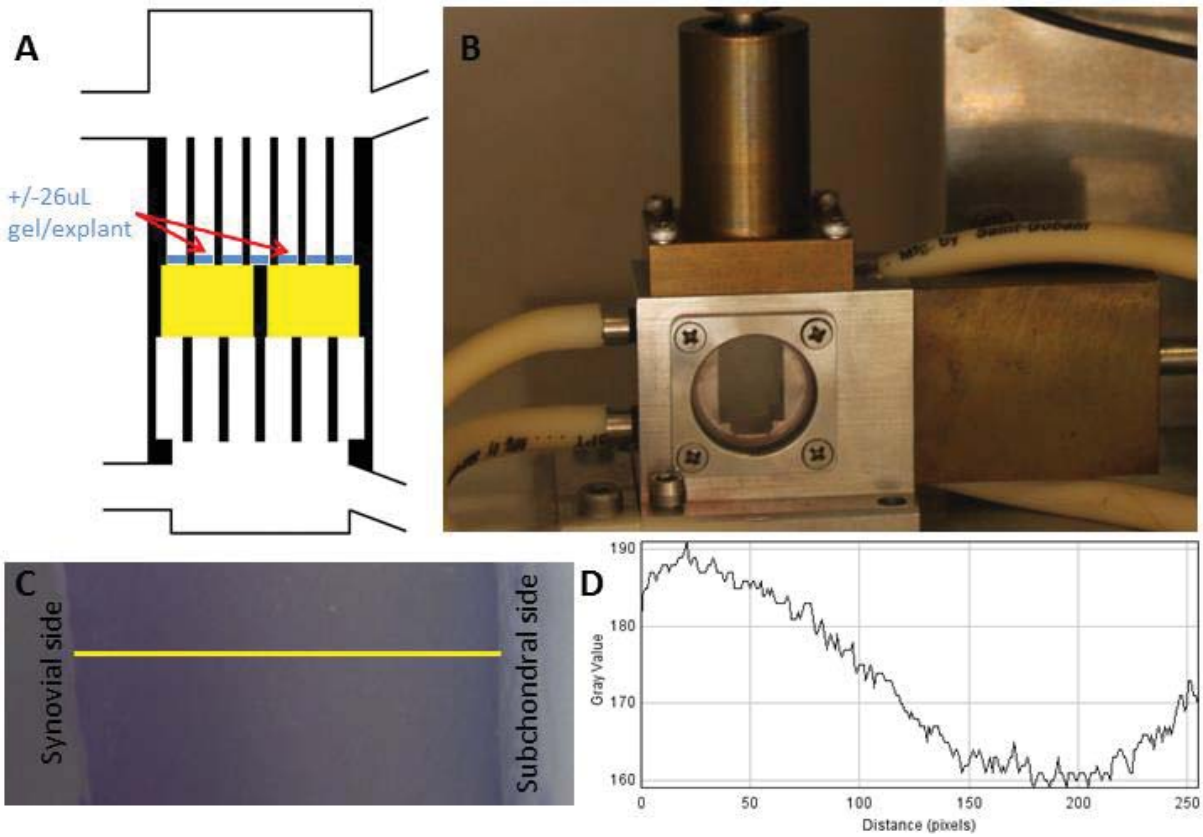

Figure 1: dual flow bioreactor for the evaluation of drug delivery systems. (A) Dual flow bioreactor, (B) schematic overview of the bioreactor chamber with the cartilage explants depicted in yellow and the loaded gel in blue as situated at the start of each condition, (C) an explant after treatment showing the blue color . The yellow line depicts the line along which (D) a plot profile was made.

Macroscopic evaluation

Directly after compression, explants were dissected and BPB stain in the middle of the explant was evaluated by stereomicroscopy (Nikon, Japan) and pictures were taken with Q-capture acquisition software (Figure 1C). After these pictures were grayscaled, a plot profile was made along the middle line (synovial to subchondral side) of the explant with ImageJ software (Figure 1C (yellow line) and 1D). Fick's law was used to estimate the diffusion coefficient after static release and release after continuous and discontinuous compression.

Estimation of the diffusion coefficient using Fick's law

When it is assumed that in a region -L < x < L the concentration of the molecule at t=0 is C_0 and at the surfaces the concentration is kept constant at C_1, the solution of Crank *et al.* can be considered. This assumes a system of non-steady state diffusion with uniform initial distribution and equal surface concentration [44].

$$\frac{C-C_0}{C_1-C_0} = 1 - \frac{4}{\pi}\sum_{n=0}^{\infty}\frac{(-1)^n}{2n+1} exp\left\{\frac{-D(2n+1)^2\pi^2 t}{4L^2}\right\} cos\frac{(2n+1)\pi x}{2L} \quad (1)$$

When n is assumed 0, equation 1 becomes:

$$\frac{C_1-C}{C_1-C_0} = \frac{4}{\pi} exp\left\{\frac{-D\pi^2 t}{4L^2}\right\} cos\frac{\pi x}{2L} \quad (2)$$

To enable calculation of the diffusion coefficient D, equation 2 can be written as [45, 46]:

$$ln\frac{C_1-C}{C_1-C_0} = \ln\left(\frac{4}{\pi} cos\frac{\pi x}{2L}\right) - \frac{D\pi^2}{4L^2} t \quad (3)$$

Assuming that the grayscale plot profile represents a concentration profile, the concentration term in equation 3 also can be written as a grayscale ratio [45, 46]:

$$ln\frac{G_1-G}{G_1-G_0} = \ln\left(\frac{4}{\pi} cos\frac{\pi x}{2L}\right) - \frac{D\pi^2}{4L^2} t \quad (4)$$

When $\ln(G_1\text{-}G)/(G_1\text{-}G_0)$ is plotted against time, the slope of this plot gives the diffusion coefficient [45, 46]:

$$slope = -\frac{D\pi^2}{4L^2} t \quad (5)$$

where G is the gray value at point x along the middle line, G_0 is the lowest gray value along the middle line and G_1 is the highest gray value along the middle line, 2L is the total length of the explant (m), x is the position in the explant where the diffusion constant is determined (m), D is the diffusion coefficient (m^2/s) and t is time (s).

Results

Effect of clearance on the penetration of bromophenol blue (BPB) into articular cartilage

We studied BPB penetration in articular cartilage after injection of an aqueous solution BPB or release of an equimolar concentration of BPB from a gel in a bioreactor in which synovial clearance, the turnover of synovial fluid, is mimicked. Visual inspection confirmed that BPB penetrated further into the cartilage when released from the gel compared to the dye that was injected in the synovial compartment (standard condition) (insets Figure 2). Quantification of the BPB distribution within the cartilage showed distinct profiles with a sharp peak close to the cartilage surface and fast declining slope in the standard condition, whereas the profile in the gel condition showed a broader peak at the synovial side and a slow declining slope (Figure 2). This indicated that bromophenol blue delivery from the gel was higher compared to the injection of an equimolar concentration of dissolved bromophenol blue in the medium compartment resembling the synovial fluid.

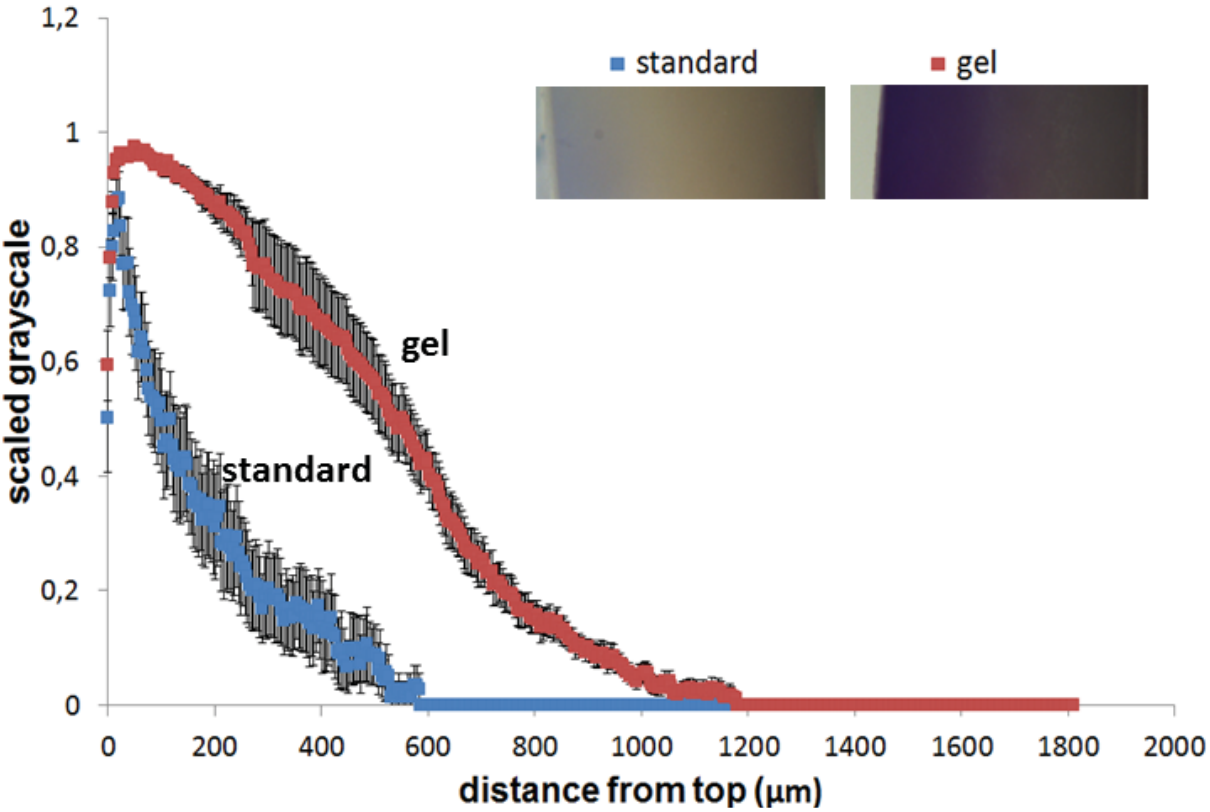

Figure 2: Influence of clearance on static bromophenol blue (BPB) delivery into articular cartilage after 1 hour. The graph represents the scaled mean grayscale profiles of BPB concentration into an explant. Insets represent explants of each condition with the synovial side on the left. Error bars represent the standard error of the mean, n=12 explants.

In an experiment using the gel setting but omitting clearance, a profile similar to the one of the gel condition in Figure 2 was observed (data not shown). This indicated that the clearance itself did not have an influence on the release behavior of BPB from the gel and was therefore not taken into account in subsequent experiments.

Effect of release duration on bromophenol blue (BPB) concentration profile within cartilage

Next, we determined how the BPB distribution changes through cartilage over time. The obtained profiles after 1, 6 and 9 hours of release without compression showed distinct profiles including a plateau that increased in length at the synovial side indicating a further penetration of the highest BPB concentration as well as a broader BPB distribution as observed by the steepness of the curve (Figure 3). It seemed that after 9 hours the BPB concentration profile did not change significantly compared to the profile after 24 hours (Figure 3). This was probably due to saturation of the tissue. These graphs show how a small molecule drug could be distributed through cartilage

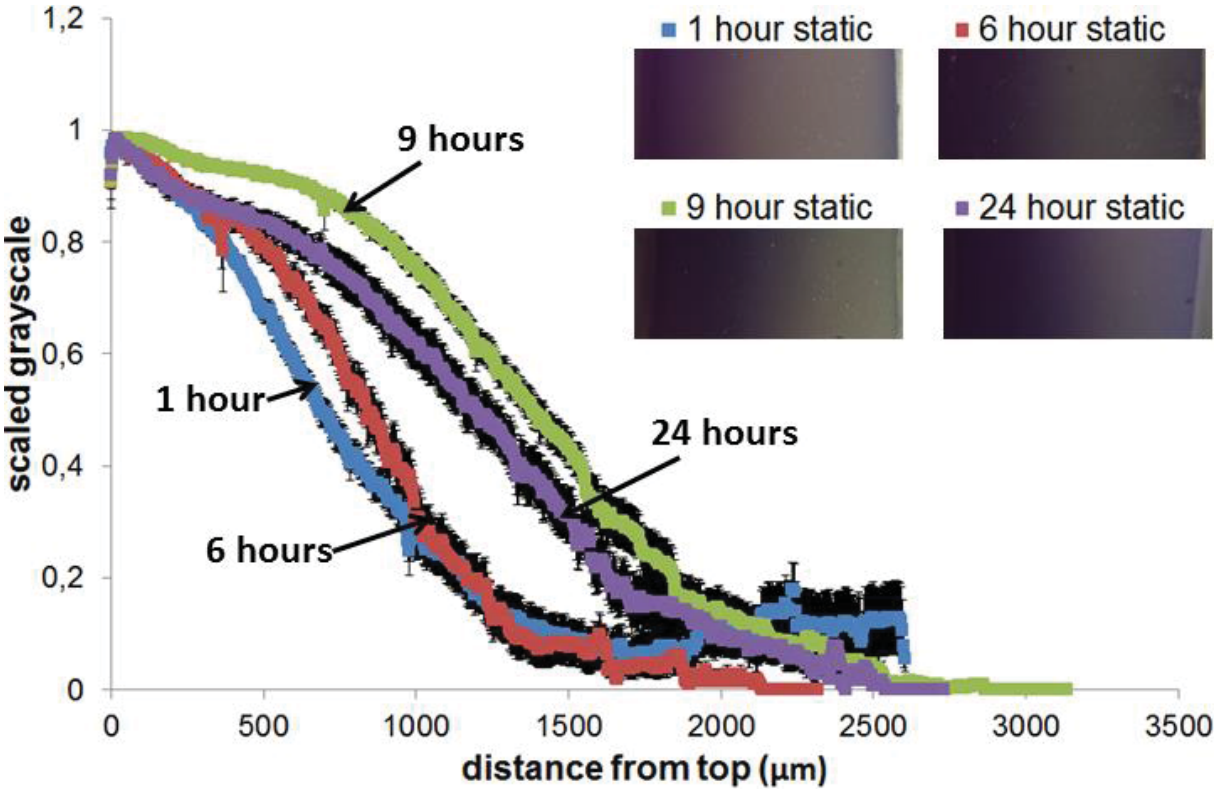

Figure 3: Characterization of the concentration profile of bromophenol blue (BPB) into articular cartilage after static incubation. The graph represents the scaled mean concentration profiles of BPB in an articular explant. Error bars represent the standard error of the mean, n=12 explants. Insets represent explants of each condition with the synovial side on the left.

tissue when a patient is not allowed to use the joint for up to 24 hours after injection of a drug depot in the knee cavity without taking synovial clearance into account.

Effect of load and frequency on bromophenol blue (BPB) penetration

When after 1 hour of compression with varying loads the concentration distribution profiles were compared, the main difference observed was that after compression with 0.05MPa the profile seemed similar to the one where no compression was applied. Under the other two conditions the profile seemed steeper. However, no significant differences were detected between the distribution profiles (Figure 4A). When the frequency was varied, a similar observation was made. After 1 hour of compression no significant differences were observed between the conditions in the distribution profiles, although under all frequencies the profiles tended to be lower compared to the non-compressed condition (Figure 4B). So, within the range of load and frequency applied in this study no differences were apparant. However, what seemed to be consistent was that the penetration of BPB under compression seemed less pronounced compared to conditions without compression (comparing the blue line with the other lines in Figure 4A and 4B) except for 0.05MPa condition. To investigate if this effect would also appear when the delivery period was prolonged, we determined the BPB profile under continuous compression over time.

Effect of free swelling and continuous compression on bromophenol blue (BPB) penetration

When the BPB profiles within the explant were compared following 6, 9 and 24 hours of continuous compression, a peak near the articular surface was observed. However, the slope after 9 and 24 hours was found to be less steep compared to that at 6 hours with the 24 hour profile being lower than the 9 hour profile (Figure 5). This finding was comparable to the trend seen after static treatment (Figure 3). Further comparison of these two figures showed that the high concentration at the synovial side ran further into the tissue when no compression was applied (Figure 3).

These data show that BPB penetration into cartilage decreases when the tissue is compressed. We hypothesize this could be enhanced by allowing the tissue to relax and regain its original form. This would induce transport of water molecules and solutes from the synovial cavity into the cartilage matrix due to mechanical stimulation. However, it should be further investigated how the penetration profile

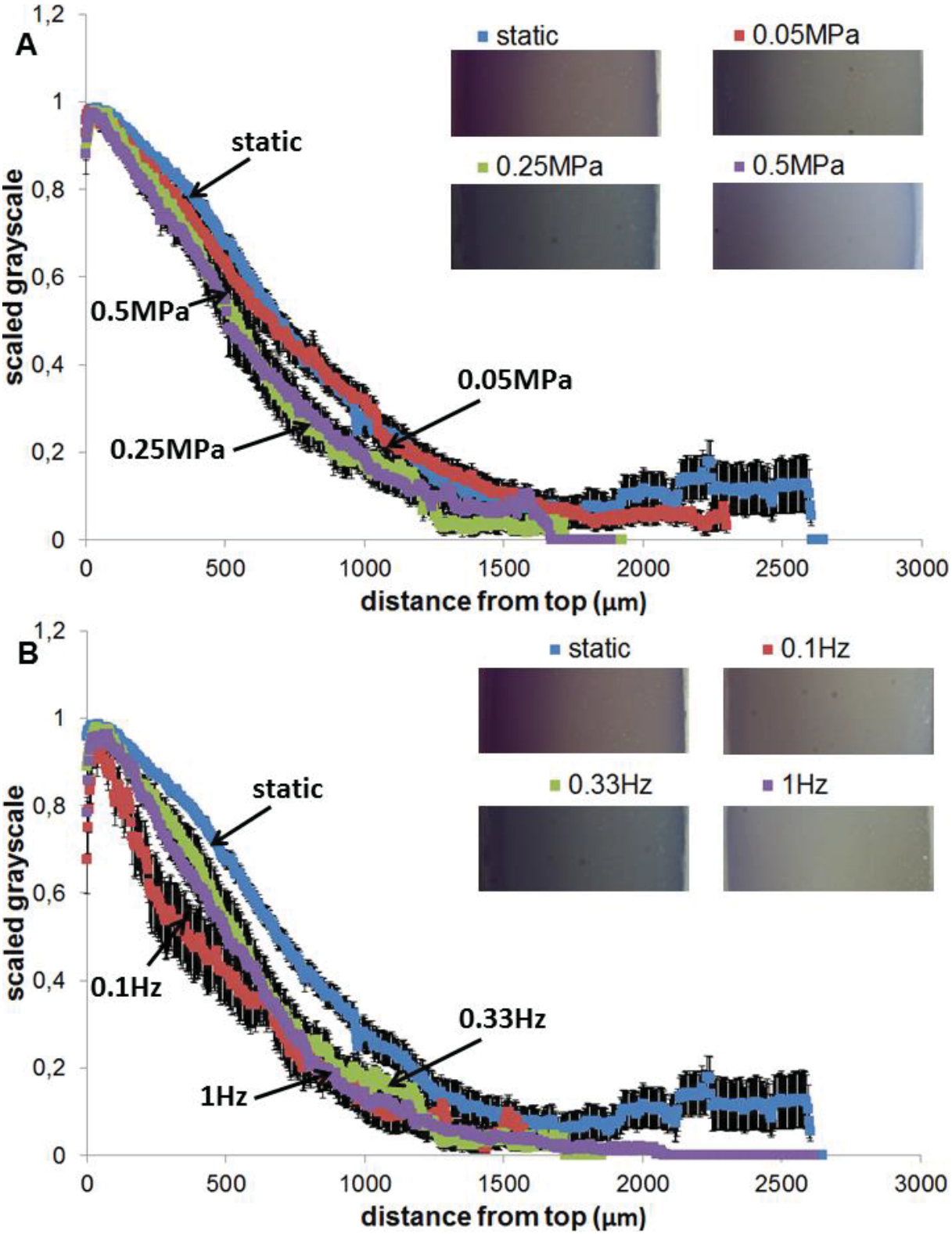

Figure 4: Influence of the amount of load (f=0.33Hz) and frequency magnitude (F=0,25MPa) on bromophenol blue (BPB) penetration in articular cartilage after 1 hour. (A) Scaled mean concentration profiles of BPB in an articular explant. Error bars represent the standard error of the mean, n=12, 9, 10 and 10 respectively. (B) Scaled mean concentration profiles of BPB in an articular explant. Error bars represent the standard error of the mean, n=12, 12, 10 and 12 respectively. Insets represent explants of each condition with the synovial side on the left.

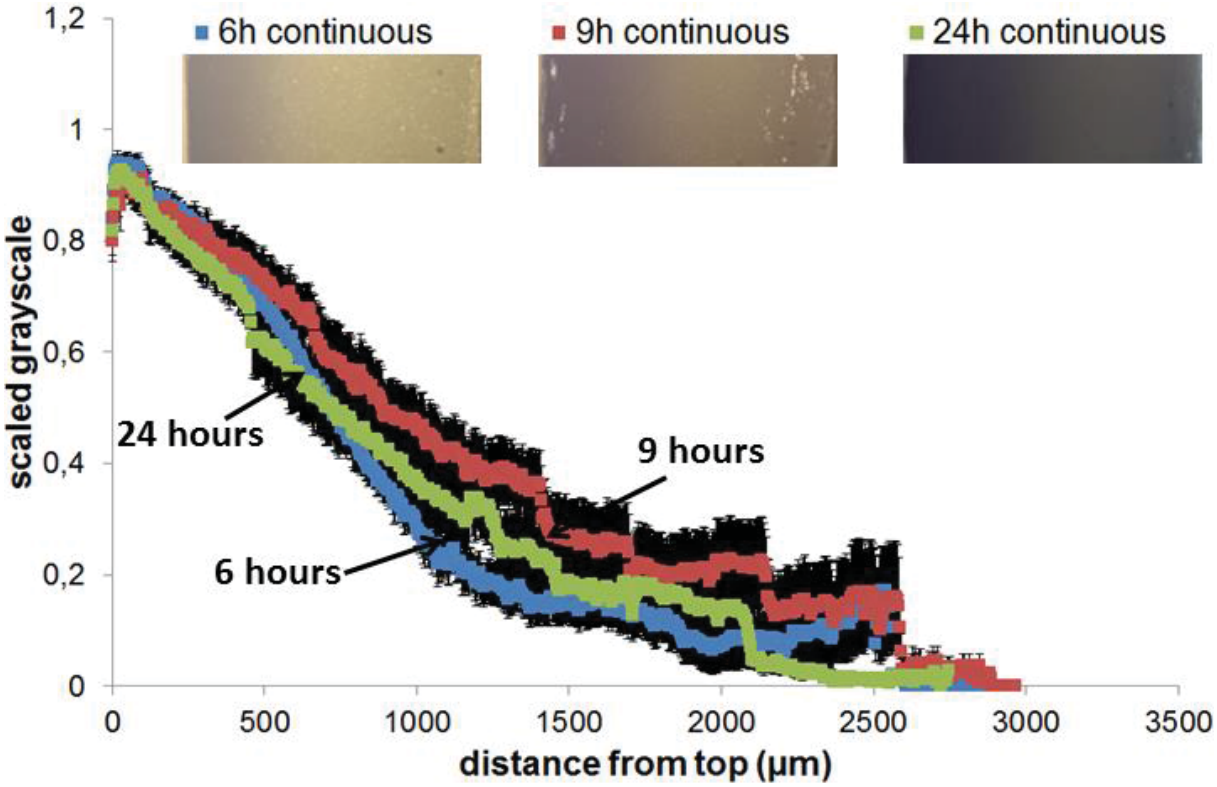

Figure 5: Influence of continuous compression on bromophenol blue (BPB) penetration into articular cartilage, F=0.25MPa, f=0.33Hz. The graph represents the scaled mean concentration profiles of BPB in an explant. Error bars represent the standard error of the mean, n=12. Insets represent explants of each condition with the synovial side on the left.

would look like when a cartilage explant is discontinuously compressed (i.e. a compression period followed by a rest period).

Estimation of the diffusion coefficients

As equation 4 shows, ln(G1-G)/(G1-G0) is a function of time t. Therefore, it was only possible to estimate the diffusion coefficient (D) at two conditions, BPB penetration after static (D(static)) release in Figure 3 and after continuous compression (D(comp)) in Figure 5. Both values were calculated at x = 1000µm. A trend line was fitted through the data points of each condition and the slope was used to calculate D according to equation 5, resulting in D(static) = $3.86*10^{-12}$ m^2/s +/- $1.47*10^{-12}$ and D(comp) = $2.04*10^{-12}$ m^2/s +/- $1.43*10^{-12}$.

Table 1 compares the diffusion coefficients of BPB (670Da) found in this study to diffusion coefficients of molecules into cartilage matrix under compressive conditions. Diffusion of tetramethylrhodamine (TMR, 430Da) into compressed bovine explants was found to be twenty five times higher compared to our findings [47, 48]. There could be several reasons for this difference: i) the diffusion matrix; TMR was allowed

to diffuse through a 650µm cartilage sheet consisting mainly of the intermediate zone, whereas in this study full thickness cartilage explants were used or ii) the mobility of the solute; TMR was administered in an aqueous solution, whereas BPB was encapsulated in a hydrogel. Alexa-hydrazide (570Da) was found to diffuse approximately one hundred times faster into a hyaluronic acid network from an aqueous solution under non-compressed conditions [49]. Collagen condenses an intact cartilage matrix resulting in lower diffusivity of solutes. This can explain the difference in diffusion coefficients. In the same study it was found that Alexa-albumin (66kDa) diffused faster into an enzymatically degraded cartilage matrix [49]. This showed that it is the complex structure of the cartilage extracellular matrix that determines the diffusion coefficient of solutes instead of just one.

Table 1: Comparison of diffusion constants in compressed articular cartilage.

Molecule	Specimen	T (°C)	Administration	Compression	D (x10^{-10} m^2/s)	Ref
Tetramethylrhodamine (430Da)	Bovine explant	4	Direct injection	+	0.52 ± 0.06	[47,48]
Fluorescein isothiocyante (FITC) tagged dextran (70kDa)	Porcine explant	?	Direct injection	+ -	0.07 0.33	[62]
Alexa-hydrazide (570Da)	HA (MW 8x10^5) HA (MW 20x10^5)	25	Direct injection	- -	~2.25 ~2.1	[49]
Alexa-albumin (66kDa)	Porcine explant	25	Direct injection	-	0.2	[49]
Bromophenol blue (670Da)	Bovine explant	37	Hydrogel injection	+ -	0.02 ± 0.01 0.04 ± 0.01	This study

Cartilage is an anisotropic tissue. Gradients of the two main matrix components, collagen type II and glycosaminoglycans, run through the tissue from synovial to subchondral side and vice versa, respectively [50]. The peak near the articular surface, which was consistent in all experiments, can be explained by BPB accumulation in this region. This means that the diffusion was delayed creating a depot in the superficial zone. This could be related to the locally high density of the collagen network. The gradual decline in the profile suggests that with increasing glycosaminoglycan concentration in the deeper zones of the matrix the retention of BPB in the cartilage matrix is decreased and thus its diffusion increased. This is consistent with the findings of Evans and Quinn [51].

Discussion

To the best of our knowledge this is the first in-depth study on the behavior of a drug depot for intra-articular injection under physiological relevant conditions *in vitro*. Drug depots have the potential to replace current drug administration approaches, as they can locally deliver a drug and release that drug for a longer time period as can be realized with conventional intra-articular injection in the treatment of osteoarthritis (OA) as reviewed by several investigators [52, 53]. Such treatment will result in prolonged activity of a drug and thus enhanced efficacy of the treatment. Most patients start using their joint shortly after the injection of the drug. However, it is yet unclear how mechanical compression affects the drug release and uptake. This raises the question if a physician should advise a patient to not or only minimally load the joint to enhance the penetration and action of the drug in cartilage. Therefore, in this study a drug delivery hydrogel was subjected to compressive loading to simulate the stimulation in the clinical situation and the resulting drug uptake by cartilage was evaluated.

Clearance of a drug by the synovial fluid can decrease the uptake of a drug as reviewed by Simkin [54]. In an environment that simulated clearance it was shown in our study that the uptake of bromophenol after conventional intra-articular injection was significantly decreased compared to injection of a gel depot. This was comparable to the findings of Jovanovic *et al.*, where they found that the delivery of silver particles under compression and convection was improved compared to release under static conditions [55]. It suggested that the concentration that can be achieved following direct injection may be lower than the minimal concentration required for the drug to work efficiently [56]. On the other hand, dye penetration from a drug depot did not seem to be hampered by clearance compared to the profile without clearance in our study.

Literature shows bioreactor studies that report values for load and frequency which induce chondrogenic differentiation and/or cartilage matrix production [57-60]. In this study, the influence of load and frequency after one hour of delivery of a small molecule was negligible compared to delivery without mechanical stimulation. Thus, to optimize the drug uptake in cartilage a patient should avoid mechanical loading of the joint directly after injection of the depot. Once uptake of a drug into cartilage has been achieved, the cartilage itself may function as a drug depot. Of note, the experiments reported in this study were performed with healthy young cartilage. Drug

penetration is determined by the composition of the tissue. Cartilage is an anisotropic tissue with varying matrix composition between superficial, middle and deep zones [50]. The estimation of the BPB diffusion coefficient and the peak near the articular surface in the BPB profiles under free swelling and continuous compression suggest that due to the complexity of the cartilage tissue its diffusion constant may not be considered homogeneous. Drug penetration is determined by several parameters such as water in- and outflow, interaction with the matrix and free diffusion. Thus, the water content as well as quantity and arrangement of matrix molecules determine the transportation and distribution within the tissue. During disease progression, the cartilage matrix degenerates and this will influence the drug uptake by cartilage. The choice of the drug for treatment should also be dependent on the degree of matrix degradation to optimize treatment outcome. Currently, techniques are developed to predict the stage of the disease, which can then be used to personalize the treatment options [61]. Another way to increase the penetration and retention of a drug in an affected joint could be achieved by enhancing the drug specificity with a moiety targeting one of the matrix components of cartilage or a drug loaded biomaterial that could attach to the degraded cartilage matrix.

Optimizing drug delivery into affected tissue is a current challenge in translational research as this will enhance our understanding and help elucidate the optimal strategy to treat patients suffering from a degenerating disease like osteoarthritis [55].

Conclusion

Our study showed that hydrogel drug depots can be the next step in an effective delivery of drugs into cartilage tissue and with favorable effects over conventional intra-articular injection. In addition, we showed that compression of cartilage will enhance drug delivery into the tissue. Further investigation will aid in developing a more patient-tailored treatment as a better understanding will allow us to determine how a drug specifically and efficiently can be delivered to each patient's tissue.

References

1. Aspden, R.M., *Osteoarthritis: a problem of growth not decay?* Rheumatology (Oxford), 2008. **47**(10): p. 1452-60.
2. Castaneda, S., et al., *Subchondral bone as a key target for osteoarthritis treatment.* Biochem Pharmacol, 2011.
3. Findlay, D.M., *Vascular pathology and osteoarthritis.* Rheumatology (Oxford), 2007. **46**(12): p. 1763-8.
4. Shim, V.B., et al., *A multiscale framework based on the physiome markup languages for exploring the initiation of osteoarthritis at the bone-cartilage interface.* IEEE Trans Biomed Eng, 2011. **58**(12): p. 3532-6.
5. Block, J.A. and N. Shakoor, *The biomechanics of osteoarthritis: implications for therapy.* Curr Rheumatol Rep, 2009. **11**(1): p. 15-22.
6. Brandt, K.D., P. Dieppe, and E. Radin, *Etiopathogenesis of osteoarthritis.* Med Clin North Am, 2009. **93**(1): p. 1-24, xv.
7. Lafeber, F.P., et al., *Unloading joints to treat osteoarthritis, including joint distraction.* Curr Opin Rheumatol, 2006. **18**(5): p. 519-25.
8. Radin, E.L., *Who gets osteoarthritis and why?* J Rheumatol Suppl, 2004. **70**: p. 10-5.
9. Wilson, D.R., E.J. McWalter, and J.D. Johnston, *The measurement of joint mechanics and their role in osteoarthritis genesis and progression.* Med Clin North Am, 2009. **93**(1): p. 67-82, x.
10. Felson, D.T., et al., *Weight loss reduces the risk for symptomatic knee osteoarthritis in women. The Framingham Study.* Ann Intern Med, 1992. **116**(7): p. 535-9.
11. Messier, S.P., et al., *Weight loss reduces knee-joint loads in overweight and obese older adults with knee osteoarthritis.* Arthritis Rheum, 2005. **52**(7): p. 2026-32.
12. Palmoski, M.J. and K.D. Brandt, *Immobilization of the knee prevents osteoarthritis after anterior cruciate ligament transection.* Arthritis Rheum, 1982. **25**(10): p. 1201-8.
13. Radin, E.L. and D.B. Burr, *Hypothesis: joints can heal.* Semin Arthritis Rheum, 1984. **13**(3): p. 293-302.
14. Intema, F., et al., *Subchondral bone remodeling is related to clinical improvement after joint distraction in the treatment of ankle osteoarthritis.* Osteoarthritis Cartilage, 2011. **19**(6): p. 668-75.
15. Intema, F., et al., *Tissue structure modification in knee osteoarthritis by use of joint distraction: an open 1-year pilot study.* Ann Rheum Dis, 2011. **70**(8): p. 1441-6.
16. Chiodo, C.P. and W. McGarvey, *Joint distraction for the treatment of ankle osteoarthritis.* Foot Ankle Clin, 2004. **9**(3): p. 541-53, ix.
17. Deie, M., et al., *A new articulated distraction arthroplasty device for treatment of the osteoarthritic knee joint: a preliminary report.* Arthroscopy, 2007. **23**(8): p. 833-8.
18. Morse, K.R., et al., *Distraction arthroplasty.* Foot Ankle Clin, 2007. **12**(1): p. 29-39.
19. Yanai, T., et al., *Repair of large full-thickness articular cartilage defects in the rabbit: the effects of joint distraction and autologous bone-marrow-derived mesenchymal cell transplantation.* J Bone Joint Surg Br, 2005. **87**(5): p. 721-9.
20. Bannuru, R.R., et al., *Therapeutic trajectory of hyaluronic acid versus corticosteroids in the treatment of knee osteoarthritis: a systematic review and meta-analysis.* Arthritis Rheum, 2009. **61**(12): p. 1704-11.
21. Bellamy, N., et al., *Intraarticular corticosteroid for treatment of osteoarthritis of the knee.* Cochrane Database Syst Rev, 2006(2): p. CD005328.
22. Zhang, W., et al., *OARSI recommendations for the management of hip and knee osteoarthritis: part III: Changes in evidence following systematic cumulative update of research published through January 2009.* Osteoarthritis Cartilage, 2010. **18**(4): p. 476-99.
23. Clarke, R., S. Derry, and R.A. Moore, *Single dose oral etoricoxib for acute postoperative pain in adults.* Cochrane Database Syst Rev, 2012. **4**: p. CD004309.
24. Derry, S. and R.A. Moore, *Single dose oral celecoxib for acute postoperative pain in adults.* Cochrane Database Syst Rev, 2012. **3**: p. CD004233.
25. Douglas, R.J., *Corticosteroid injection into the osteoarthritic knee: drug selection, dose, and injection frequency.* Int J Clin Pract, 2012. **66**(7): p. 699-704.
26. Kwon, D.R., G.Y. Park, and S.U. Lee, *The effects of intra-articular platelet-rich plasma injection according to the severity of collagenase-induced knee osteoarthritis in a rabbit model.* Ann Rehabil Med, 2012. **36**(4): p. 458-65.
27. Lo, G.H., et al., *Intra-articular hyaluronic acid in treatment of knee osteoarthritis: a meta-analysis.* JAMA, 2003. **290**(23): p. 3115-21.

28. Holland, T.A., Y. Tabata, and A.G. Mikos, *Dual growth factor delivery from degradable oligo(poly(ethylene glycol) fumarate) hydrogel scaffolds for cartilage tissue engineering.* J Control Release, 2005. **101**(1-3): p. 111-25.
29. Liu, X., X. Jin, and P.X. Ma, *Nanofibrous hollow microspheres self-assembled from star-shaped polymers as injectable cell carriers for knee repair.* Nat Mater, 2011. **10**(5): p. 398-406.
30. Park, H., et al., *Delivery of TGF-beta1 and chondrocytes via injectable, biodegradable hydrogels for cartilage tissue engineering applications.* Biomaterials, 2005. **26**(34): p. 7095-103.
31. Park, J.S., et al., *Determination of dual delivery for stem cell differentiation using dexamethasone and TGF-beta3 in/on polymeric microspheres.* Biomaterials, 2009. **30**(27): p. 4796-805.
32. Wang, X., et al., *Growth factor gradients via microsphere delivery in biopolymer scaffolds for osteochondral tissue engineering.* J Control Release, 2009. **134**(2): p. 81-90.
33. Wenk, E., et al., *Microporous silk fibroin scaffolds embedding PLGA microparticles for controlled growth factor delivery in tissue engineering.* Biomaterials, 2009. **30**(13): p. 2571-81.
34. Edwards, S.H., *Intra-articular drug delivery: the challenge to extend drug residence time within the joint.* Vet J, 2011. **190**(1): p. 15-21.
35. Godwin, M. and M. Dawes, *Intra-articular steroid injections for painful knees. Systematic review with meta-analysis.* Can Fam Physician, 2004. **50**: p. 241-8.
36. Jose, S., et al., *Thermo-sensitive gels containing lorazepam microspheres for intranasal brain targeting.* Int J Pharm, 2012.
37. Shahbazi, M.A. and M. Hamidi, *The impact of preparation parameters on typical attributes of chitosan-heparin nanohydrogels: particle size, loading efficiency, and drug release.* Drug Dev Ind Pharm, 2012.
38. Son, J.S., et al., *Drug delivery from hydroxyapatite-coated titanium surfaces using biodegradable particle carriers.* J Biomed Mater Res B Appl Biomater, 2012.
39. Zhang, X., et al., *Hydrotropic polymeric mixed micelles based on functional hyperbranched polyglycerol copolymers as hepatoma-targeting drug delivery system.* J Pharm Sci, 2012.
40. Spitters, T.W., et al., *A dual flow bioreactor with controlled mechanical stimulation for cartilage tissue engineering.* Tissue Eng Part C Methods, 2013.
41. Petit, A., et al., *Modulating rheological and degradation properties of temperature-responsive gelling systems composed of blends of PCLA-PEG-PCLA triblock copolymers and their fully hexanoyl-capped derivatives.* Acta Biomater, 2012. **8**(12): p. 4260-7.
42. Petit, A., et al., *Effect of polymer composition on rheological and degradation properties of temperature-responsive gelling systems composed of acyl-capped PCLA-PEG-PCLA.* Biomacromolecules, 2013. **14**(9): p. 3172-82.
43. Sandker, M.J., et al., *In situ forming acyl-capped PCLA-PEG-PCLA triblock copolymer based hydrogels.* Biomaterials, 2013. **34**(32): p. 8002-11.
44. Crank, J., *The mathematics of diffusion*. 2d ed. 1975, Oxford, Eng: Clarendon Press. viii, 414 p.
45. Samprovalaki, K., P.T. Robbins, and P.J. Fryer, *Investigation of the diffusion of dyes in agar gels.* Journal of Food Engineering, 2012. **111**(4): p. 537-545.
46. Samprovalaki, K., P.T. Robbins, and P.J. Fryer, *A study of diffusion of dyes in model foods using a visual method.* Journal of Food Engineering, 2012. **110**(3): p. 441-447.
47. Quinn, T.M., P. Kocian, and J.J. Meister, *Static compression is associated with decreased diffusivity of dextrans in cartilage explants.* Arch Biochem Biophys, 2000. **384**(2): p. 327-34.
48. Quinn, T.M., V. Morel, and J.J. Meister, *Static compression of articular cartilage can reduce solute diffusivity and partitioning: implications for the chondrocyte biological response.* J Biomech, 2001. **34**(11): p. 1463-9.
49. Lee, J.I., et al., *Measurement of diffusion in articular cartilage using fluorescence correlation spectroscopy.* BMC Biotechnol, 2011. **11**: p. 19.
50. Woodfield, T.B., et al., *Polymer scaffolds fabricated with pore-size gradients as a model for studying the zonal organization within tissue-engineered cartilage constructs.* Tissue Eng, 2005. **11**(9-10): p. 1297-311.
51. Evans, R.C. and T.M. Quinn, *Solute diffusivity correlates with mechanical properties and matrix density of compressed articular cartilage.* Arch Biochem Biophys, 2005. **442**(1): p. 1-10.
52. Aly, M.N., *Intra-articular drug delivery: a fast growing approach.* Recent Pat Drug Deliv Formul, 2008. **2**(3): p. 231-7.
53. Chevalier, X., *Intraarticular treatments for osteoarthritis: new perspectives.* Curr Drug Targets, 2010. **11**(5): p. 546-60.

54. Simkin, P.A., *Assessing biomarkers in synovial fluid: consider the kinetics of clearance.* Osteoarthritis Cartilage, 2013. **21**(1): p. 7-9.
55. Jovanovic, Z., et al., *Bioreactor validation and biocompatibility of Ag/poly(N-vinyl-2-pyrrolidone) hydrogel nanocomposites.* Colloids Surf B Biointerfaces, 2013. **105**: p. 230-5.
56. Patrignani, P., et al., *Managing the adverse effects of nonsteroidal anti-inflammatory drugs.* Expert Rev Clin Pharmacol, 2011. **4**(5): p. 605-21.
57. Brama, P.A., et al., *Effect of loading on the organization of the collagen fibril network in juvenile equine articular cartilage.* J Orthop Res, 2009. **27**(9): p. 1226-34.
58. Burton-Wurster, N., et al., *Effect of compressive loading and unloading on the synthesis of total protein, proteoglycan, and fibronectin by canine cartilage explants.* J Orthop Res, 1993. **11**(5): p. 717-29.
59. Buschmann, M.D., et al., *Stimulation of aggrecan synthesis in cartilage explants by cyclic loading is localized to regions of high interstitial fluid flow.* Arch Biochem Biophys, 1999. **366**(1): p. 1-7.
60. Elder, S.H., et al., *Chondrocyte differentiation is modulated by frequency and duration of cyclic compressive loading.* Ann Biomed Eng, 2001. **29**(6): p. 476-82.
61. Ding, C., Y. Zhang, and D. Hunter, *Use of imaging techniques to predict progression in osteoarthritis.* Curr Opin Rheumatol, 2013. **25**(1): p. 127-35.
62. Leddy, H.A. and F. Guilak, *Site-specific effects of compression on macromolecular diffusion in articular cartilage.* Biophys J, 2008. **95**(10): p. 4890-5.

6

Chapter 7
Short communication: Are Microspheres a Treatment Option in Osteoarthritis?

Spitters TWGM, Duque L, Zuidema J, Steendam R, Karperien M

Abstract

Microspheres are under evaluation to serve as a drug depot for intra-articular injection. They can provide a means to achieve long-term controlled release of a drug. The choice of the polymer is a delicate one, as the eventual mechanical properties of the microspheres should be compatible with the mechanical forces exerted in the wearing joint. Spheres which are too stiff could potentially abrase the articular surface, whereas too soft ones could be squeezed, thereby burst-releasing their content.

In this study we assessed the behavior of monodispersed D-L-Lactide/L-Lactide copolymer microspheres in an *in vitro* joint environment subjected to cyclic mechanical loading. Similar volumes of microspheres of 5, 15 and 30µm were loaded into a simulated joint cavity during compression of an osteochondral explant.

After compression, the articular surface showed indentations when it was treated with 5µm or 15µm spheres. Also, especially in the 15µm spheres, cracks and surface modifications were observed after compression. However, only a minimal amount of the 30µm spheres could be retraced on the articular surface. The deepest indentations on the articular surface were observed after treatment with the 5µm microspheres. With increasing diameter of the microspheres the diameter of the indentations increased. This indicated that the depth of the indentation decreased.

In our opinion, this *in vitro* evaluation shows that microspheres can be used as a drug delivery system. In particular the 30µm spheres did not seem to leave indentations. However, our findings suggest this should be assessed for microspheres of different polymers individually.

Keywords: microspheres, drug delivery, bioreactor, osteoarthritis

Chapter seven: Microspheres in Osteoarthritis Treatment?

Introduction

Intra-articular injection of dissolved medicines proves to be ineffective in long-term repression of clinical symptoms in a disease like osteoarthritis [1]. This is due to the high clearance rate of synovial fluid. Therefore, current strategies aim at creating depots which serve as a long-term release system within the synovial cavity. Several approaches have been developed as reviewed by Chevalier [2]. Microspheres are of interest as they provide a dispersion of the loaded drug within the joint. This can result in a more homogeneous distribution of the drug compared to conventional intra-articular injection. As the degradation rate of the microsphere polymer can be tailored, the release profile of the loaded drug can be extended over a longer period of time. However, little is known about the microsphere behaviour in an articulating environment. It could be hypothesized that a mismatch in compressive strength between articular cartilage and microspheres could lead to abrasions on the articular surface or uncontrolled release of the loaded drug. An inappropriately high compressive strength of the spheres could potentially leave indentations that could not regain its original shape. Moreover, if the spheres become stuck in the joint, the forces could become too high and cause the spheres to crack resulting in a uncontrolled release of the loaded drug. A too low compressive strength could lead to crushing of the microspheres, which can result in a local burst release of the loaded drug. Also, it has to be taken into account that the mechanical properties of articular cartilage change during progression of a degenerative disease like osteoarthritis decreases over time [3]. The aim of this study was to evaluate the effect of microsphere treatment on healthy articular surface in a simulated joint environment subjected to cyclic compression.

Materials and methods

Microsphere production

SynBiosys polymers are made by chain-extending at least two chemically distinct prepolymers (having hydroxyl end groups) with 1,4-diisocyanate. SynBiosys polymers are divided in amorphous and phase separated polymers. Amorphous polymers consist of at least two prepolymers that are amorphous. Amorphous polymers generally have one Tg, since the prepolymers mix and give rise to one amorphous phase. Phase separated polymers consist of at least one semi-crystalline prepolymer and at least one amorphous polymer. Phase separated polymers have at least one Tm and one Tg. Prepolymers are made by ring opening polymerization of cyclic monomers initiated by either polyethylene glycol (PEG) or 1,4-butanediol (BDO).

Both the amorphous and the phase separated polymers may contain PEG, that render the polymers swellable (to some extent) in water. Amorphous polymers can only contain a small amount of PEG (up to ~10 wt%), since larger amounts would lead to a Tg below room temperature, leading to sticky material. Also, the polymer would slowly dissolve in water (i.e. uncontrolled swelling). Phase separated polymers can contain large amounts of PEG, up to ~50 wt%. The presence of the semicrystalline prepolymer ensures that the material is non-sticky. The crystalline areas act as physical crosslinks that enable controlled swelling of the polymer (i.e. the polymer does not dissolve slowly in water).

For the phase-separated polymers poly(ε-Caprolactone) and poly(L-lactide) are commonly used as semi-crystalline prepolymers. poly(ε-Caprolactone) and poly(L-lactide) have a Tm of 60 and 120 °C, respectively. Poly(ε-Caprolactone) based polymers are very suitable for extrusion, as they allow extrusion at temperatures as low as ~50 °C. Due to the high Tm of poly(L-lactide), poly(L-lactide) can only be extruded at elevated temperature (> 100 °C). Poly(L-lactide) based polymers are very suitable for making microspheres with the double emulsion process, as the semi-crystalline poly(L-lactide) ensures that the microspheres are non-sticky. Microspheres cannot be made with phase separated polymers based on poly(ε-Caprolactone), as the material is too sticky after extraction of dichloromethane to yield microspheres. Most likely the crystallization is of poly(ε-Caprolactone) is too low in the time frame of processing.

Material source

Knees of 10-12 month old calves were collected from the local abattoir. Femoral condyles were exposed by removing the muscles and patella. Then, osteochondral explants of 7mm in diameter were collected with a custom made puncher and placed into a polycarbonate insert as described previously [4].

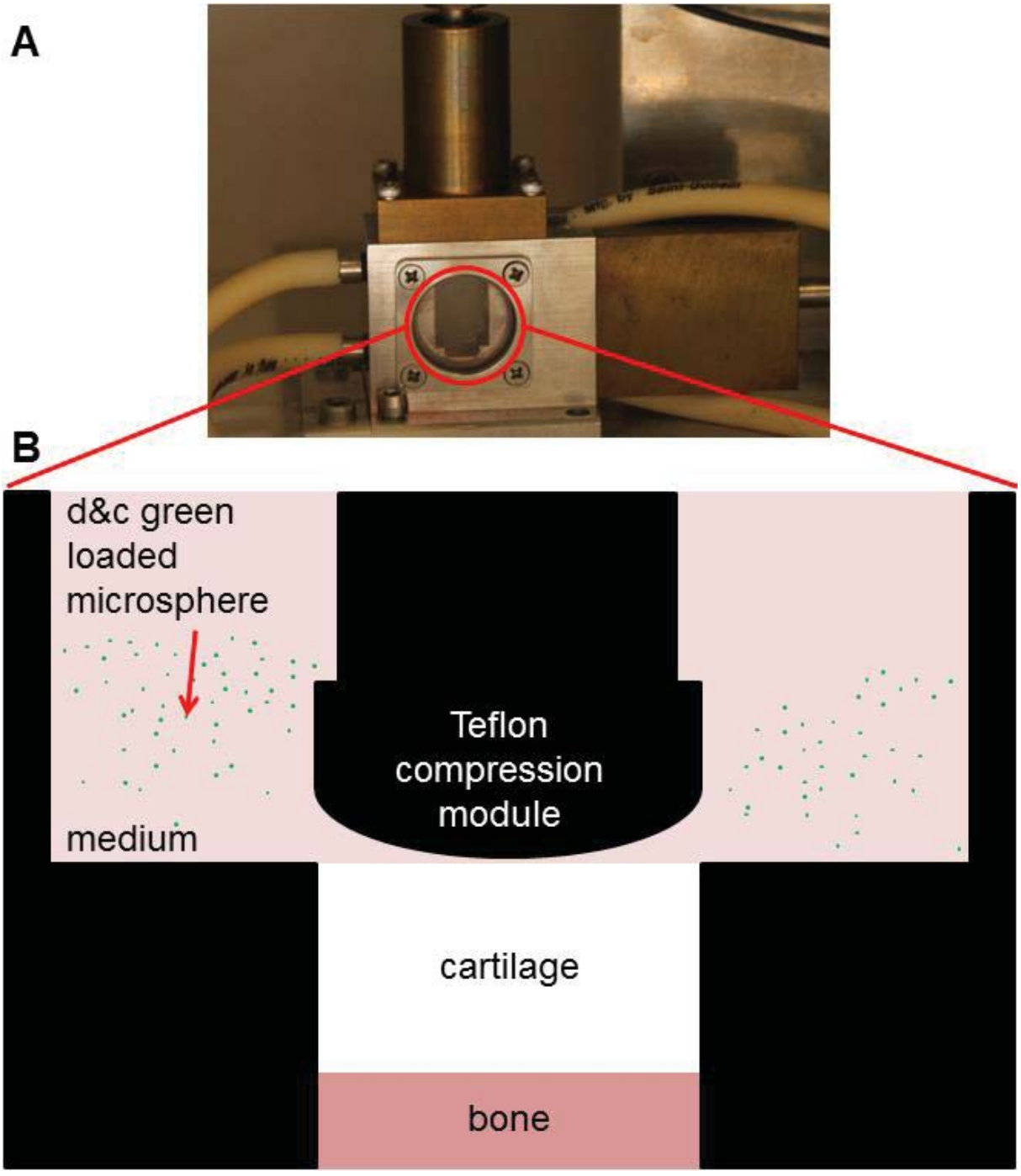

Figure 1: (A) Dual flow bioreactor, (B) schematic overview of the reactor chamber indicating the compression module, the explant and where the microspheres where injected in the chamber.

Explant culture

Explants were placed into a dual compartment bioreactor as previously described [4]. Subsequently, eight microliter monodispersed microspheres suspension (200mg microspheres/mL) was introduced in the top compartment of the bioreactor. Compression was applied with a load of 0.13MPa or 0.26MPa (frequency 0.33Hz, compression time per cycle 50%) for 1 hour. Figure 1 shows a schematic representation of the explant, microspheres and the loading direction in the used bioreactor set up.

Scanning electron microscopy (SEM)

After culture the explants were fixated in 10% buffered formalin at 4°C overnight. Then, the explants were dehydrated in an ethanol series, critical point dried (Balzers) and gold sputtered (Cressington sputter coater). SEM was performed using a Philips XL30 electron microscope (Philips, The Netherlands).

Image analysis

The diameter of the microspheres and indentations caused by the spheres were quantified using ImageJ software.

Results

Scanning electron microscopy showed that all microspheres indented the articular surface (Figure 2A). The amount of spheres that could be retraced on the surface after compression decreased with increasing diameter of microspheres. This could be explained that with increasing microsphere diameter less spheres where injected. However, smaller microspheres could more easily be trapped between the compression module and the articular surface. In the highest load tested 15μm and 30μm microspheres were observed that had cracks on their surface or the surface structure itself was modified (yellow arrows in Figure 2A). This indicated that part of the microspheres could not withstand the mechanical forces in such an environment.
Microscopic evaluation showed that these microspheres where pressed into the articular surface (Figure 2B). Quantifying the indentations made by the microspheres showed that the 5μm spheres left the deepest indentations compared to the 15μm and 30μm spheres, as measured by the diameter of the shadow around the spheres. Treatment with the 15μm and 30μm diameter microspheres resulted in indentations that increased with increasing diameter. The diameter of the indentations also increased with increasing load when treated with 15μm microspheres, whereas this increase was not observed after treatment with the 30μm spheres. This indicated that the impact of the indentations was less compared to the ones caused by the 5μm spheres. However, a large number of indentations caused by the 15μm spheres was still detected indicating that the tissue could not relax properly in those spots. As only a small number of indentations was visible on the surface after treatment with the 30μm microspheres, it could be imagined that the tissue at those sites was not deformed indefinite or that these spheres were kept in suspension better than the spheres of the other diameters. Interesting was the decrease of the diameter of the 30μm spheres after compression, which could be due to swelling. The cracks and surface modifications that were observed in the 15μm and 30μm conditions could not be contributed to e.g. surface tension. This parameter is expected to increase with increasing diameter. So, the bigger microspheres are expected to resist the mechanical load better than the smaller ones.

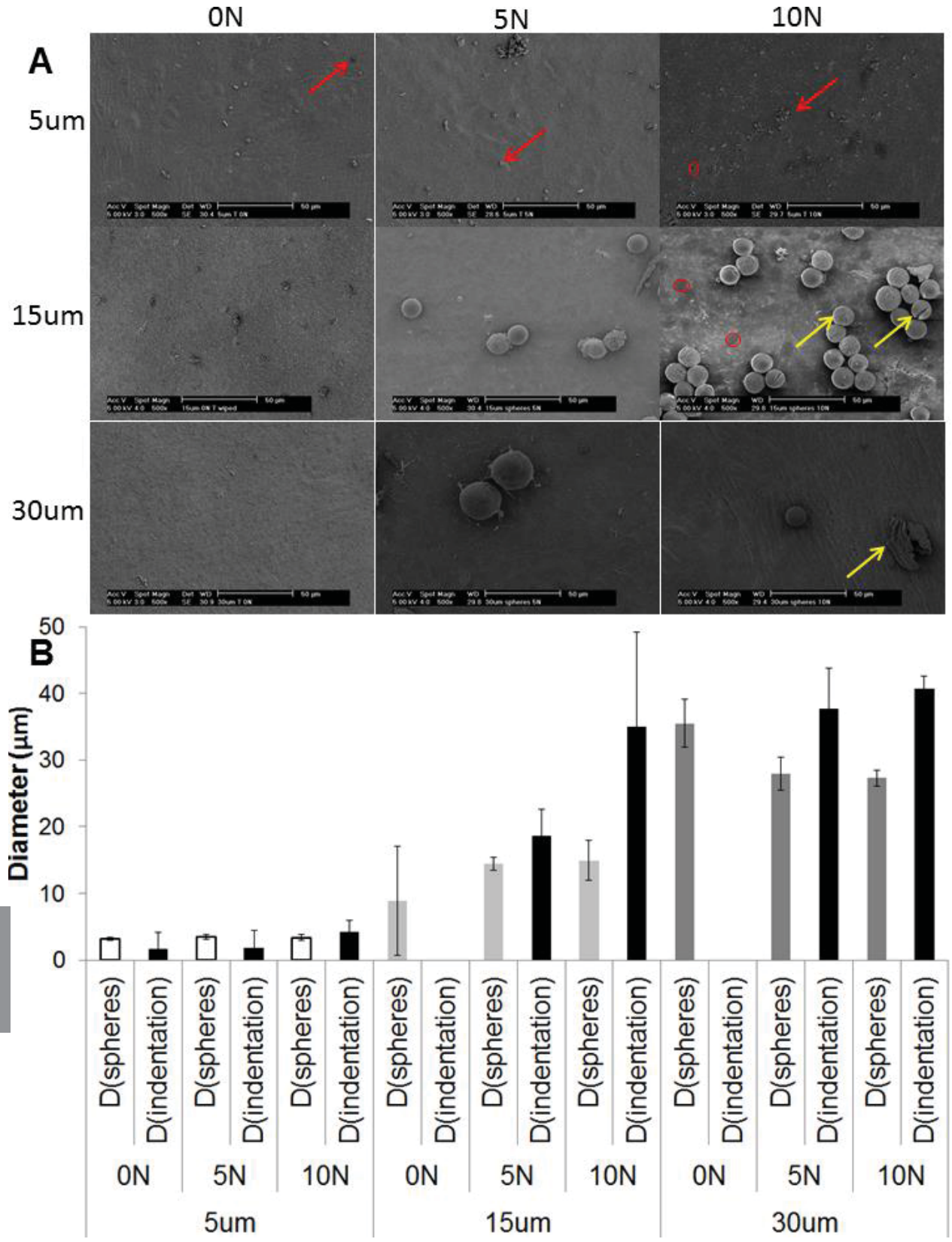

Figure 2: Scanning electron images of the articular surfaces treated with microspheres. The red arrows indicate the 5µm microspheres. The red circle indicates in empty indentation. The yellow arrows indicate microspheres with cracks or surface modification. (B) Quantification of the diameter of the detected spheres and indentations.

Discussion

Microsphere-based therapies for intra-articular injection aim at prolonged release of the loaded drug. In a dynamic environment like the joint cavity two parameters have to be considered for effective therapy. First, the microspheres should stay intact during residence in the joint space to prevent a burst and uncontrolled release. Second, the microspheres should not negatively affect the already degraded articular surface during movement of the joint. As little is known about the behavior of microspheres in an articular environment, the aim of this study was to evaluate the effect of microsphere treatment on the articular surface in a simulated joint environment.

Monodispersed microspheres of three sizes were tested on their abrasive behavior on the articular surface and their resistance to mechanical load. It was observed that the 5μm and 15μm microspheres left deeper indentations than those of 30μm as measured by the smaller shadow ring around the spheres. This can implicate that the compressive modulus of the largest spheres matches the one of articular cartilage better than the ones of the two smaller microspheres. This allowed the surface to relax to its original shape. A reason that fewer 30μm microspheres were found on the surface compared to the other conditions is that less cells were injected. Another possibility is that the interaction with the articular surface of the smaller spheres was stronger compared to the interaction of the larger ones, as, due to water flow in the top compartment the latter ones are more easily removed from the articular surface.

Another interesting observation was that especially the 15μm microspheres showed cracks in their surface and a majority of the spheres showed surface modifications. It is possible that the spheres of this size could not withstand the strain and burst. This would make the release of the loaded drug uncontrollable. The 5μm spheres consistently showed a smaller diameter than expected. This could be due to processing procedures but also due to compression as these spheres left a deep indentation where they became trapped.

These experiments were conducted with healthy cartilage. However, during osteoarthritis the cartilage matrix is progressively degraded and the compressive strength decreases. This means that the compressive modulus of the spheres should be tailored to this situation. This can even be extended further as the compressive modulus of the cartilage matrix in the different stages of the disease will change, the

treatment should be customized during the treatment period and optimized for the start of the treatment.

This study showed that the PLLA microspheres in the range of 5-15μm will act abrasively the cartilage surface and undergo morphological changes in a compressive environment. In contrast, 30μm microspheres only indented the cartilage surface minimally. Therefore, it can be concluded that in this study PLLA microspheres of 30μm seemed the most suitable size to be used as a therapy in osteoarthritis treatment.

References

1. Douglas, R.J., Corticosteroid injection into the osteoarthritic knee: drug selection, dose, and injection frequency. Int J Clin Pract, 2012. 66(7): p. 699-704.
2. Chevalier, X., Intraarticular treatments for osteoarthritis: new perspectives. Curr Drug Targets, 2010. 11(5): p. 546-60.
3. Temple-Wong, M.M., et al., Biomechanical, structural, and biochemical indices of degenerative and osteoarthritic deterioration of adult human articular cartilage of the femoral condyle. Osteoarthritis Cartilage, 2009. 17(11): p. 1469-76.
4. Spitters, T.W., et al., A dual flow bioreactor with controlled mechanical stimulation for cartilage tissue engineering. Tissue Eng Part C Methods, 2013.

7

Chapter 8
Dextran-Based Hydrogel Compositions in Cartilage Defect Repair

Tim W.G.M. Spitters, Barbara Slowinska, Rong Wang, Pieter Dijkstra, Marcel Karperien

8

Abstract

Due to the low self-healing capacity of cartilage, traumatic focal cartilage defects can initiate further degradation of the matrix eventually leading to osteoarthritis. Current surgical interventions and tissue engineering approaches have not come up with a definite solution. *In situ* gelation hydrogels seem to be suitable candidates to treat focal cartilage defects. These can be used as cell-free or in cell-based therapies. As *in vivo* models are expensive and give answers about the long term effects of a particular treatment, we propose to evaluate new therapies for tissue engineering in an *ex vivo* model that simulates the natural environment in key aspects. A static dual compartment bioreactor was used to evaluate the behaviour of a dextran-based hydrogel in an osteochondral defect model. In hydrogels supplemented with type 1 collagen cell migration from the surrounding tissue was observed. Cell distribution and matrix deposition in the gel and gel integration with the host extracellular matrix will be the focus of future experiments. In our opinion, this bioreactor system can aid in the preclinical evaluation of tissue engineering approaches.

Keywords: cartilage, osteochondroal defect, bioreactor, in vitro model, dextran-based hydrogel

Introduction

Cartilage defects due to trauma or disease can lead to the initiation of osteoarthritis. Reconstruction of the tissue can prevent the onset of this degenerative disease. In the context of regenerative medicine, several options for therapy are being investigated, such as articular chondrocyte implantation (ACI), microfracturing and scaffold implantation (with or without cells) [1-6]. The first two techniques, although showing promising clinical results, can lead to donor site morbidity. In addition, questions are raised about the quality of the repair tissue [7-9]. Scaffolds can be used to stabilize a defect until its repair by the body itself. Mechanical properties of both scaffold and tissue have to match to prevent friction between the two components and further deterioration of the tissue. *In vitro* preculture of a cartilaginous construct can be an alternative to produce an implant of clinically relevant size. However, cell expansion *ex vivo* can lead to dedifferentiation and unexpected responses to growth factor stimuli [10]. Therefore, current efforts focus on the creation of an *in vitro* environment that resembles the *in vivo* environment in key aspects [11-17]. Bioreactors for cartilage tissue engineering can provide the means to optimise the nutrient supply and mechanical environment. By resembling the natural milieu, bioreactors also can be used as a tool in the preclinical evaluation of cartilaginous constructs when equipped with real-time imaging [18, 19].

Scaffolds for cartilage tissue engineering come in a wide variety, but can roughly be divided in natural and synthetic polymers. Polymers can be cast as a solid structure to which cells can attach or as a hydrogel in which cells are embedded. While both natural and synthetic polymers have their advantages, we hypothesized that the use of natural polymers would provide the cells with an environment to which they more easily can adapt. Furthermore, natural polymers may possess cues relevant for tissue formation which lack in synthetic materials. Recently, our group developed a sugar-based hydrogel (Dex-TA gel) suitable for cartilage tissue engineering in terms of viability and matrix deposition [20-22]. These *in situ* gelating hydrogels have been proposed to be suitable candidates for cartilage tissue engineering purposes [21, 22]. Combined with chemoattractants, migration of chondrocytes and stromal cells towards these hydrogels was shown [23]. However, cellular invasion into the gels has not yet been established. In this study, these Dex-TA gels were supplemented with type 1 collagen and hyaluronic acid, the two main components of cartilage, to provide

the cells with a scaffold that facilitates cellular invasion into the hydrogels. Cell migration was followed in an osteochondral defect model in a dual compartment bioreactor. Complementing the gel with collagen and hyaluronic acid rendered a scaffold that allowed cellular ingrowth from the surrounding tissue.

Materials and Methods

Dextran synthesis and preparation of hydrogel compositions

Dextran-tyramine was synthesized as previously described by Jin *et al* [21]. Moreira *et al.* found that adding 50% of platelet rich plasma (PRP) had a chemotractive effect on chondrocytes [24]. Concentrations of collagen (coll) and hyaluronic acid (HA) were determined after the dry weight of these components in native cartilage matrix [25]. As collagen I is more widely available than collagen II, for proof-of-principle this type was mixed in first. Collagen dissolved in 0.01N hydrogenchloride was used (PureCol®, Advanced Biomatrix, USA). Hyaluronic acid was prepared from sodium hyaluronate (15-30kDa, contipro.com) by dissolving it in phosphate buffered saline. Solutions of PRP, coll and HA were added to 10mg Dex-TA (degree of substitution 15) and volume of the mixture was increased to 100μL with Dulbecco's Modified Eagle's Medium (DMEM). The final concentrations of collagen and hyaluronic acid were 3mg/mL and 1.65mg/mL (Table 1) respectively.

Table 1: Final concentrations of gel components in 100μL gel

Gel composition	Dex-TA (mg/mL)	Platelet rich-plasma (%)	Type 1 collagen (mg/mL)	Hyaluronic acid (mg/mL)
Dex-TA	10	-	-	-
Dex-TA + PRP	10	50	-	-
Dex-TA + coll	10	-	3	-
Dex-TA + HA	10	-	-	1.65
Dex-TA + PRP + coll	10	50	3	-
Dex-TA + PRP + HA	10	50	-	1.65
Dex-TA + coll + HA	10	-	3	1.65
Dex-TA + PRP + coll + HA	10	50	3	1.65

Cell sources

Bovine osteochondral explants were isolated as described before [15]. Bovine chondrocytes (bCHs) were isolated from femoral articular cartilage by means of collagenase type II digestion (150U/mL; Worthington, USA) overnight. Subsequently, collagenase suspension was filtered through a 200 micron cell strainer and centrifuged at 300g for 10 minutes at 4°C. The pellet was then washed in phosphate buffered saline (PBS) and centrifuged. This procedure was repeated once before cells were resuspended in Dulbecco's Modified Eagle's Medium (DMEM) (Gibco, USA) and counted using a Burkner counting chamber. Cells were used immediately after isolation.

Medium composition

Bioreactor cultures were performed in differentiation medium (dif.med) which consisted of DMEM supplemented with 100U/mL penicillin/100µg/mL streptomycin, 20mM ascorbic acid, 40µg/mL proline, 100µg/mL sodium pyruvate and 1% Insulin Transferrin and Selenium premix.

Gelation times of Dex-TA hydrogel compositions

Gelation times were measured in a tilting vial assay. Individual components were pipetted into a vial in the proper concentration. Then, horseradish peroxide and H_2O_2 were added as described before [21]. Upon addition of the enzyme and catalyst, the vial was tilted and the time until complete gelation was measured.

Migration assay

The cell attractive capacity of the different Dex-TA compositions were tested in a CytoSelect™ cell migration assay (BioLabs, USA). Hydrogel compositions (150µL) were pipetted in the bottom plate of the assay. Then, the transwell plate was put on top and 100µL of a $10*10^6$ bCH/mL cell suspension in dif.med was added to each transwell. The number of migrated chondrocytes was assessed after 24 hours by carefully removing the transwells from the hydrogels and carefully removing the medium from the transwells. Subsequently, the transwells were placed in a lysis buffer and incubated for 30 minutes at 37°C. Then, GR Dye was added to the solution and the 100µL of the solution was added to a white 96-well plate and fluorescence was read at a spectrophotometer LS50B (Perkin Elmer). The different gel compositions were plain Dex-TA, Dex-TA+PRP, Dex-TA+coll, Dex-TA+HA, Dex-TA+PRP+coll, Dex-TA+PRP+HA, Dex-TA+coll+HA, Dex-TA+PRP+coll+HA. As a control differentiation medium was used. Fluorescence values were shown relative to the control.

Bioreactor culture

Agarose plugs of 7mm in diameter and 4mm in height (Figure 1A) were produced in previously described custom-made molds [15] and transferred to a similar molds with a perforated support. Then, a 2mm deep defect was made with a biopsy plunger (Brymill, USA) with a diameter of 3mm (Figure 1A). Defects were filled with 14µL

Dex-TA solution and gelation was initiated by adding 14µL of a 150U/mL horseradish peroxide/0.3% H_2O_2 solution. These constructs were transferred to previously described static bioreactors [15] and, after they were transferred to custom made 4-well plates, top and bottom compartments were filled with 2mL and 10mL differentiation medium respectively. Subsequently, 500,000 cells were seeded in the top compartment. Culture was performed for 7 days in humidified conditions at 37°C.

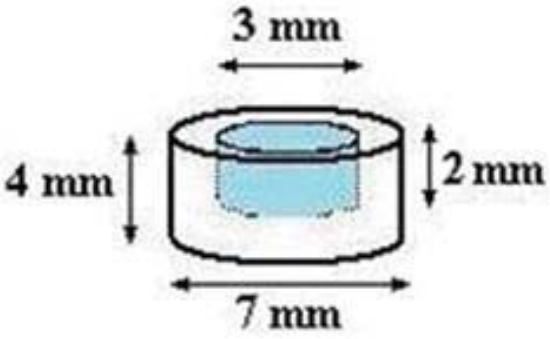

Figure 1: (A) schematic representation of explant dimensions. The blue area represents a focal defect filled with the Dex-TA based hydrogel.

Defects were made in a similar way in the cartilage layer of the osteochondral explants. Culture conditions were also similar to the culture described above.

Biochemical analysis

DNA quantification

Before analysis, constructs were incubated in a proteinase K (PK) digestion buffer (1µg/mL PK, 1µg/mL pepstatin A, 18.5µg/mL iodoacetamide, Sigma) and went through a freeze/thaw cycle. DNA content was quantified with a CyQuant kit (Invitrogen, USA) according to manufacturer's protocol and fluorescence was measured at 480nm using a spectrophotometer LS50B (Perkin Elmer). DNA concentrations were calculated from a λ DNA standard curve

Viability

Cell viability in the defect model was assessed after 7 days of culture with a live/dead assay according to manufacturer's protocol (Invitrogen, New York, USA). Live (green) and dead (red) cells were visualized with separate FITC and Texas Red filters on a fluorescence microscope (Nikon Eclipse E600) and microphotographs were taken with Qcapture acquisition software. These pictures were overlaid in Photoshop.

Histology

For histology, explants and constructs were dissected, top to bottom, and fixed in a 0.5% L-lysine/phosphate buffered paraformaldehyde fixative for 24 hours at 4°C.

Subsequently, explants and constructs were washed in phosphate buffered sucrose solution for 24 hours at 4°C and washed in acetone until the solution became clear. Then, explants and constructs were incubated overnight in cryomatrix before they were embedded in cryomatrix and sectioned in a cryotome into 10µm thick longitudinal sections and then mounted onto Superfrost® Plus (Thermo Fisher Scientific, USA) glass slides.

Alcian Blue staining

Proteoglycan deposition and distribution was visualized by staining sections with Alcian Blue (AB). Sections were hydrated for 10 minutes in demi water and stained with AB solution for 30 minutes. Afterwards they were washed in running tap water and dehydrated in a sequence of 96% EtOH, 100% EtOH and xylene for 2 minutes each. Section were dried and mounted with mounting medium.

Picrosirius Red

To visualize collagen fibers sections were stained with the Picrosirius Red staining kit (BioSciences, San Jose, USA) according to the manufacturer's protocol. Shortly, sections were hydrated for 10 minutes in demi water, stained with Haematoxylin for 8 minutes and rinsed in distilled water followed by staining with Picrosirius Red. The stained sections were washed in 70% EtOH for 45 seconds and dehydrated in a graded ethanol series.

Slides were scanned with a Nanozoomer 2.0 RS (Hamamatsu, Japan) and captured with its proprietary NDP.Scan software (Hamamatsu, Japan).

Results

Collagen and hyaluronic acid supplementation of Dex-TA hydrogels enhanced chondrocyte migration in a transwell assay

Gelation in reaction tubes showed no color differences between the different hydrogel compositions and efficient gel formation was observed in each condition (Figure 2A). However, gelation times increased with the number of additives, although the gelation time of the Dex-TA+coll+HA condition was longer compared to the Dex-TA+PRP+coll+HA composition (Table 2).

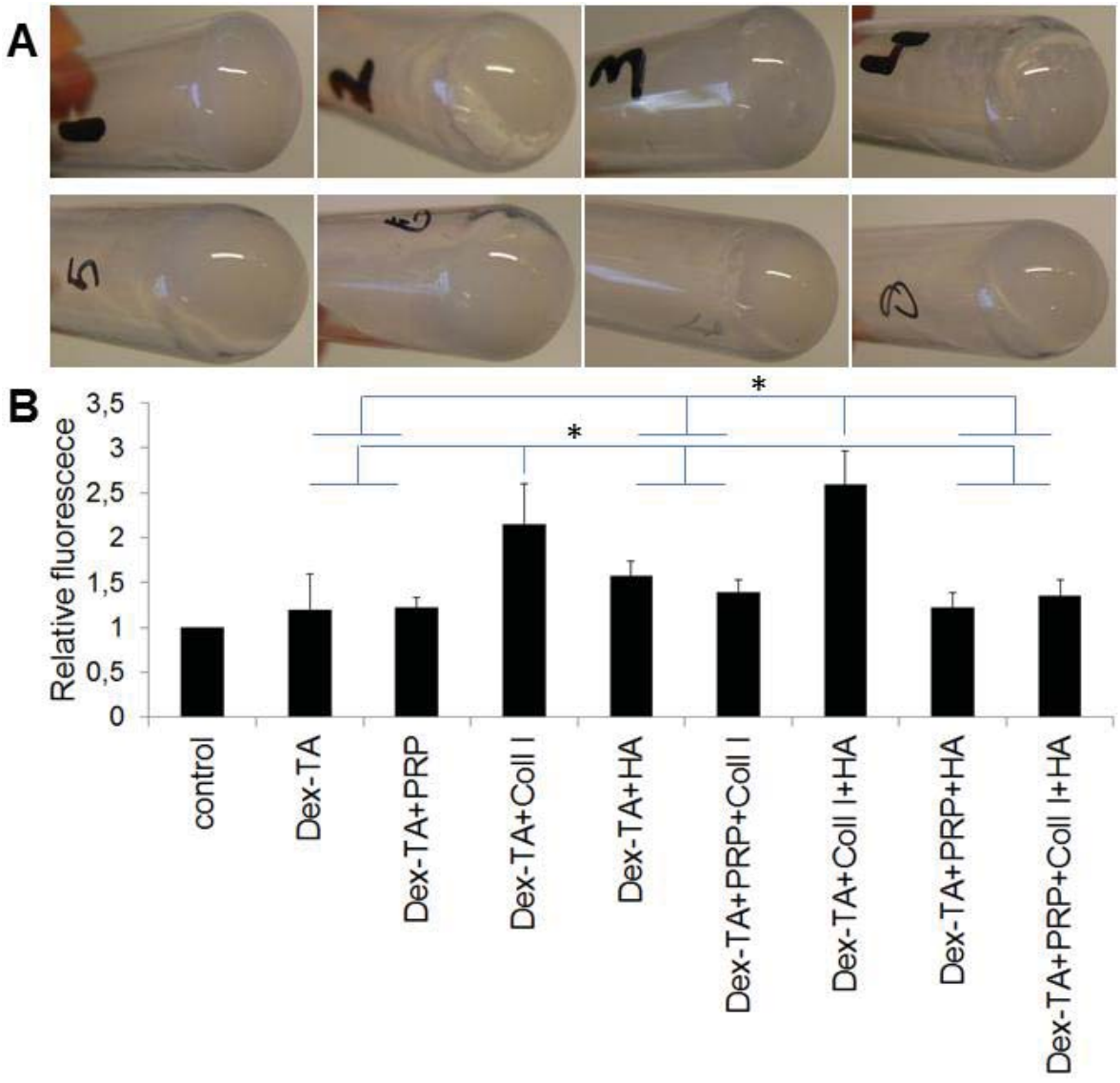

Figure 2: Characterisation of Dex-TA compositions in a cell migration assay. (A) gelation in reaction tubes: 1) Dex-TA, 2) Dex-TA+platelet rich plasma (PRP), 3) Dex-TA+collagen I (coll), 4) Dex-TA+hyaluronic acid (HA), 5) Dex-TA+PRP+coll, 6) Dex-TA+PRP+HA, 7) Dex-TA+coll+HA, 8) Dex-TA+PRP+coll+HA. In each of these compositions efficient gel formation was observed. (B) The effect of hydrogel supplements was assessed in a 24-hour migration assay. P0 bovine chondrocytes that crossed the transwell membrane were quantified. Control is cells migrated towards chondrogenic differentiation medium. Data is expressed as fold change relative to the control which was set as 1, n = 6, * = $P<0.05$.

DNA quantification of migrated cells revealed that, relative to the control, chondrocyte migration towards Dex-TA hydrogels was similar compared to the control (Figure 2B). In contrast to previously published data, supplementation of Dex-TA hydrogel with PRP did not increase cell migration [24]. This is likely due to the use of a different source of PRP, which is well known for its high variability in biological responses [26-28]. Also, supplementation of Dex-TA hydrogels with solely HA did not have an effect. On the other hand when type I collagen was added, either with or without HA, chondrocyte migration was significantly enhanced. Remarkably, the presence of PRP tended to have an inhibitory effect on cell migration stimulated by type 1 collagen. Therefore, the gel compositions containing collagen with or without HA were tested in a defect model to investigate the migratory behaviour of chondrocytes.

Table 2: Gelation times of different Dex-TA hydrogel compositions

Gel composition (numbers correspond to Figure 2A)	**Approximate gelation time (s)**
1: Dex-TA	25
2: Dex-TA + platelet lysate	25
3: Dex-TA + collagen	30
4: Dex-TA + hyaluronic acid	30
5: Dex-TA + platelet lysate + collagen	50
6: Dex-TA + platelet lysate + hyaluronic acid	50
7: Dex-TA + collagen + hyaluronic acid	85
4: Dex-TA + platelet lysate + collagen + hyaluronic acid	60

Isolated chondrocytes did not migrate into Dex-TA hydrogel compositions in a agarose defect model

To test the ingrowth of isolated p0 chondrocytes (CHs) into Dex-TA based hydrogels, CHs were seeded on top of a Dex-TA filled focal defect created in an agarose cylinder. Alcian blue staining showed that the chondrocytes did not enter the gel, but formed a monolayer on the top of the agarose cylinder with a Dex-TA hydrogel filled defect (Figure 3A). Matrix accumulation was observed in the regions where the cell monolayer was located.

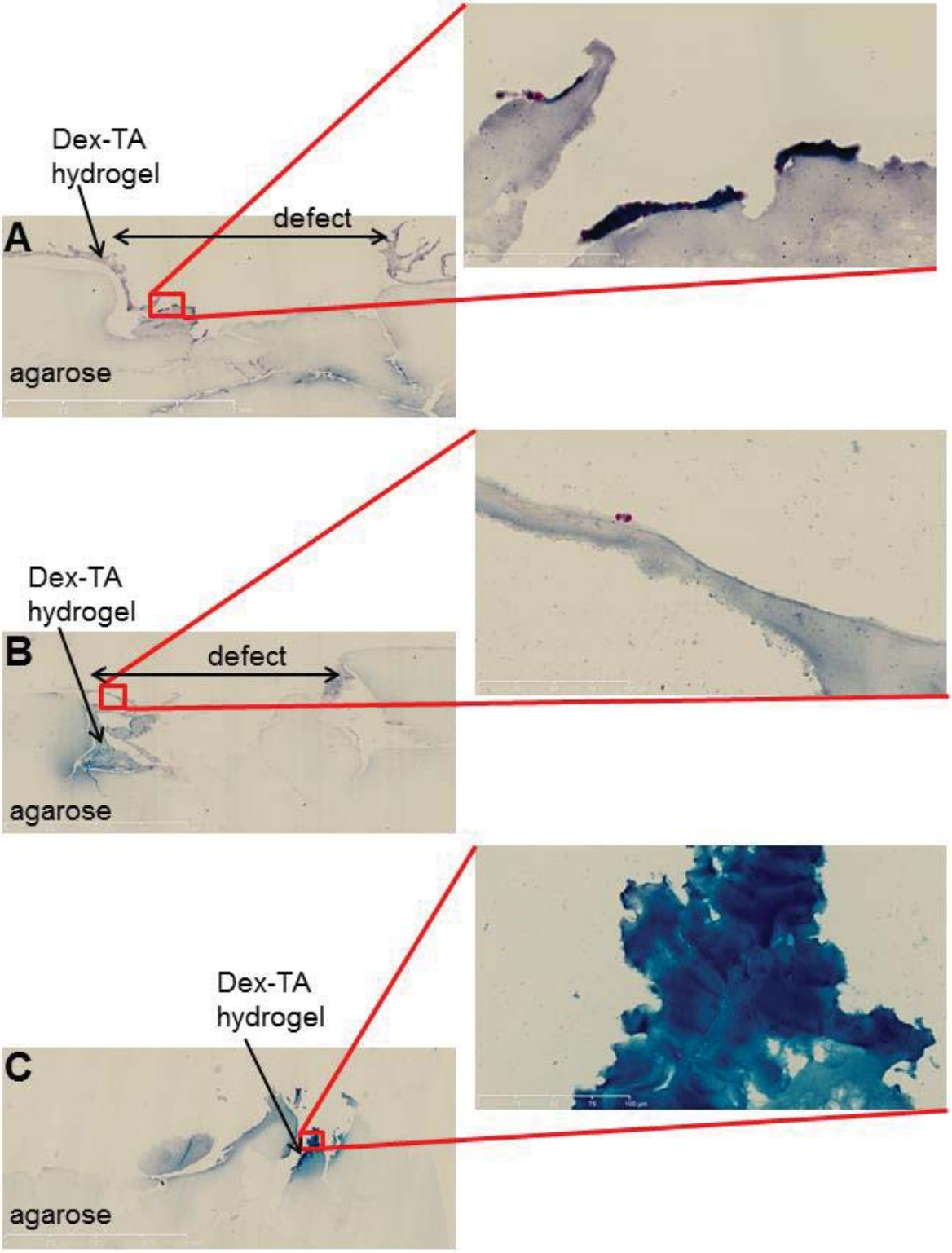

Figure 3: Migration of P0 bovine chondrocytes in an agarose defect model with cells seeded on top of the hydrogels. Alcian blue counterstained with nuclear fast red revealed that cells attached to the hydrogel compositions, but did not migrate into the gel. Agarose defects filled with (A) Dex-TA, (B) Dex-TA+coll and (C) Dex-TA+coll+HA.

Only a few or no cells were detected on top of or in the Dex-TA gels supplemented with collagen or collagen and hyaluronic acid (Figure 3B and 3C). Also, no matrix

production was observed around the detected cells. Thus, histological analysis did not provide evidence for chondrocytes migration into the Dex-TA hydrogels.

Chondrocyte invasion of Dex-TA hydrogels in an osteochondral defect model

Before cultures were started, the effects on cell viability of the procedure to create a cartilage defect and subsequent filling of the defect with an injectable hydrogel were investigated. Using live/dead analysis minimal cell death was observed both after punching the defect and after filling the defect with a Dex-TA hydrogel (Figure 4).

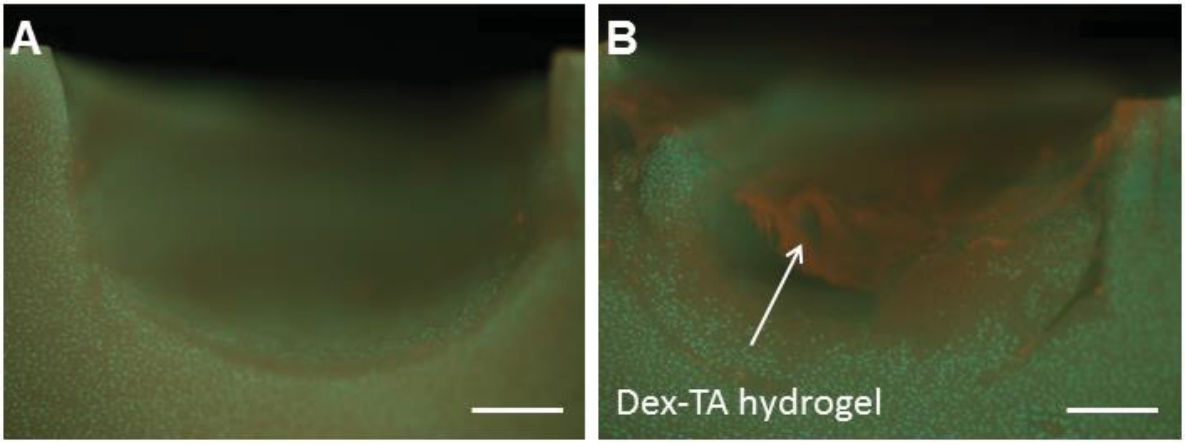

Figure 4: Live/dead pictures of an osteochondral explant with a defect (A) without a Dex-TA hydrogel, (B) with a Dex-TA hydrogel. Scale bar represents 500µm. Live cells stain green, dead cells stain red. The red backgroud stain of the dextran gel is likely due to autofluorescence.

During processing for histological analysis, the Dex-TA gel was unfortunately lost. Alcian blue/nuclear fast red staining showed cellular invasion in both the gel supplemented with collagen (Dex-coll) and with collagen and hyaluronic acid (Dex-coll-HA) (Figure 5A and 5B). In the Dex-coll gel cells were observed closely to the border with the tissue (Figure 5A, red arrows). Further, it seemed that cells were migrating through the cartilage as these were not located in a chondron (Figure 5A, yellow arrows), although it cannot be excluded that this is observation is a processing or cutting artefact. Also, cells were detected in the Dex-coll-HA gel and it seemed in higher quantities compared to the Dex-coll gel. Chondrocytes in this gel did not show the natural round morphology, but seemed stretched (Figure 5B, red arrows). This is in accordance with the shape of a migratory cell. Of note, these figures are not representative pictures, but observations, as not all histological pictures showed cells. This showed that migration from the cartilage into the gels occurred seldom. These preliminary data provide evidence that supplementation of Dex-TA hydrogels with a collagen or hyaluronic acid could stimulate cell migration into the gels.

However, further experiments and comparison to unsupplemented Dex-TA gel are necessary to elucidate the exact effect of collagen and hyaluronic acid addition to Dex-TA hydrogels.

This showed that migration from the cartilage into the gels was not homogeneous. But it did show that enhancing the Dex-TA hydrogels with a collagen or hyaluronic acid could stimulate cell migration into the gels.

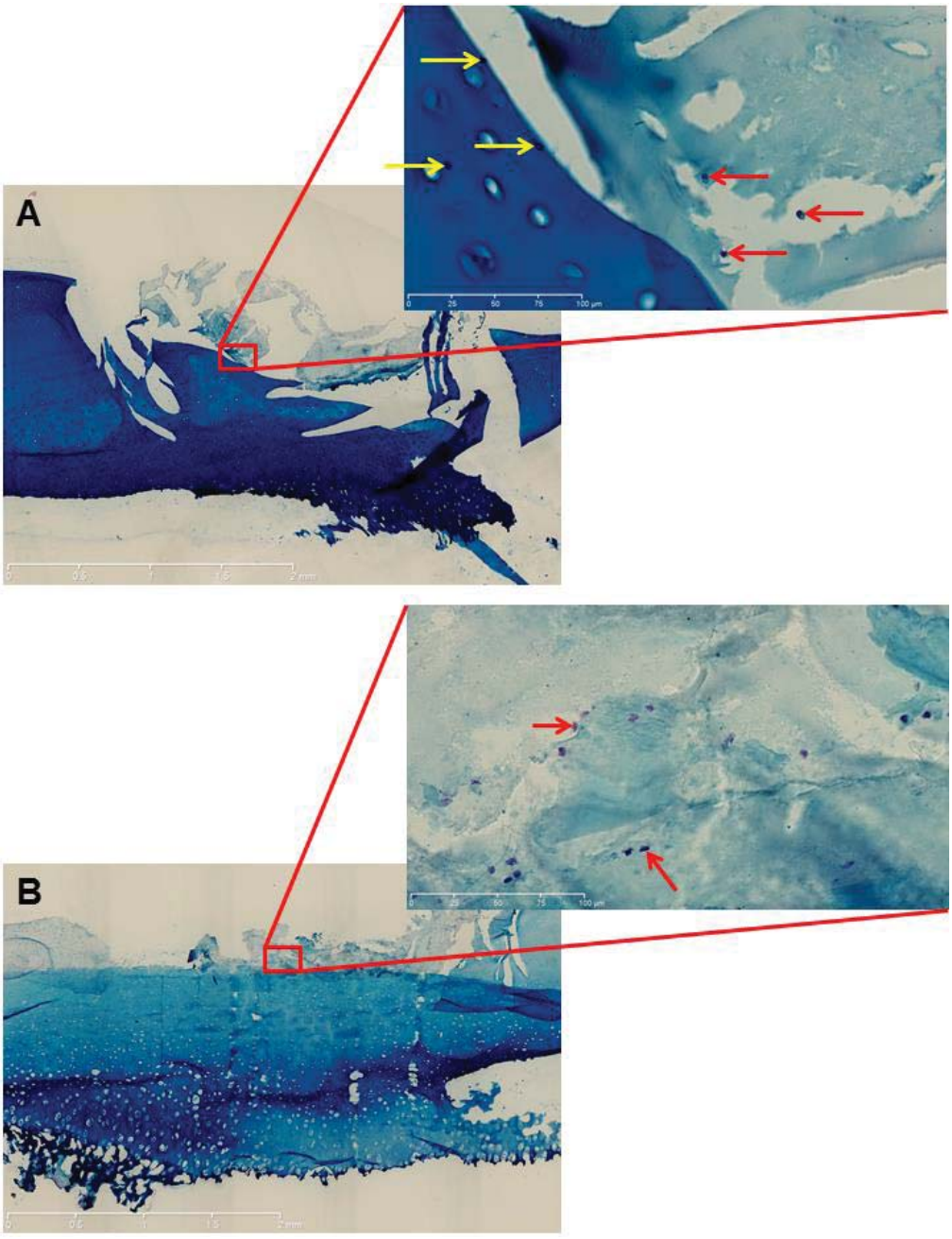

Figure 5: Migration of bovine chondrocytes into hydrogels from articular cartilage in an osteochondral defect model. Alcian blue counterstained with nuclear fast red revealed that cells seemed to migrate into Dex-TA hydrogels supplemented with type I collagen and/or hyaluronic acid. Cartilage defects were filled with (A) Dex-TA+coll and (B) Dex-TA+coll+HA. Yellow arrows indicate possible migrating cells in cartilage, red arrows indicate chondrocytes in Dex-TA hydrogel.

Discussion

When left untreated, cartilage defects can progress over time into osteoarthritis [29, 30]. To overcome the limitations of current surgical techniques, polymers are developed which can act as a material to fill a defect until new extracellular matrix is deposited in the affected site and tissue function is restored. The most accurate evaluation systems to date are expensive *in vivo* models. Thus, an *in vitro* system that resembles the natural environment in most key features could serve as an advantageous, cost-effective alternative preclinical evaluation system.

In this preliminary study, we used a dual compartment bioreactor for osteochondral tissue engineering to investigate cell migration into a novel hydrogel for cartilage tissue engineering [15, 22]. This novel hydrogel is based on chemically modified natural polymers that cross-link enzymatically *in situ*. This gel has the potential to be used as a filler of focal cartilage defects. Importantly, during *in situ* cross-linking this gel firmly attaches to cartilage by covalent cross linking of the chemically modified polymers to tyrosine residues in collagen [23]. By incorporating chemoattractant cues, this injectable hydrogel could be developed into a cell-free treatment option for cartilage repair. In this preliminary study we have set the first steps to develop such a chemoattractant hydrogel by supplementation of the dextran based hydrogel with natural polymers like type 1 collagen and hyaluronic acid. Previously we have shown that supplementation of a Dex-TA hydrogels with heparin-TA resulted in a chemoattractant gel providing the rationale for developing a cell attracting hydrogel solely based on natural polymers [20]. Indeed, supplementation of a Dex-TA hydrogel with type 1 collagen or with hyaluronic acid increased chemoattraction of cells in a cell migration assay. Remarkably, freshly isolated p0 chondrocytes did not migrate into the different gel compositions when placed on top of the Dex-TA hydrogel used to fill up an artificial defect in an agarose cylinder. In contrast, cells embedded in native tissue seemed to migrate towards and into the hydrogel-filled defect created in an osteochondral plug *ex vivo*. A hypothesis could be that the generation of the defect induced cells, remaining on the edges of the defect side, to migrate. Another possibility is that due to the defect the chemical environment of the cells on the edges changed, inducing cellular proliferation and migration. This would corroborate with results described in chapter 4 and 5 of this thesis in which we show the differential effect of growth factor and nutrient concentration distributions on cellular behaviour.

Many studies have reported cell migration towards drug depots loaded with known chemoattractants as reviewed by Schmidt [31]. For the hydrogel used in this study it was reported that a hydrogel/platelet lysate combination had a positive effect on cell attraction [24]. However, this could not be confirmed in this study, which could be due to the batch of platelet lysate used. Using a more defined chemoattractant could aid in determining the processes involved in the migration into and remodelling of new hydrogels for the treatment of cartilage defects. Supplementation of an injectable *in situ* gelating hydrogel of a defined composition of natural polymers with a selected number of growth factors could potentially further augment chemoattraction.

Fibroblast growth factor-18 (FGF-18) has recently been associated with a strong effect on chondrocyte migration [32, 33]. A gel composed of chemoattractant natural polymers supplemented with FGF18 could thus have a dual function: (1) stabilize the defect site preventing further degradation of the matrix and (2) as a temporary scaffold to allow cellular invasion of cells derived from the defect's surroundings and facilitating matrix deposition by cells. Important for the first function is the integration of the gel with the host tissue, which in literature has been described as a challenge due to the interaction with the host matrix [34]. In our study, signs of integration by collagen fibers have been observed (Figure 6), which was in accordance with previous reports [23]. This integration should be further improved. In addition, one

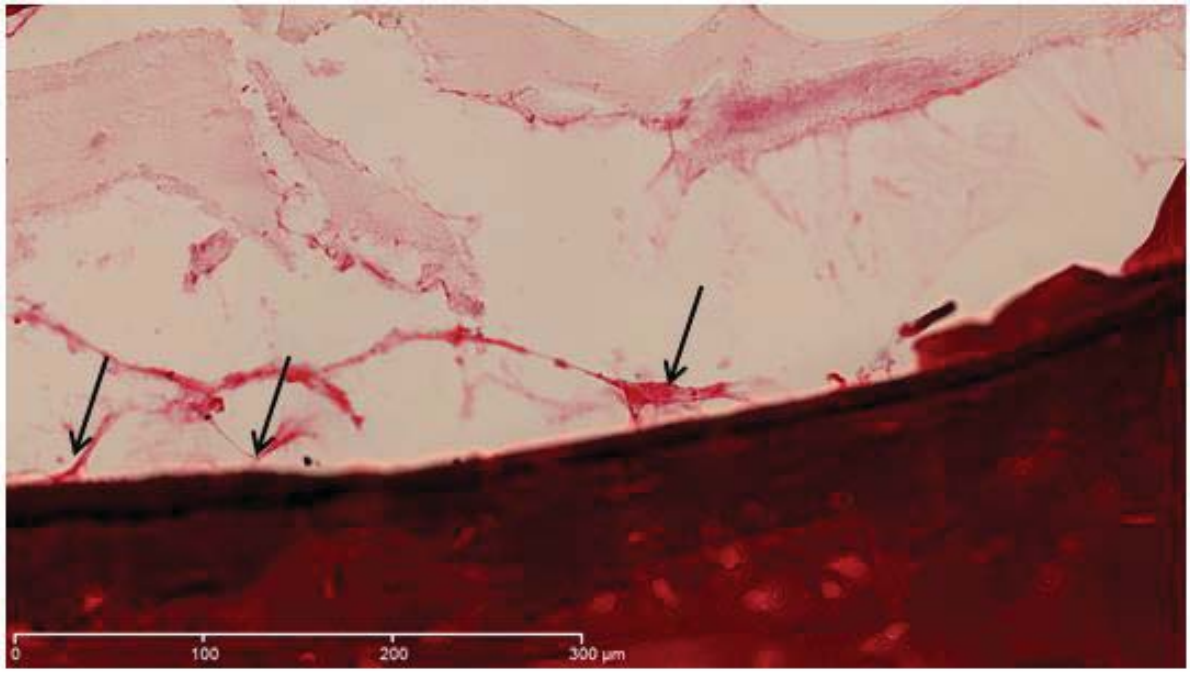

Figure 6: Picrosirius Red Staining of Dex-TA+coll+HA hydrogels showing attachment of the gel to the host tissue by collagen fibers (arrows). Most likely due to tyramine - tyrosine crosslinks.

may expect that ingrowth of cells derived from adjacent native tissue into the hydrogel may further facilitate tissue – construct integration.

Cellular invasion may be derived from the cartilage itself, the bone marrow compartment, the synovial fluid and/or synovium. Various stem or progenitor cell populations have been identified in the diseased joint [35, 36]. It has been postulated that these cells are an attempt of the joint to repair itself. The hydrogel may provide the proper environment for these cells to initiate successful repair, which otherwise will fail.

Another important parameter regarding novel therapies is that they have to withstand the mechanical environment in the knee joint. Due to the articulating motion of the joint, the connection between the host tissue and the implanted material can get lost leading to further deterioration of the tissue. The herein described system can also be equipped with controlled mechanical stimulation [15] and will thus be a suitable system to answer these kind of questions. This system will be more advantageous to investigate the short term effect of a therapy compared to *in vivo* models, especially when equipped with real time monitoring to visualize the maturation and behaviour of the construct in an environment that closely resembles the natural situation.

Although our bioreactor model has provided first preliminary results demonstrating its potential use for developing a cell-free treatment for focal cartilage defects, various aspects in analysis should be improved. For example, due to the different properties of the hydrogel versus the native cartilage, histological artefacts might arise, hence protocols for histological analysis need optimization.

In conclusion, this study provides the first preliminary evidence that chondrocytes near borders of defects may have the capacity to free themselves from their surrounding chondron and may migrate into the defect site provided a proper scaffold for cell migration is available. Furthermore, our previously developed bioreactor seems very well suited to investigate and optimize the chemoattractant properties of an *in situ* gelating hydrogel, thereby providing the first steps in the development of a cell-free treatment of focal cartilage defects.

References

1. Bartlett, W., et al., *Autologous chondrocyte implantation versus matrix-induced autologous chondrocyte implantation for osteochondral defects of the knee: a prospective, randomised study.* J Bone Joint Surg Br, 2005. 87(5): p. 640-5.
2. Kon, E., et al., *Articular Cartilage Treatment in High-Level Male Soccer Players: A Prospective Comparative Study of Arthroscopic Second-Generation Autologous Chondrocyte Implantation Versus Microfracture.* Am J Sports Med, 2011.
3. Steadman, J.R., et al., *Outcomes of microfracture for traumatic chondral defects of the knee: average 11-year follow-up.* Arthroscopy, 2003. 19(5): p. 477-84.
4. Steadman, J.R., W.G. Rodkey, and K.K. Briggs, *Microfracture to treat full-thickness chondral defects: surgical technique, rehabilitation, and outcomes.* J Knee Surg, 2002. 15(3): p. 170-6.
5. Delcogliano, M., et al., *Use of innovative biomimetic scaffold in the treatment for large osteochondral lesions of the knee.* Knee Surg Sports Traumatol Arthrosc, 2013.
6. Filardo, G., et al., *Treatment of knee osteochondritis dissecans with a cell-free biomimetic osteochondral scaffold: clinical and imaging evaluation at 2-year follow-up.* Am J Sports Med, 2013. 41(8): p. 1786-93.
7. Knutsen, G., et al., *A randomized trial comparing autologous chondrocyte implantation with microfracture. Findings at five years.* J Bone Joint Surg Am, 2007. 89(10): p. 2105-12.
8. Kreuz, P.C., et al., *Is microfracture of chondral defects in the knee associated with different results in patients aged 40 years or younger?* Arthroscopy, 2006. 22(11): p. 1180-6.
9. Kreuz, P.C., et al., *Results after microfracture of full-thickness chondral defects in different compartments in the knee.* Osteoarthritis Cartilage, 2006. 14(11): p. 1119-25.
10. Wu, L., et al., *Extracellular Matrix Domain Formation As an Indicator of Chondrocyte Dedifferentiation and Hypertrophy.* Tissue Eng Part C Methods, 2013.
11. Grad, S., et al., *Effects of simple and complex motion patterns on gene expression of chondrocytes seeded in 3D scaffolds.* Tissue Eng, 2006. 12(11): p. 3171-9.
12. Heywood, H.K., M.M. Knight, and D.A. Lee, *Both superficial and deep zone articular chondrocyte subpopulations exhibit the Crabtree effect but have different basal oxygen consumption rates.* J Cell Physiol, 2010. 223(3): p. 630-9.
13. Malda, J., et al., *Oxygen gradients in tissue-engineered PEGT/PBT cartilaginous constructs: measurement and modeling.* Biotechnol Bioeng, 2004. 86(1): p. 9-18.
14. Rosa, S.C., et al., *Role of glucose as a modulator of anabolic and catabolic gene expression in normal and osteoarthritic human chondrocytes.* J Cell Biochem, 2011. 112(10): p. 2813-24.
15. Spitters, T.W., et al., *A dual flow bioreactor with controlled mechanical stimulation for cartilage tissue engineering.* Tissue Eng Part C Methods, 2013.
16. Thorpe, S.D., et al., *Modulating gradients in regulatory signals within mesenchymal stem cell seeded hydrogels: a novel strategy to engineer zonal articular cartilage.* PLoS One, 2013. 8(4): p. e60764.
17. Wimmer, M.A., et al., *Tribology approach to the engineering and study of articular cartilage.* Tissue Eng, 2004. 10(9-10): p. 1436-45.
18. Jovanovic, Z., et al., *Bioreactor validation and biocompatibility of Ag/poly(N-vinyl-2-pyrrolidone) hydrogel nanocomposites.* Colloids Surf B Biointerfaces, 2013. 105: p. 230-5.
19. Popp, J.R., et al., *An Instrumented Bioreactor for Mechanical Stimulation and Real-Time, Nondestructive Evaluation of Engineered Cartilage Tissue.* Journal of Medical Devices-Transactions of the Asme, 2012. 6(2).
20. Jin, R., et al., *Chondrogenesis in injectable enzymatically crosslinked heparin/dextran hydrogels.* J Control Release, 2011. 152(1): p. 186-95.
21. Jin, R., et al., *Enzymatically crosslinked dextran-tyramine hydrogels as injectable scaffolds for cartilage tissue engineering.* Tissue Eng Part A, 2010. 16(8): p. 2429-40.
22. Jin, R., et al., *Enzymatically-crosslinked injectable hydrogels based on biomimetic dextran-hyaluronic acid conjugates for cartilage tissue engineering.* Biomaterials, 2010. 31(11): p. 3103-13.
23. Moreira Teixeira, L.S., et al., *Self-attaching and cell-attracting in-situ forming dextran-tyramine conjugates hydrogels for arthroscopic cartilage repair.* Biomaterials, 2012. 33(11): p. 3164-74.
24. Moreira Teixeira, L.S., et al., *The effect of platelet lysate supplementation of a dextran-based hydrogel on cartilage formation.* Biomaterials, 2012. 33(14): p. 3651-61.
25. Cole, B.J. and M.M. Malik, *Articular cartilage lesions: a practical guide to assessment and treatment*. 2004: Springer Science+Business Media.

26. Cho, H.S., et al., *Individual variation in growth factor concentrations in platelet-rich plasma and its influence on human mesenchymal stem cells.* Korean J Lab Med, 2011. 31(3): p. 212-8.
27. Kalen, A., et al., *The content of bone morphogenetic proteins in platelets varies greatly between different platelet donors.* Biochem Biophys Res Commun, 2008. 375(2): p. 261-4.
28. Singh, R.P., et al., *Quality assessment of platelet concentrates prepared by platelet rich plasma-platelet concentrate, buffy coat poor-platelet concentrate (BC-PC) and apheresis-PC methods.* Asian J Transfus Sci, 2009. 3(2): p. 86-94.
29. Linden, B., *Osteochondritis dissecans of the femoral condyles: a long-term follow-up study.* J Bone Joint Surg Am, 1977. 59(6): p. 769-76.
30. Messner, K. and J. Gillquist, *Cartilage repair. A critical review.* Acta Orthop Scand, 1996. 67(5): p. 523-9.
31. Schmidt, M.B., E.H. Chen, and S.E. Lynch, *A review of the effects of insulin-like growth factor and platelet derived growth factor on in vivo cartilage healing and repair.* Osteoarthritis Cartilage, 2006. 14(5): p. 403-12.
32. Ellsworth, J.L., et al., *Fibroblast growth factor-18 is a trophic factor for mature chondrocytes and their progenitors.* Osteoarthritis Cartilage, 2002. 10(4): p. 308-20.
33. Yamaoka, H., et al., *Involvement of fibroblast growth factor 18 in dedifferentiation of cultured human chondrocytes.* Cell Prolif, 2010. 43(1): p. 67-76.
34. Hunter, C.J. and M.E. Levenston, *Maturation and integration of tissue-engineered cartilages within an in vitro defect repair model.* Tissue Eng, 2004. 10(5-6): p. 736-46.
35. Katagiri, H., et al., *Transplantation of aggregates of synovial mesenchymal stem cells regenerates meniscus more effectively in a rat massive meniscal defect.* Biochem Biophys Res Commun, 2013. 435(4): p. 603-9.
36. Nakamura, T., et al., *[Bone and Cartilage Diseases and Regeneration. Articular cartilage regenerative therapy with synovial mesenchymal stem cells in a pig model].* Clin Calcium, 2013. 23(12): p. 1741-9.

Chapter 9
General Discussion

Abstract

In vitro models that mimic the native environment can aid in the production of tissues that are similar to their natural equivalents. Here, a dual compartment bioreactor equipped for controlled mechanical stimulation is described. We show proof-of-principle how such bioreactor can be used for establishing gradients of nutrients, growth factors and catabolic enzymes in three dimensional tissue engineered constructs and explants. Moreover, we provide evidence how such gradients affect matrix deposition and distribution. In addition, we describe how such a bioreactor can be used in the evaluation of intra-articular drug delivery systems.

Gradients in cartilage tissue engineering

During embryonic development morphogen gradients play an important role in cell guidance and cell fate [1-3]. Cellular organization and organ development are controlled by specific morphogen distributions [4, 5]. After maturation, most tissues are dependent on vascularization for nutrient and growth factor supply. Due to the constant refreshment of blood, more or less stable concentrations of these factors within the tissue are maintained. However, cartilage, due to its avascular nature, is largely dependent on diffusion of growth factors and nutrients from the synovial side of the tissue to the mineralized cartilage residing at the subchondral bone plate. The diffusion is facilitated by compression forces on cartilage which induce exchange of water molecules in the cartilaginous extracellular matrix with the synovial fluid. The inward and outward flux of water induced by cyclic loading of cartilage aids in the replenishment of nutrient and growth factor levels and expels metabolic waste products. This particular nutrient supply results in the formation of nutrient and growth factor gradients. In this thesis we show that both these parameters influence metabolic rates, matrix deposition and matrix distribution in a three dimensional construct.

The design of our bioreactor set up was focused on these parameters, namely, cyclic loading and nutrient supply by diffusion to create nutrient and growth factor gradients. Figure 1 shows schematic representations of a static dual compartment bioreactor and a dynamic dual flow bioreactor equipped with cyclic compression. In both systems cartilage explants or tissue engineered constructs divide a top and bottom chamber. Complete separation of the two compartments allows for exposure of the constructs to two different medium compositions. This is intended to provide an

environment to differentiate progenitor or stem cells into two different lineage within one construct.

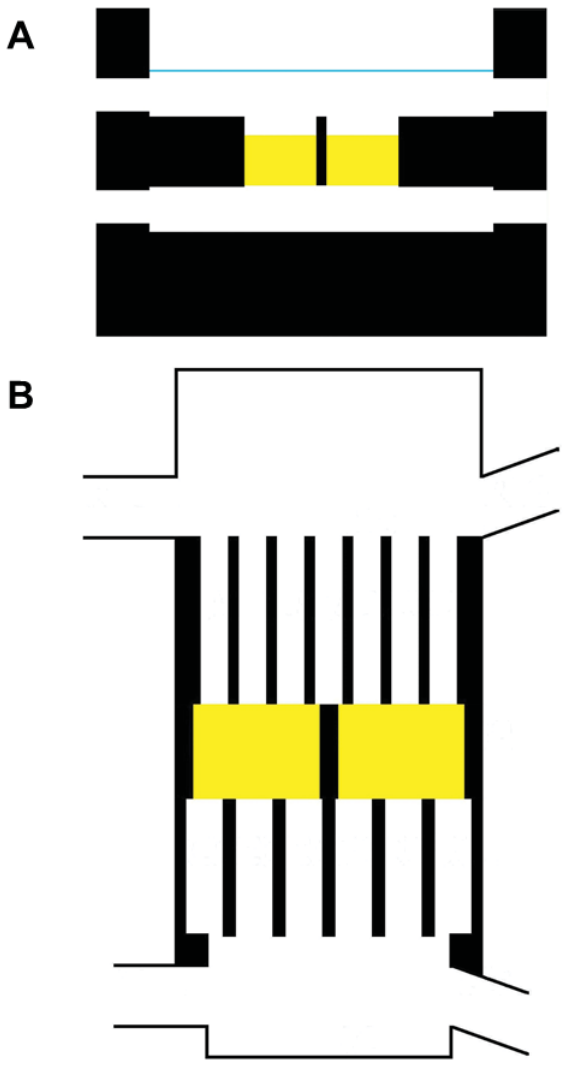

Figure 1: Schematic representation of a static (A) and dynamic (B) dual compartment bioreactor. The latter one is equipped for top down cyclic compression. Tissue engineered constructs separating the top and bottom compartment are represented in yellow. The dimensions of these cubes are 4.5x4.5x4mm.

Interestingly, the GAG/DNA data in constructs cultured in a glucose gradient showed the same trend compared to the GAG/DNA ratios of native cartilage as reported by Woodfield *et al* [6]. Prolonged cultures have to determine if glucose gradients alone can induce this native GAG/DNA gradient. Further, we show that opposing gradients of growth factors and their respective antagonists induce sharp differences cell response. Most probably growth factor gradients will aid in facilitating the formation of gradual matrix distribution and induce zonal differentiation of chondrocytes. The interplay of nutrient and growth factor gradients has not been studied in this thesis. This interplay will add to the complexity of *in vitro* culture of cartilage constructs. In cartilage also oxygen gradients exist and low oxygen concentration in the medium has a positive effect on matrix deposition by chondrocytes [7-10]. Mathematical models have predicted how an oxygen gradient could look like in articular cartilage [11-13]. However, culturing chondrocyte constructs in such oxygen gradients *in vitro* has not yet been accomplished, although it will play a pivotal role in producing cartilaginous implants that are already adapted to the native situation. This likely will increase the integration of the construct with the surrounding tissue upon implantation.

The addition of mechanical stimulation of these constructs will add another degree of complexity not only to produce functional load bearing tissue but also to establish

zonal organization of collagen fibers in a tissue engineered construct. Kock *et al*. showed that sliding indentation induces collagen production by chondrocytes and that collagen bundles are formed towards the direction of the stimulus [14]. Thus, solely compression from the top, as applied in our system, will not provide sufficient cues to orientate collagen fibers in the fountain-like shape found in cartilage. Therefore, optimizing the compression module in such a way that both articulating as top-down compression can be applied is of importance to create an implantable construct that can function in load absorption and distribution, one of the main functions of cartilage [15].

But will bioreactor systems have a role in the production of tissue engineered products in clinically relevant amounts? Can the production be upscaled to such quantities that it is cost-effective? Are there possibilities to decrease the culture time to shorten the patients' waiting time for an implant? Or will they be merely a tool in deducing mechanisms and parameters for three dimensional culture of tissue engineered constructs and pathophysiology? In my opinion, the bioreactor field should focus on these questions to advance further in the exploration of tissue engineered constructs towards a more patient-specific therapy. Some of the published systems are being commercialized at the moment [16, 17]. Therefore, also other applications of our system were explored.

Preclinical Evaluation of Treatment Strategies

Recreating the natural articular cartilage environment *in vitro* allows for the evaluation of new therapies in a simulated knee joint. Animal experiments are expensive. Providing an equivalent alternative to evaluate a newly developed therapy can lower the associated costs. In addition, it is well recognized that each animal model has limitations and can only partly represent the situation in humans. Although animal experiments will stay important in preclinical research, being able to prescreen new therapies cost-effectively ensures a more direct approach in selecting the most promising candidate for biomedical therapies [18].

We explored the possibility of evaluating newly developed treatment options for joint diseases. A hydrogel and microspheres for intra-articular drug delivery, and a biomimicking hydrogel were tested in a dual compartment bioreactor regarding their effectiveness and biocompatibility. By injecting a hydrogel drug depot we observed that drug delivery into the cartilage is increased compared to direct injection of a drug

in the synovial fluid. Further, drug penetration will be most optimal if the patient does not use the joint continuously after injection.

The microspheres were tested for their grinding effect on the articular surface. This effect was not observed after treatment with the 30μm spheres, although less of these spheres were injected in the top compartment compared to the smaller microspheres. In animal studies done in parallel with ours it was seen that the 30μm spheres also performed best (unpublished data). Therefore, larger spheres seem to be the best candidate for drug delivery in the joint. However, the release profile in such an environment could not yet be determined and thus the local action of the drug is yet unknown. Importantly, our system only includes two tissues, articular cartilage and subchondral bone, whereas the joint consists of multiple tissues that interact to maintain joint homeostasis. One of these tissues is the synovium. *In vitro* cocultures of synovium and articular cartilage have shown that the communication between these tissues is important in maintaining the balance between anabolic and catabolic processes [19]. Thus, adding a compartment harboring the synovium will make the model more representative. Furthermore, current experiments were conducted in the presence of a watery medium, whereas in the native situation the joint cavity is filled with synovial fluid which is more viscous. This will influence the formation of gradients as diffusion through a viscous fluid is slower than a non-viscous one [20]. Furthermore, this will have an impact on the way forces during loading are conducted on the cartilage surface.

In an osteochondral defect model cell migration towards a hydrogel filled defect was observed. This shows that the current system can be used to elucidate mechanisms involved in cartilage repair and evaluating new therapies.

Conclusion

In this thesis we describe the validation of a dual compartment/flow bioreactor. Its design supports the controllable creation of nutrient, growth factor and growth factor antagonists through three-dimensional hydrogel constructs. Finally, we explored the application of this bioreactor system in the evaluation of drug delivery systems for the treatment of cartilage defects and degenerative cartilage diseases.

References

1. Cho, H.S., et al., *Individual variation in growth factor concentrations in platelet-rich plasma and its influence on human mesenchymal stem cells.* Korean J Lab Med, 2011. **31**(3): p. 212-8.
2. Kim, H.K., I. Oxendine, and N. Kamiya, *High-concentration of BMP2 reduces cell proliferation and increases apoptosis via DKK1 and SOST in human primary periosteal cells.* Bone, 2013. **54**(1): p. 141-50.
3. Zhang, J. and Y. Li, *Fibroblast growth factor 21, the endocrine FGF pathway and novel treatments for metabolic syndrome.* Drug Discov Today, 2013.
4. Arkell, R.M., N. Fossat, and P.P. Tam, *Wnt signalling in mouse gastrulation and anterior development: new players in the pathway and signal output.* Curr Opin Genet Dev, 2013. **23**(4): p. 454-60.
5. Idkowiak, J., G. Weisheit, and C. Viebahn, *Polarity in the rabbit embryo.* Semin Cell Dev Biol, 2004. **15**(5): p. 607-17.
6. Woodfield, T.B., et al., *Polymer scaffolds fabricated with pore-size gradients as a model for studying the zonal organization within tissue-engineered cartilage constructs.* Tissue Eng, 2005. **11**(9-10): p. 1297-311.
7. Das, R., et al., *Control of oxygen tension and pH in a bioreactor for cartilage tissue engineering.* Biomed Mater Eng, 2008. **18**(4-5): p. 279-82.
8. Heywood, H.K., D.L. Bader, and D.A. Lee, *Rate of oxygen consumption by isolated articular chondrocytes is sensitive to medium glucose concentration.* J Cell Physiol, 2006. **206**(2): p. 402-10.
9. Malda, J., et al., *Oxygen gradients in tissue-engineered PEGT/PBT cartilaginous constructs: measurement and modeling.* Biotechnol Bioeng, 2004. **86**(1): p. 9-18.
10. Strobel, S., et al., *Anabolic and catabolic responses of human articular chondrocytes to varying oxygen percentages.* Arthritis Res Ther, 2010. **12**(2): p. R34.
11. Moretti, M., et al., *An integrated experimental-computational approach for the study of engineered cartilage constructs subjected to combined regimens of hydrostatic pressure and interstitial perfusion.* Biomed Mater Eng, 2008. **18**(4-5): p. 273-8.
12. Raimondi, M.T., et al., *Breakthroughs in computational modeling of cartilage regeneration in perfused bioreactors.* IEEE Trans Biomed Eng, 2011. **58**(12): p. 3496-9.
13. Zhou, S., Z. Cui, and J.P. Urban, *Nutrient gradients in engineered cartilage: metabolic kinetics measurement and mass transfer modeling.* Biotechnol Bioeng, 2008. **101**(2): p. 408-21.
14. Kock, L.M., et al., *Tuning the differentiation of periosteum-derived cartilage using biochemical and mechanical stimulations.* Osteoarthritis Cartilage, 2010. **18**(11): p. 1528-35.
15. Wimmer, M.A., et al., *Tribology approach to the engineering and study of articular cartilage.* Tissue Eng, 2004. **10**(9-10): p. 1436-45.
16. Timmins, N.E., et al., *Three-dimensional cell culture and tissue engineering in a T-CUP (tissue culture under perfusion).* Tissue Eng, 2007. **13**(8): p. 2021-8.
17. Wendt, D., et al., *Uniform tissues engineered by seeding and culturing cells in 3D scaffolds under perfusion at defined oxygen tensions.* Biorheology, 2006. **43**(3-4): p. 481-8.
18. Jovanovic, Z., et al., *Bioreactor validation and biocompatibility of Ag/poly(N-vinyl-2-pyrrolidone) hydrogel nanocomposites.* Colloids Surf B Biointerfaces, 2013. **105**: p. 230-5.
19. Beekhuizen, M., et al., *Osteoarthritic synovial tissue inhibition of proteoglycan production in human osteoarthritic knee cartilage: establishment and characterization of a long-term cartilage-synovium coculture.* Arthritis Rheum, 2011. **63**(7): p. 1918-27.
20. Kwan, C., et al., *Effects of intra-articular sodium pentosan polysulfate and glucosamine on the cytology, total protein concentration and viscosity of synovial fluid in horses.* Aust Vet J, 2012. **90**(8): p. 315-20.

Acknowledgements

The work presented in this thesis would not have been possible without the help and support of others. Prof.Dr. Marcel Karperien and Prof.Dr. Clemens van Blitterswijk thank you for giving me the opportunity to do my PhD thesis in your group. Marcel, as my daily supervisor, thank you for all the biological input and support at times I needed direction. Further, I want to thank Prof.Dr. Weinans, Prof.Dr.Ir. Verdonschot, Prof. de Boer, Dr. Schulz, Dr.Ir. Martens and Dr. van Donkelaar for taking place in my graduation committee.

All my (former) colleagues from DBE, Giulia, Emilie, Tom, Parthiban, Sieger, Leilei, Rong, Jetse, Jan, Aart, Piet, Janine, Sanne, Ingrid, Janneke, Nicole, Ellie, Jeroen, Liliana, Mijke, Jos, Milou and Elahe, thank you for all your insightful, interesting and useful comments, remarks and discussions. I learned a lot of you guys and you made the work environment one in which you can finish a PhD. Jacqueline thank you for all your help and input on technical details.

Andrea, Erik, Wim, Paul and Max thanks for all the fun and sociable moments. I hope we will have continue our friendship also when we are not in The Netherlands anymore. My other TR colleagues also your input in discussions and sociability is much appreciated.

Raymond, Evelien, Samuel and Barbara, thank you for your hard work during your BSc or MSc theses. I learned a lot from you, I hope I could transfer some knowledge to you too. Good luck in your future careers!

Christian, Dirk, Frank Simon and Tim, my supervisors during my BSc or MSc thesis, thank you for the opportunity to develop myself as a researcher. All the guidance you gave made sure I could finish my PhD thesis.

Teris a special thanks for you. I can definitely say that without you this thesis would never had happened from my hand. Thank you for believing in me and giving me one more chance.

Ruben and Ernst, my paranymphs, we go back a long time already. And therefore we never need many words to say that we respect each other, so I won't break with that tradition ;-).

Mom, dad, Hilde, Rik, Henk and Jessie, although there has been quite some distance between us the last 12 years, I have never forgotten my family. And maybe I have not always shown you were always with me. Therefore, I thank you very much for all your patience, trust and confidence in me!
And last, but for sure not least, Natalie, although we are not together for a long time yet, you mean a lot to me. Thank you for the patience and the proof reading during my writing period! You kept me motivated to finish this thesis.

Curriculum Vitae

Tim Spitters was born December 21st, 1981 in Waalwijk, The Netherlands. He started the study Biotechnology at Wageningen University in 2001. During his Bachelor he specialized in Microbial Physiology and worked on the isolation and characterization of micro-organisms involved in anaerobic methane oxidation under supervision of Dr. Christian Jagersma and Prof. Dr. Ir. Fons Stams. He then continued his Masters specializing in Medical Biotechnology. His Master thesis was performed at the department of Tissue Engineering at the University of Twente under the supervision of Dr. Frank Janssen, Dr. Ir. Dirk Martens and Prof. Dr. Clemens van Blitterswijk and was entitled *Bioreactors in Bone Tissue Engineering: The effect of whole bone marrow seeding and hypoxia on the production of osteogenic constructs*. This was followed by a six-month internship at the University of Canterbury and the University of Otago, New Zealand, under the supervision of Dr. Simon Ströbel and Dr. Tim Woodfield and was entitled *Bioreactors in Cartilage Tissue Engineering: The production of chondrogenic constructs with a high local cell density - a novel method of guiding cells during seeding*. After his return to The Netherlands he started his PhD thesis, of which the results are described in this book, in the department of Tissue Engineering and continued in the Department of Developmental BioEngineering at the University of Twente under the supervision of Prof. Dr. Marcel Karperien.

List of Publications

Peer-reviewed articles

Gustavo A. Higuera, Deborah Schop, **Tim W.G.M. Spitters**, Riemke van Dijkhuizen-Radersma, Madelon Bracke, Joost D.de Bruijn, Dirk Martens, Marcel Karperien, Anton van Boxtel, and Clemens A. van Blitterswijk, 2011, *Patterns of Amino Acid Metabolism by Proliferating Human Mesenchymal Stem Cells*, Tissue Engineering Part A, 18 (5 and 6)

Tim W.G.M. Spitters, Jeroen C.H. Leijten, Filipe D. Deus, Ines B.F. Costa, Aart A. van Apeldoorn, Clemens A. van Blitterswijk and Marcel Karperien, 2013, *A Dual Flow Bioreactor with Controlled Mechanical Stimulation for Cartilage Tissue Engineering*, Tissue Engineering Part C, 19 (10)

Manuscripts in preparation

Tim W.G.M. Spitters, Carlos Miguel Domingues Mota, Barbara Slowinska, Lorenzo Moroni, Marcel Karperien, *Glucose gradients influence zonal matrix deposition in 3D agarose constructs,* submitted

Tim W.G.M. Spitters, Dimitrios Stamatialis, Audrey Petit, Mike W.G. de Leeuw, Marcel Karperien, *Delivery of small molecules from a drug delivery system into articular cartilage is dependent on clearance, compression, frequency and tissue relaxation*, submitted

Tim W.G.M. Spitters, Tim B.F. Woodfield, Marcel Karperien, *Bioreactors Design and Application in Musculoskeletal Tissue Engineering*, submitted

Tim W.G.M. Spitters, Jacqueline Plass, Marcel Karperien, *Creating growth factor gradients to control cell behavior in three dimensional constructs*

Tim W.G.M. Spitters, Barbara Slowinska, Rong Wang, Piet Dijkstra, Marcel Karperien, *Enhancement of Dex-TA gels with collagen and hyaluronic acid induces migration from chondrocytes from cartilage into the hydrogel*

Tim W.G.M. Spitters, Luisa Duque, Johan Zuidema, Rob Steendam, Marcel Karperien, *Are microspheres a treatment option in osteoarthritis?*

Gustavo A. Higuera, Hugo Fernandes, **T.W.G.M. Spitters**, Nils Aufferman, Roman Truckenmueller, Maryana Escalante, Reinout Stoop, Jan de Boer, Vinod Subramaniam, Marcel Karperien, Clemens van Blitterswijk, Anton van Boxtel, and Lorenzo Moroni, *Spatiotemporal proliferation of mesenchymal stem cells influence stanniocalcin-1 expression and angiogenesis potential*

Selected abstracts for oral presentations

T.W.G.M. Spitters, H.A.M. Fernandes, J.C.H. Leijten, F.D. Deus, A.A. van Apeldoorn, C.A. van Blitterswijk, M. Karperien, *Novel bioreactor approach for cartilage tissue engineering*, Dutch Biotechnology Association, 2011

T.W.G.M. Spitters, H.A.M. Fernandes, J.C.H. Leijten, F.D. Deus, A.A. van Apeldoorn, C.A. van Blitterswijk, M. Karperien, *Novel bioreactor approach for cartilage tissue engineering*, TERMIS, 2011,

T.W.G.M. Spitters, D. Stamatialis, A. Petit, M.G.W. De Leeuw, M. Karperien, *Evaluation of small molecule delivery from a hydrogel in a simulated knee joint environment*, 2013, Annual BMM/TerM/DCTi meeting

Selected abstracts for poster presentations

S. Stroebel, **T.W.G.M. Spitters**, J Malda, T.B.F. Woodfield, *Perfusion seeding of chondrocytes into 3D printed polymer scaffolds*, ESB, 2009

T.W.G.M. Spitters, J.C.H. Leijten, F.D. Deus, IB Ferreira da Costa, A.A. van Apeldoorn, C.A. van Blitterswijk, M. Karperien, *Novel bioreactor approach for cartilage tissue engineering*, Dutch Biomaterials and Tissue Engineering Conference, 2012

T.W.G.M. Spitters, D. Stamatialis, A. Petit, M.G.W. De Leeuw, M. Karperien, *Evaluation of small molecule delivery from a hydrogel in a simulated knee joint environment*, 2013

wat je blijkt te doen,
heb je gedaan.
Wat je ook overkomen is:
het is al gebeurd.
van belang is alleen de vraag:
en nu?
Jon Kabat-Zinn

(what you appear to do,
you have done,
what has happened to you,
it has past,
the only question that matters is:
what now?)

veni, vidi, superstites
(ik kwam, ik zag, ik heb het overleefd)
(I came, I saw, I have survived)
after Julius Ceasar